AD_____

Award Number: W81XWH-07-1-0208

TITLE: How MMPs impact bone responses to metastatic prostate cancer

PRINCIPAL INVESTIGATOR: Conor C. Lynch

CONTRACTING ORGANIZATION: Vanderbilt University
Nashville TN, 37232

REPORT DATE: April 2011

TYPE OF REPORT: Final

PREPARED FOR: U.S. Army Medical Research and Materiel Command
Fort Detrick, Maryland 21702-5012

REPORT DOCUMENTATION PAGE

Form Approved
OMB No. 0704-0188

1. REPORT DATE *(DD-MM-YYYY)*	**2. REPORT TYPE**	**3. DATES COVERED** *(From - To)*
04/30/2011	Final	1 FEB 2007 – JAN 30 2010

4. TITLE AND SUBTITLE
How MMPs impact bone responses to metastatic prostate cancer

5a. CONTRACT NUMBER
W81XWH-07-1-0208

5b. GRANT NUMBER

5c. PROGRAM ELEMENT NUMBER

6. AUTHOR(S)
Conor C Lynch
conor.lynch@vanderbilt.edu

5d. PROJECT NUMBER

5e. TASK NUMBER

5f. WORK UNIT NUMBER

7. PERFORMING ORGANIZATION NAME(S) AND ADDRESS(ES)
Vanderbilt University

Nashville TN, 37232

8. PERFORMING ORGANIZATION REPORT NUMBER

9. SPONSORING / MONITORING AGENCY NAME(S) AND ADDRESS(ES)
U.S. Army Medical Research and Materiel Command
Fort Detrick, Maryland 21702-5012

10. SPONSOR/MONITOR'S ACRONYM(S)

11. SPONSOR/MONITOR'S REPORT NUMBER(S)

12. DISTRIBUTION / AVAILABILITY STATEMENT
Approved for public release; distribution unlimited

13. SUPPLEMENTARY NOTES

14. ABSTRACT
Using an animal model of prostate tumor progression in the bone we have previously shown that MMPs, namely MMP-2,-3,-9 and -13, are overexpressed at the tumor bone interface and these MMPs are for the most part expressed by the host cells of the bone. To test the contribution of MMPs in prostate tumor progression in the bone, we have generated mice that are immunocompromized and deficient for MMP-2,-3 and -9 during the current period. We have found that MMP-9 does not contribute to prostate tumor progression in the bone since no difference in osteolytic or osteoblastic responses between wild type and MMP-9 deficient animals were detected by Faxitron, CT, SPECT and histomorphometry. These results, while negative, are important for the generation of selective MMP inhibitors that lack the deleterious side effects associated with broad spectrum inhibitors. In addition, we have also identified PTHrP as an MMP substrate and postulate that MMP processing of PTHrP may be a mechanism through which MMPs can contribute to tumor induced osteolysis.

15. SUBJECT TERMS
Osteolysis, osteoblastic changes, prostate progression in bone, matrix metalloproteinases, MMPs, receptor activator of nuclear kappa B ligand, RANKL, bone metastasis.

16. SECURITY CLASSIFICATION OF:			**17. LIMITATION OF ABSTRACT**	**18. NUMBER OF PAGES**	**19a. NAME OF RESPONSIBLE PERSON**
a. REPORT	**b. ABSTRACT**	**c. THIS PAGE**			**19b. TELEPHONE NUMBER** *(include area code)*
U	U	U	UU	61	USAMRMC

Table of Contents

Page

Introduction……..1

Body……..2

Key Research Accomplishments……..11

Reportable Outcomes……12

Conclusion…… 13

References……14

Summary and Introduction……..

Summary

The DOD New investigator award has been of great importance to the establishment of my career. I have been able to complete the majority of the objectives set forth, particularly in Aim 1 and have been able to utilize the preliminary data generated during the award period to successfully obtain NCI-RO1 funding (1RO1CA143094-01A1). During the summer of 2010, I also have taken a new position at the Moffitt Caner Center in Tampa, FL, USA. The move somewhat curtailed my ability to complete some of the objectives set forth in specific Aim 2. However, the research will be completed at the Moffitt Cancer Center and the DOD new investigator award will be acknowledged in any

publications arising from the work. I would like to take the opportunity to thank the DOD PCRP for their support and look forward to contributing to and participating in PCRP programs throughout my career in Prostate Cancer Research.

Introduction

This year, in the United States alone, of the approximately 29,000 men who die from prostate cancer, 80% will have evidence of bone metastasis (1, 2). Prostate bone metastases cause several complications for patients such as hypercalcemia, spontaneous bone fracture and debilitating pain that dramatically affects their quality of life. To progress in the bone, the invading prostate tumor cells induce radical changes in bone matrix homeostasis by stimulating osteoblastic and osteolytic changes (3). These changes result in an actively remodeling bone tumor microenvironment, rich in mitogenic signals that promote tumor growth. In turn, the growth of the tumor exacerbates the osteoblastic and osteolytic changes in a manner that has been well described as the 'vicious cycle' (4). Using an animal model of tumor progression in the bone, we have previously identified a group of enzymes known as matrix metalloproteinases (MMPs) as being highly overexpressed at the tumor bone interface in comparison to the tumor area alone. In a bid to understand the importance of these MMPs, namely MMP-2, -3, -9 and -13, in prostate tumor progression in the bone, we aim to generate MMP null animals and compare those animals to their wild type counterparts. While the MMPs are important in the turnover of the extracellular matrix, it has become apparent that the MMPs are also capable of regulating cell:cell communication by processing various cytokines and growth factors to active soluble forms (5). These soluble factors often influence biological processes including survival, proliferation, angiogenesis and osteoclast activation. Therefore, understanding which MMPs are important in contributing to prostate tumor progression in the bone and identifying the mechanisms that govern the vicious cycle can provide valuable targets for therapeutic development.

Body……..

Accomplishments

Aim 1. *Determine the stromal contribution of MMPs that are markedly overexpressed at the tumor:bone interface namely, MMP-2,-3,-9 and -13 to prostate cancer induced osteoblastic and osteolytic changes in the bone*.

a) Generate immunocompromized RAG-$2^{-/-}$ mice that are deficient in MMP-2, MMP-3 and MMP-13 by crossing RAG-$2^{-/-}$ mice with $MMP^{-/-}$ mice that are both available on the C57Bl/6 background (Months 1-12).
b) Using our pre-clinical animal models, we will test the contribution of stromal MMP-9 to tumor induced osteoblastic and osteolytic change in readily available immunocompromized RAG-$2^{-/-}$ MMP-9 deficient mice (Months 1-12).
c) Test the contribution of stromal MMP-2, MMP-3 and MMP-13 to tumor induced osteoblastic and osteolytic change using our pre-clinical model (Months 11-30).
d) Identify the expression of stromal MMPs in human clinical samples of prostate bone metastases (Months 20-36).

The proposed animal model used in the study involved the transplantation of moderately differentiated rat prostate adenocarcinoma to the calvaria of immunocompromized wild type and MMP deficient mice. To achieve this, we crossed C57Bl/6 RAG-2 (recombinase activating gene-2) deficient mice with either C57Bl/6 MMP-2, -3 or -13 deficient animals in order to generate F2/F3 animals that are immunocompromized and deficient for the desired MMP. As of January 2010, we generated, RAG-$2^{-/-}$;MMP-$3^{-/-}$ and RAG-$2^{-/-}$; MMP-$13^{-/-}$ animals and have made preliminary observations with these animals in terms of prostate tumor induced osteolytic and osteoblastic changes. Initial attempts to generate RAG-$2^{-/-}$;MMP-$2^{-/-}$ null mice were successful and our initial observations suggested that MMP-2 did impact the progression of prostate cancer in bone. However, breeding of the animals to generate sufficient numbers in order repeat experiments has proven difficult. These studies have now been placed on hold while we focus on MMP-13 and mechanistic studies.

Host MMP-9 impacts angiogenesis in the prostate tumor-bone microenvironment but does not impact tumor induced osteolytic and/or osteoblastic changes.

In the initial 12 months of the project, we focused on assessing the impact of host derived MMP-9 in tumor induced osteolytic and osteoblastic changes. We observed that the cell responsible for bone destruction, the osteoclast, was the major cellular source of MMP-9 in the prostate tumor-bone microenvironment in our animal model. The clinical relevance of this observation was also tested. In collaboration with Dr. Bob Vessella, University of Washington (6, 7), we assessed the expression of MMP-9 in 10 human samples of prostate to bone metastasis and observed that again, osteoclasts were a major cellular source of MMP-9 in the **human** prostate tumor-bone microenvironment. To test whether host MMP-9 contributed to prostate tumor induced osteolysis or osteogenesis, we utilized immunocompromized animals that were either wild type or null for host MMP-9. In repeated studies, with at least 10 animals per group, we determined that MMP-9 does not have any effect on tumor progression in the bone using both whole animal imaging modalities such as microCT and microSPECT and traditional histomorphometry approaches. While there was a trend towards a decrease in osteolysis in the MMP-9 deficient animals, this decrease did not prove to be statistically significant (Figure 1). While these data suggest that MMP-9 does not contribute to tumor progression in the bone, it should be stated that the role of MMP-9 in 1) the metastasis of prostate cancer to the

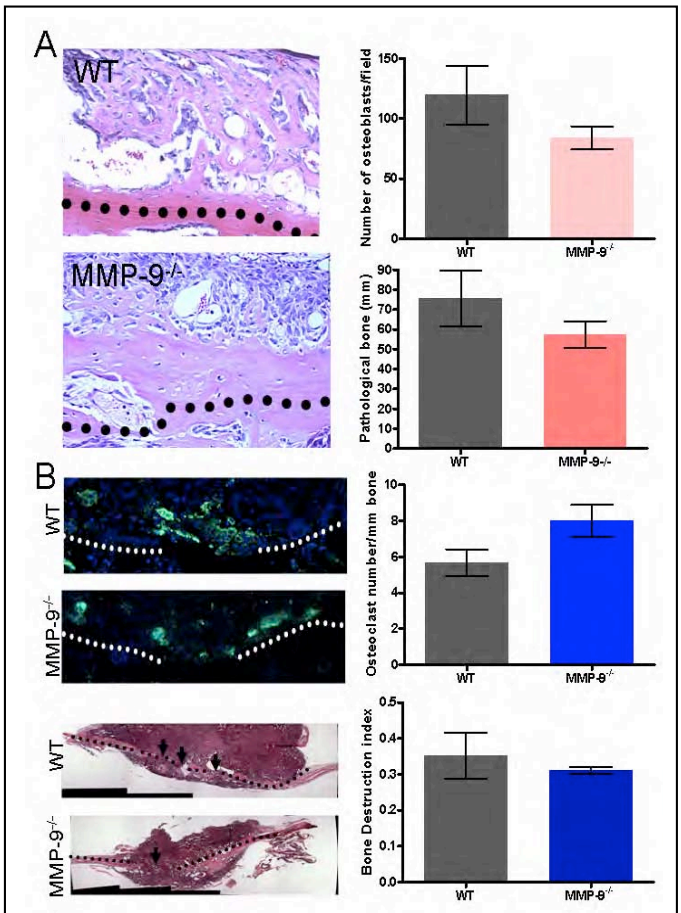

Fig. 1. Host MMP-9 does not contribute to prostate tumor induced osteolytic or osteoblastic changes. **A:** The amount of pathological bone (dashed line) was assessed in sections from WT (n=24) and MMP-9 deficient (n=37) animals at week 3. The number of osteoblasts generating pathological bone was also measured. **B:** The numbers of TRAP positive multinucleated osteoclasts (green) at the tumor bone interface (dashed line) in multiple sections revealed no difference in numbers between the WT and MMP-9 deficient groups. DAPI (blue) was used as a nuclear stain. No differences in the bone destruction indices were observed. Arrows indicate areas of osteolysis.

bone or 2) in the initial survival/establishment of the prostate tumor cells in the bone microenvironment can not be ruled out since these steps are not recapitulated in our animal model. Previous studies have shown that MMP-9 is important in mediating angiogenesis in the tumor microenvironment (8) and using the endothelial antigen CD-31 as a marker for angiogenesis, we found decreased angiogenesis in the MMP-9 null group. In follow-up experiments we identified that while MMP-9 did not impact the ability of myeloid cells to become mature multi-nucleated osteoclasts, there was a significant decrease in the ability of the MMP-9 null osteoclasts to mediate the bioavailability of the potent angiogenic factor vascular endothelial growth factor A (VEGF-A_{164}) (Figure 2). This observation explains, in part, the reduced vascularity of the tumors in the MMP-9 null animals. These results therefore demonstrate that while host, specifically osteoclast derived MMP-9, does not contribute to tumor induced osteolysis and osteogenesis, it does contribute to angiogenesis in the tumor-bone microenvironment. Furthermore, our results resonate with emerging studies from other groups that establish the osteoclast as an angiogenic cell (9, 10). These data have recently been reported in the journal *Molecular Cancer Research* and the publication is appended (11).

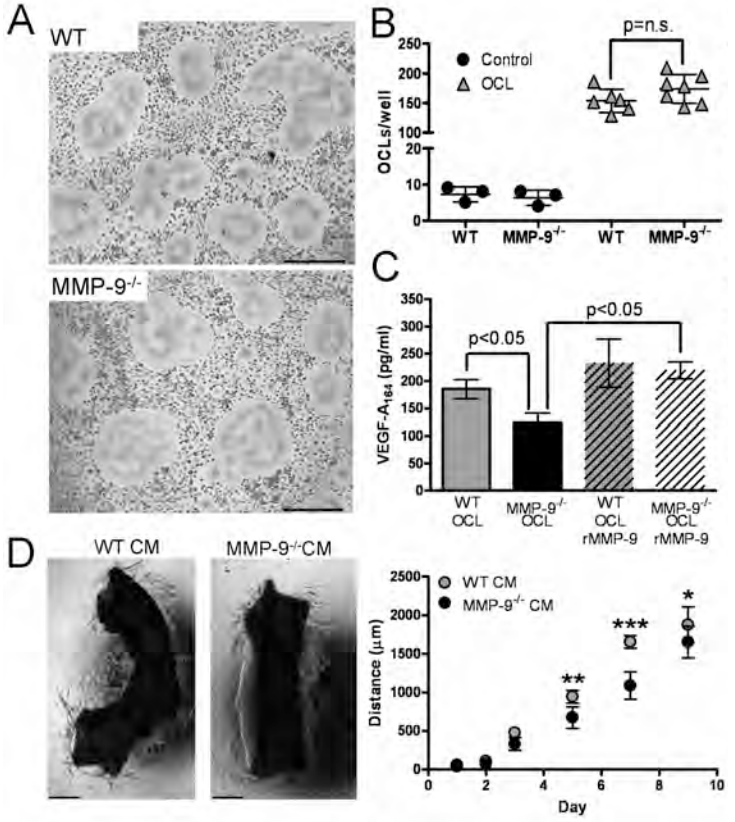

Fig. 2. Osteoclast derived MMP-9 regulates VEGF-A_{164} bioavailability and angiogenesis. *A,* Representative photomicrographs of mature multinucleated osteoclasts generated from $CD11b^{+ve}$ myeloid precursor cells isolated from WT or MMP-$9^{-/-}$ mice after 10 days of culture in osteoclast differentiation media. Scale bars represent 50μm. *B,* Quantitation of the number of osteoclasts generated by treatment with control or osteoclast (OCL) differentiation media. Only multinucleated (>3/cell) TRAcP positive cells were counted. *C,* Quantitation of VEGF-A_{164} levels in conditioned media derived from WT or MMP-$9^{-/-}$ osteoclast (OCL) cultures in the presence or absence of 100ng/ml recombinant MMP-9. *D,* Representative photomicrographs of mouse thoracic aortas stimulated with WT or MMP-$9^{-/-}$ osteoclast culture conditioned media (CM) at day 7. The average distance of sprout migration was calculated from photomicrographs on a daily basis. Scale bar represents 1mm. n.s. denotes non-significant (p>0.05) p values. * denotes p<0.05, ** denotes that p<0.01, *** denotes that p<0.001.

Host MMP-13 has a protective role in the prostate tumor-bone microenvironment

Murine MMP-13 is considered to be the ortholog of human MMP-1, and MMP-13 deficient animals have been reported as having a delay in endochondral ossification during skeletal development with thickened trabecular bone persisting in the animals (12, 13). In collaboration with Dr. Stephen Krane, we generated immunocompromized MMP-13 deficient mice. Histological analysis of the calvaria from these animals at 6 weeks of age and their age matched wild type counterparts were similar with respect to the amount of bone and number of osteoclasts (data not shown). Surprisingly, preliminary studies using our animal model suggested that host MMP-13 plays a protective role in preventing tumor induced osteolytic and osteoblastic changes (Figure 3). At three weeks post implantation, immunocompromized wild type and MMP-13 deficient animals were sacrificed. Histological analysis revealed that in comparison to wild type controls, MMP-13 deficient sections had higher numbers of osteoblasts and osteoclasts which was consistent with increase bone formation and destruction respectively. These data are unexpected since MMP-13 has been described as the rate limiting collagenase for murine skeletal development and suggest that in the pathological context of the tumor bone microenvironment, *host MMP-13 inhibits the vicious cycle and plays a protective role in the tumor-bone microenvironment*.

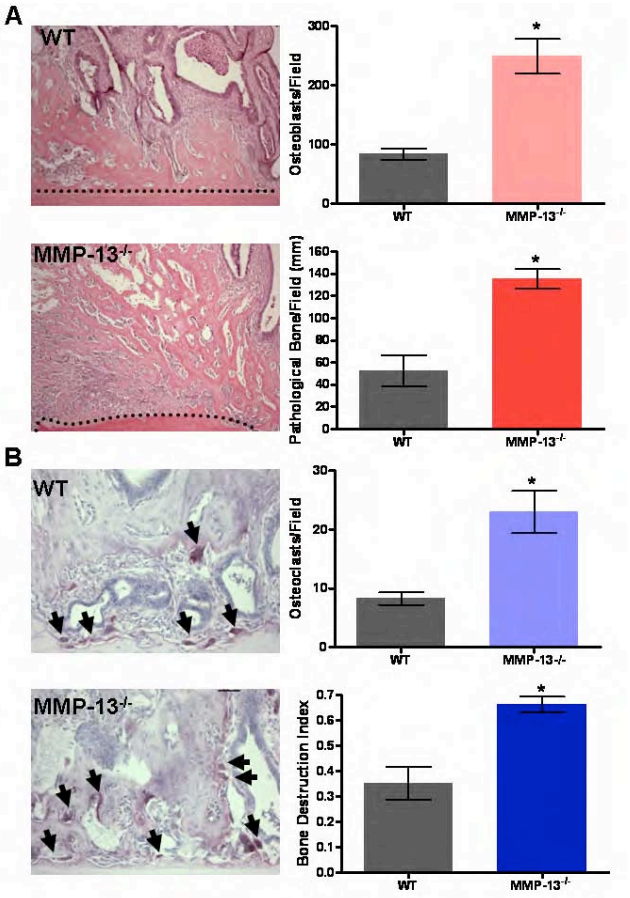

Fig. 3. MMP-13 has a protective role in prostate tumor induced osteoblastic and osteolytic changes. **A:** The number of osteoblasts and the amount of pathological bone in multiple sections (10x fields) were calculated in MMP-13 (n=7) and wild type mice (n=5). **B:** The number of TRAP stained (red) multinucleated osteoclasts (arrows) per field in addition to the to the bone destruction index in multiple sections were also calculated. Asterisk denotes statistical significance with $p<0.05$.

The concept of MMPs as playing a protective role during tumor progression has been reported for MMP-3 and MMP-8 during skin carcinogenesis and progression in mice but to our knowledge

MMP-13 has not been described as being protective in a pathological context (14, 15). These studies and the mechanisms underlying the observations are still being explored in detail by my group. The studies will continue past the life-span of the award but the award will be acknowledged upon publication.

Our collected data illustrated that MMP-7, -9 and -13 are highly expressed in the prostate tumor-bone microenvironment but on an individual basis, they clearly play very different roles with respect to tumor induced osteoblastic and osteolytic changes. In the final year of the proposal, we observed that host MMP-3 did not impact the prostate cancer progression in bone. Given that our overall objective is to identify individual MMPs that play roles in prostate cancer progression in bone, we will include this data in our prospective MMP-13 publication, since, while negative data, is nonetheless informative with respect to the selective design of MMP inhibitors. In our previous report (2010), we identified that MMP-2 contributes to prostate cancer progression in bone. However, breeding of the mice to generate sufficient numbers has proven difficult. This may be due to unforeseen developmental issues, i.e. knocking out RAG-2 and MMP-2 may impact mouse development. We have put these studies on hold while we focus on MMP-13 and our mechanistic studies. Future strategies for assessing the contribution of MMP-2 may require the use of an alternative approach. For example, the use of C57BL/6 prostate cancer tissue derived from the TRAMP or LADY model of prostate cancer progression would allow us to use immunocompetent MMP-2 null mice on a C57BL/6 background. However, we will first need to assess whether the murine prostate cancer would induce osteolytic or osteoblastic changes. These efforts will be the performed in future studies. Currently we are focused on focused on identifying how MMP-13 can protect against prostate tumor progression in the bone microenvironment using our animal model. We anticipate that the results of these studies will be published within the next 12 months.

Conclusions from Aim 1. Initially we set out to test whether individual host MMPs contributed to prostate tumor progression in bone using a unique animal model. Our results and preliminary findings

show that in some cases, individual MMPs can contribute (MMP-7 (MMP-2, tentatively)? while others can be protective (MMP-13), play more subtle roles (MMP-9) or not be involved (MMP-3). These findings illustrate the diverse roles MMPs play in the tumor-bone microenvironment and support the rationale for the development of specific or highly selective inhibitors. The data collected during this award highlights the individual roles that MMPs can play in the prostate tumor-bone microenvironment and provides a shortlist of MMPs (MMP-7 and MMP-9) that could be therapeutically targeted for the treatment of prostate to bone metastases.

Aim 2. *Identify and test MMP processed substrates that mediate prostate tumor induced osteolytic and osteoblastic change.*

a) Identify and test candidate MMP substrates that mediate prostate tumor induced osteolytic and osteoblastic change.
b) Determine the contribution of MMP solubilized RANKL vs. MMP resistant RANKL in mediating osteoclastogenesis

In aim 2, we took a candidate approach in a bid to identify the potential factors that MMPs process in order to mediate tumor induced osteolysis. Bone is a rich reservoir of growth factors such as transforming growth factorβ (TGFβ) and insulin like growth factor-1 (IGF-1) and both of these factors have been implicated in driving the 'vicious cycle' (4). Given that various MMPs have been reported as processing the molecules that keep these growth factors in a latent state such as latency TGFβ binding proteins (LTBPs) and IGF binding proteins (IGF-BPs) we envisaged that these would be excellent candidate molecules through which MMPs could contribute to osteolytic and osteoblastic changes in the bone microenvironment.

MMP-2 is a key regulator of TGFβ bioavailability

In our initial studies, we examined the presence of active TGFβ using ELISA techniques. While we observed that there is more active TGFβ at the tumor bone interface in comparison to the tumor area alone, we found no difference in the levels of active TGFβ between wild type, MMP-7 and MMP-9 null animals (Figure 4). Given the labile nature of TGFβ we have taken multiple approaches into identifying the activity status of the cytokine in wild type and MMP null animals. Using procedures described by Barcellos-Hoff et al.(16), we generated frozen sections of non-decalcified bone using the Cryo-Jane Tape transfer system. The approach allowed us to visualize latent and active TGFβ and the effectors of TGFβ such as phospho SMAD2 in the tumor-bone microenvironment using microscopy (Figure 4).

In parallel studies, we localized the major cellular sources of the MMPs under investigation in human and murine tumor-bone microenvironments. Surprisingly, we identified that osteoblasts and osteocytes are major sources of MMP-2. In Specific aim 1, our initial studies revealed that host MMP-2 contributed to tumor progression in the bone microenvironment. Thus far we have not generated enough animals to test whether differences in the levels of active TGFβ exist between the wild type and MMP-2 null immunocompromized animals. Therefore, in order to test if osteoblast derived MMP-2 is regulating the bioavailability of TGFβ we isolated primary osteoblast cultures from immunocompetent MMP null animals and tested the ability of the MMP null osteoblasts to produce active TGFβ *in vitro*. Our initial experiments have provided exciting results. We have identified that osteoblast derived MMP-2 plays a major role in facilitating

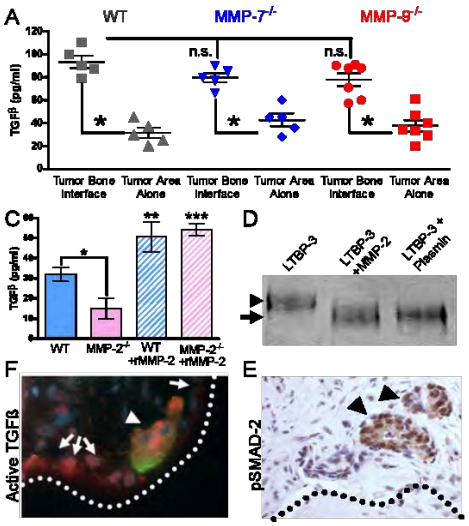

Fig. 4. TGFβ activation in the tumor bone microenvironment. **A:** The levels of TGFβ in lysates of the calvarial prostate tumor-bone interface and tumor area alone were measured by ELISA in WT and MMP-7, MMP-9 null mice. Asterisk denotes statistical significance ($p<0.05$). n.s. denotes non-significance. **C:** ELISA of active TGFβ in WT and MMP-2 null conditioned media (CM) derived from primary osteoblasts (n≥4 primary cultures per group). Samples were normalized for total protein. Recombinant MMP-2 (rMMP-2; 20ng/ml for 3 hours at 37°C) was also added to osteoblast CM and TGFβ activation was assessed. Asterisk denotes $p<0.05$. ANOVA analysis followed by a Tukey comparison of all conditions revealed that rMMP-2 addition enhanced TGFβ activation. Double asterisk denotes $p<0.01$, triple asterisk denotes $p<0.001$). **D:** WT osteoblast CM was incubated with 50ng of rMMP-2 overnight or 1μg of plasmin. Western blot analysis for LTBP-3 shows processing of full length LTBP-3 (arrow head) to a lower molecular weight form (arrow) presumably resulting in the activation of TGFβ. **E:** Immunofluorescent detection of active TGFβ at the tumor bone interface (red; arrows) in frozen sections. Dashed line indicates tumor bone interface while arrow head indicates TRAcP positive (green) multinucleated (DAPI;blue) mature osteoclasts. **F:** pSMAD-2 (arrow head; brown), a down stream effector of TGFβ signaling, was detected in cancer cells proximal to the tumor bone interface.

TGFβ activation and for first time have shown that LTBP-3 which is predominantly expressed in the skeleton is a major player in this process. In our preliminary observations, we have found that osteoblast derived MMP-2 contributes to tumor progression in the bone microenvironment and that the regulation of TGFβ bioavailability is the major molecular mechanism underlying this phenomenon (Figure 4). We are currently repeating these experiments using our animal model system but are also using other models in order to test the role of osteoblast derived MMP-2 in tumor progression in the bone microenvironment. We anticipate that the findings of these studies will be published within the next 6 months.

PTHrP is a novel MMP substrate

In the metastatic bone:tumor microenvironment, parathyroid related hormone (PTHrP) has been identified as a powerful mediator of osteolysis (17). Pro-PTHrP has three isoforms that are 139, 141 or 173 amino acids in length. These isoforms are subsequently enzymatically processed to yield the mature form of $PTHrP_{1-36}$ (amino acids 1-36). Thus far the enzymes implicated in generating mature PTHrP have been; endothelin converting enzyme-1 (ECE-1); ECE-2 and neprilysin which are not MMPs but are members of the metazincin family of proteinases. Interestingly, prostate specific antigen (PSA) which is a serine protease has also been shown to process PTHrP but in a different region that generates a 23 amino acid form of

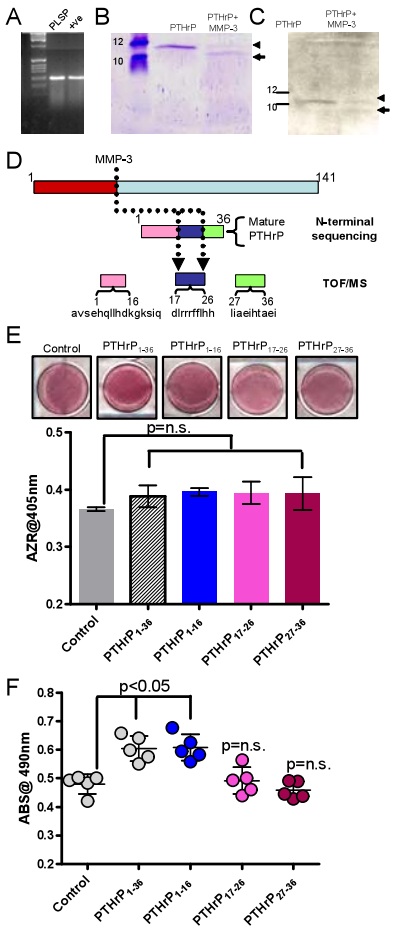

Fig. 5. PTHrP is an MMP substrate. **A:** RT-PCR analysis of PTHrP expression by the prostate cancer tissue (PLSP). +ve refers to positive control. **B:** Mature PTHrP (100ng; arrow head) was incubated for 1 hour at 37°C either alone or with 100ng of active MMP-3. Arrow indicates cleavage product. Markers are in kDa. **C:** Immunoblot analysis also demonstrates PTHrP processing using an antibody directed to the C-terminus (Santa Cruz; sc-20728). **D:** N-terminal amino acid sequencing revealed that MMP-3 generated $PTHrP_{1-36}$. **F.** MALDITOF-MS showed that MMP-3 was capable of further processing of $PTHrP_{1-36}$. Similar analyses revealed no degradation of full length PTHrP in the absence of MMPs. **E-F:** MC3T3-E1 (10^5 cells per 6 well in triplicate) were incubated with 50nM $PTHrP_{1-36}$ or equimolar concentrations of PTHrP fragments corresponding to MMP-3 products. No difference in mineralization was determined by day 21 using alizarin red and spectrophotometry (E). However, treatment with $PTHrP_{1-16}$ significantly stimulated MC3T3 cell growth as assessed by MTT assay (F).

$PTHrP_{1-23}$ (18). This is thought to abolish the activity of the hormone but some studies suggest that smaller molecular weight versions of PTHrP can have differential effects compared to $PTHrP_{1-36}$ (19).

Since PTHrP can be processed by members of the metazincin family and given the presence of MMPs in the tumor bone microenvironment, we asked whether MMPs could process PTHrP. Using recombinant $PTHrP_{1-141}$, we observed that MMP-3 and MMP-7 generate mature $PTHrP_{1-36}$ (Figure 5). Further examination by mass spectroscopy revealed that MMP-3 and MMP-7 further processed $PTHrP_{1-36}$ into smaller fragments, namely $PTHrP_{1-16}$, $PTHrP_{17-26}$ and $PTHrP_{27-34}$. A number of the MMP generated PTHrP products have reported cellular functions. For example, $PTHrP_{1-16}$ has sequence similarities to endothelin-1 (ET-1). ET-1 has been identified as a major factor involved in promoting osteoblastic responses via the ET_A receptor (20). $PTHrP_{1-16}$ has been shown to bind to ET_A in cardiomyocytes but apparently has no impact on ET_A signaling when overexpressed in CHO cells (21, 22). However, the precise role of $PTHrP_{1-16}$ in osteoblast function is unclear. Other MMP-3 generated fragments such as $PTHrP_{27-36}$ can mediate protein kinase C signaling via the PTHR-1 receptor (23) but again, the precise role of this fragment in addition to $PTHrP_{17-26}$ in osteoblast function remain unclear. Our initial experiments identified that the MMP generated fragments can impact the behavior of the osteoblasts with respect to growth but it does not appear that the fragments impact osteoblast differentiation and invasion. We are currently further assessing the in vitro and in vivo relevance of the MMP generated PTHrP products and they will be the focus of future studies.

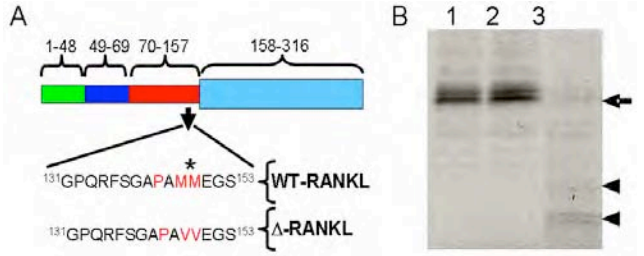

Fig. 6. A: MMP-7 processes RANKL in the juxtamembrane region at amino acid position 142 (see figure 10 for additional information). To generate a non-cleavable mutant RANKL, the methionines at positions 142 and 143 in addition to the proline at position 140 were mutated by single nucleotide substitution using a site directed mutagenesis kit (Stratagene). Methionine to Valine (ATG to GTG) and Proline to Leucine (CCA to CTA) **B:** Wild type and Δ-RANKL full length cDNAs were in vitro translated using the Promega TnT *in vitro* translation system with S^{35} labeled methionine. **1:** Δ-RANKL alone. **2-3:** Δ-RANKL(2) or wild type RANKL(3) incubated with 100ng of MMP-7 overnight at 37°C. Arrow indicates full length unglycosylated Δ-RANKL at approx 40kDa. Arrow heads denote cleavage products.

MMPs generate an active soluble form of RANKL.

We have previously demonstrated that membrane bound receptor activator of nuclear κ B ligand (RANKL) which is essential for osteoclast maturation and activation is sensitive to shedding from the cell

surface by MMP-3 and MMP-7 (24) and have found that the mechanism is not only relevant in the prostate tumor-bone microenvironment but also in the breast (25). Experiments in this study have resulted in the generation of non-cleavable of RANKL and future studies are focused on testing the ability of the non-cleaved RANKL to stimulate osteoclast activation via direct cell:cell contact and generating knock in animals (Figure 6).

Conclusions from Aim 2

Using a candidate approach we have found that MMPs that are highly expressed in the tumor-bone microenvironment (MMP-2, -3, -7) can process the factors that drive the vicious cycle. MMPs have primarily been considered as playing important roles in matrix degradation and while this may be true, clearly they are also playing key roles in regulating the availability and bioactivity of key factors such as PTHrP, RANKL and TGFβ. These discoveries are innovative and will be the focus of my group's research efforts at the Moffitt Cancer Center, Tampa, FL.

Key Research Accomplishments……..

- Generated RAG-2;MMP-2, RAG-2;MMP3, RAG-2;MMP-13 null animals
- Identified osteoclasts as a major source of MMP-9 in the human and murine prostate tumor-bone microenvironments
- Demonstrated that host derived MMP-9 does not contribute to tumor progression in the bone but does impact angiogenesis
- Determined that host MMP-13 plays a protective role in preventing tumor induced osteolytic and osteoblastic changes
- Identified in preliminary studies that host MMP-2 contributes to tumor progression in the bone microenvironment.
- Identified higher levels of TGFβ at the tumor bone interface in comparison to the tumor area alone in wild type animals

- Identified that osteoblast derived MMP-2 is a major regulator of TGFβ bioavailability
- Identified that MMP-3 and MMP-7 are capable of generating mature PTHrP
- Identified that MMP generated PTHrP fragments impact osteoblast behavior
- Generated a non-cleavable version of RANKL

Reportable Outcomes……

Manuscripts (Appended)

1) Lynch CC. (2011) MMPs as master regulators of the vicious cycle of bone metastasis. Bone. 48: 44-53
2) Bruni-Cardoso A, Johnson LC, Peterson TE, Vessella RL and **Lynch CC**. (2010). Osteoclast MMP-9 directly affects angiogenesis in the prostate tumor-bone microenvironment. Mol. Cancer Res. 8 (4): 459-70.
3) Fowler JA, Mundy, GR, Lwin ST, **Lynch CC** and Edwards CM (2009). A murine model of myeloma that allows genetic manipulation of the host microenvironment. Disease Models and Mechanisms. Nov-Dec;2(11-12):604-11. PMCID: PMC2776114
4) Thiolloy S, Halpern JL, Holt GE, Schwartz HE, Mundy GR, Matrisian LM and **Lynch CC**. (2009). Host derived MMP-7, but not MMP-9 impacts mammary tumor induced osteolysis. Cancer Res. August 15, 69:6747-55.

Book Chapters

1) Lynch CC and Matrisian LM (2008). Matrix metalloproteinases as key regulators of tumor-bone interaction. The Cancer Degradome, Proteases and Cancer Biology. Edwards DR, Hoyer-Hansen G, Blasi F and Sloane BF (Eds). Springer, NY. Chapter 27, p541-566
2) Mundy GR, Edwards CM, Edwards JR, Lynch CC, Sterling JA and Zhuang J. (2008). Localized Osteolysis. Principals of Bone Biology. (3rd Edition) Biezikian J, Craig Z, Martin TJ (Eds) Academic Press, Inc., San Diego, CA. Chapter 64, p1391-1413.

3) Fingleton B and Lynch CC (2009). Cancer in context: The importance of the tumor microenvironment. Cell-Extracellular Matrix Interactions in Cancer. Zent R and Pozzi A (Eds). Springer, NT, Chapter 3, p75-100.

Presentations

DOD ImPaCt, Orlando, FL, 2011.

Tumor Microenvironment Steering Committee Meeting, Nashville, TN, 2009.

Cancer And Bone Society, Arlington, VA. October, 2009.

Gordon Research Conference-Matrix Metalloproteinases, Les Dialebtres, Switzerland, August 2009.

Growth Factor and Signaling Symposium, Ames, Iowa, September, 2008

Joint AACR and Metastasis Research Society Meeting, Vancouver, BC, Canada, August, 2008

Tumor host interaction and angiogenesis meeting, Monte Verita, Ascona, Switzerland, October 2007.

Tumor microenvironment (TMEN) meeting, Vanderbilt University, Nashville, TN, September, 2007.

Grants

NCI-(1RO1CA143094-01A1). 01-JUL-10-30-JUN-15.

Role: Principal Investigator.

Title: Host MMP-mediated regulation of the vicious cycle of prostate to bone metastases

Overall Conclusions……

Our results have shown that individual MMPs can have differential effects in the tumor-bone microenvironment. Previously, MMP inhibitors failed in the clinical setting, primarily due to a lack of understanding as to how MMPs contribute to tumor progression. In animals models of osteolysis, broad spectrum MMP inhibitors have been successful in preventing tumor induced osteolysis and growth (26-28). Therefore, in order to apply MMP inhibitors in the clinical setting, our results suggest that the selective targeting of MMP-2, MMP-7 and MMP-9 while sparing the activity of other

metalloproteinase family members such as MMP-13 would be of benefit for the treatment of prostate to bone metastases. Finally, as a new investigator award mechanism, this grant from the DOD has been essential in allowing me to become an independent and established investigator. Based on my results acquired from this application, I have been successfully obtained funding from the NIH (1RO1CA143094-01A1) and have taken a new position at the Moffitt Cancer Center, Tampa. FL. Therefore, I am extremely grateful for the DOD in allowing me this opportunity to kick start my career in identifying cures for prostate to bone metastases.

References……

1. www.cancer.org. Cancer Facts and Figures. American Cancer Society 2008.
2. Bubendorf L, Schopfer A, Wagner U, et al. Metastatic patterns of prostate cancer: an autopsy study of 1,589 patients. Human Pathology 2000; 31: 578-83.
3. Keller ET, Brown J. Prostate cancer bone metastases promote both osteolytic and osteoblastic activity. Journal of Cellular Biochemistry 2004; 91: 718-29.
4. Mundy GR. Metastasis to bone: causes, consequences and therapeutic opportunities. Nature Reviews Cancer 2002; 2: 584-93.
5. Lynch CC, Matrisian LM. Matrix metalloproteinases in tumor-host cell communication. Differentiation 2002; 70: 561-73.
6. Roudier MP, Morrissey C, True LD, Higano CS, Vessella RL, Ott SM. Histopathological assessment of prostate cancer bone osteoblastic metastases. J Urol 2008; 180: 1154-60.
7. Roudier MP, Vesselle H, True LD, et al. Bone histology at autopsy and matched bone scintigraphy findings in patients with hormone refractory prostate cancer: the effect of bisphosphonate therapy on bone scintigraphy results. Clin Exp Metastasis 2003; 20: 171-80.
8. Bergers G, Brekken R, McMahon G, et al. Matrix metalloproteinase-9 triggers the angiogenic switch during carcinogenesis. Nature Cell Biology 2000; 2: 737-44.

9. Coleman RE, Guise TA, Lipton A, et al. Advancing treatment for metastatic bone cancer: consensus recommendations from the Second Cambridge Conference. Clin Cancer Res 2008; 14: 6387-95.

10. Cackowski FC, Roodman GD. Perspective on the osteoclast: an angiogenic cell? Ann N Y Acad Sci 2007; 1117: 12-25.

11. Bruni-Cardoso A, Johnson LC, Vessella RL, Peterson TE, Lynch CC. Osteoclast-Derived Matrix Metalloproteinase-9 Directly Affects Angiogenesis in the Prostate Tumor-Bone Microenvironment. Mol Cancer Res 2010.

12. Inada M, Wang Y, Byrne MH, et al. Critical roles for collagenase-3 (Mmp13) in development of growth plate cartilage and in endochondral ossification. Proceedings of the National Academy of Sciences of the United States of America 2004; 101: 17192-7.

13. Stickens D, Behonick DJ, Ortega N, et al. Altered endochondral bone development in matrix metalloproteinase 13-deficient mice 2. Development 2004; 131: 5883-95.

14. Balbin M, Fueyo A, Tester AM, et al. Loss of collagenase-2 confers increased skin tumor susceptibility to male mice. Nat Genet 2003; 35: 252-7.

15. McCawley LJ, Crawford HC, King LE, Jr., Mudgett J, Matrisian LM. A protective role for matrix metalloproteinase-3 in squamous cell carcinoma. Cancer Res 2004; 64: 6965-72.

16. Barcellos-Hoff MH, Derynck R, Tsang ML, Weatherbee JA. Transforming growth factor-beta activation in irradiated murine mammary gland. J Clin Invest 1994; 93: 892-9.

17. Guise TA. Molecular mechanisms of osteolytic bone metastases. Cancer 2000; 88: 2892-8.

18. Cramer SD, Chen Z, Peehl DM. Prostate specific antigen cleaves parathyroid hormone-related protein in the PTH-like domain: inactivation of PTHrP-stimulated cAMP accumulation in mouse osteoblasts. J Urol 1996; 156: 526-31.

19. Ruchon AF, Marcinkiewicz M, Ellefsen K, et al. Cellular localization of neprilysin in mouse bone tissue and putative role in hydrolysis of osteogenic peptides. J Bone Miner Res 2000; 15: 1266-74.

20. Yin JJ, Mohammad KS, Kakonen SM, et al. A causal role for endothelin-1 in the pathogenesis of osteoblastic bone metastases. Proc Natl Acad Sci U S A 2003; 100: 10954-9.

21. Langlois C, Letourneau M, Turcotte K, Detheux M, Fournier A. PTHrP fragments 1-16 and 1-23 do not bind to either the ETA or the ETB endothelin receptors. Peptides 2005; 26: 1436-40.

22. Schluter KD, Katzer C, Piper HM. A N-terminal PTHrP peptide fragment void of a PTH/PTHrP-receptor binding domain activates cardiac ET(A) receptors. Br J Pharmacol 2001; 132: 427-32.

23. Miao D, Tong XK, Chan GK, Panda D, McPherson PS, Goltzman D. Parathyroid hormone-related peptide stimulates osteogenic cell proliferation through protein kinase C activation of the Ras/mitogen-activated protein kinase signaling pathway. J Biol Chem 2001; 276: 32204-13.

24. Lynch CC, Hikosaka A, Acuff HB, et al. MMP-7 promotes prostate cancer-induced osteolysis via the solubilization of RANKL 1. Cancer Cell 2005; 7: 485-96.

25. Thiolloy S, Halpern J, Holt GE, et al. Osteoclast-derived matrix metalloproteinase-7, but not matrix metalloproteinase-9, contributes to tumor-induced osteolysis. Cancer Res 2009; 69: 6747-55.

26. Lee J, Weber M, Mejia S, Bone E, Watson P, Orr W. A matrix metalloproteinase inhibitor, batimastat, retards the development of osteolytic bone metastases by MDA-MB-231 human breast cancer cells in Balb C nu/nu mice. European Journal of Cancer 2001; 37: 106-13.

27. Winding B, NicAmhlaoibh R, Misander H, et al. Synthetic matrix metalloproteinase inhibitors inhibit growth of established breast cancer osteolytic lesions and prolong survival in mice. Clinical Cancer Research 2002; 8: 1932-9.

28. Nemeth JA, Yousif R, Herzog M, et al. Matrix metalloproteinase activity, bone matrix turnover, and tumor cell proliferation in prostate cancer bone metastasis. Journal National Cancer Institute 2002; 94: 17-25.

APPENDED PUBLICATIONS

Published OnlineFirst March 23, 2010; DOI:10.1158/1541-7786.MCR-09-0445

Molecular Cancer Research

Osteoclast-Derived Matrix Metalloproteinase-9 Directly Affects Angiogenesis in the Prostate Tumor –Bone Microenvironment

Alexandre Bruni-Cardoso, Lindsay C. Johnson, Robert L. Vessella, et al.

Mol Cancer Res 2010;8:459-470. Published OnlineFirst March 23, 2010.

Published OnlineFirst March 23, 2010; DOI:10.1158/1541-7786.MCR-09-0445

Molecular Cancer Research

Osteoclast-Derived Matrix Metalloproteinase-9 Directly Affects Angiogenesis in the Prostate Tumor–Bone Microenvironment

Alexandre Bruni-Cardoso[1], Lindsay C. Johnson[2], Robert L. Vessella[4], Todd E. Peterson[2], and Conor C. Lynch[3]

Abstract

In human prostate to bone metastases and in a novel rodent model that recapitulates prostate tumor–induced osteolytic and osteogenic responses, we found that osteoclasts are a major source of the proteinase, matrix metalloproteinase (MMP)-9. Because MMPs are important mediators of tumor-host communication, we tested the effect of host-derived MMP-9 on prostate tumor progression in the bone. To this end, immunocompromised mice that were wild-type or null for MMP-9 received transplants of osteolytic/osteogenic-inducing prostate adenocarcinoma tumor tissue to the calvaria. Surprisingly, we found that that host MMP-9 significantly contributed to prostate tumor growth without affecting prostate tumor–induced osteolytic or osteogenic change as determined by microcomputed tomography, microsingle-photon emission computed tomography, and histomorphometry. Subsequent studies aimed at delineating the mechanism of MMP-9 action on tumor growth focused on angiogenesis because MMP-9 and osteoclasts have been implicated in this process. We observed (*a*) significantly fewer and smaller blood vessels in the MMP-9 null group by CD-31 immunohistochemistry; (*b*) MMP-9 null osteoclasts had significantly lower levels of bioavailable vascular endothelial growth factor-A_{164}; and (*c*) using an aorta sprouting assay, conditioned media derived from wild-type osteoclasts was significantly more angiogenic than conditioned media derived from MMP-9 null osteoclasts. In conclusion, these studies show that osteoclast-derived MMP-9 affects prostate tumor growth in the bone microenvironment by contributing to angiogenesis without altering prostate tumor–induced osteolytic or osteogenic changes. *Mol Cancer Res; 8(4); 459–70. ©2010 AACR.*

Introduction

Prostate to bone metastases induce mixed lesions containing areas of extensive bone destruction (osteolysis) and formation (osteogenesis) that are mitigated by the principal cells of the bone, osteoclasts and osteoblasts, respectively (1). The highjacking of the normal bone remodeling process by the metastatic prostate cancer cells results in an increase in growth factors and cytokines that subsequently can stimulate tumor growth, thus generating what has been called a "vicious cycle" (2). Therefore, understanding the molecular mechanisms that facilitate the interaction between the multiple cell types in the tumor-bone microenvironment can provide new targets for therapies that will be effective in controlling and/or curing prostate to bone metastases.

Matrix metalloproteinases (MMP) are a family of 23 enzymes that collectively are capable of processing extracellular matrix components including those that comprise the bone matrix (3). Given their role in bone matrix resorption, it is not surprising that osteoclasts express a large repertoire of MMPs. However, recent analyses have identified that osteoclast-derived MMPs can control cell behavior in the tumor microenvironment by regulating the bioavailability/bioactivity of nonmatrix-related molecules, for example, receptor activator of nuclear κB ligand and kit ligand (4, 5). Despite their role in bone matrix synthesis, osteoblasts also express several MMPs (6, 7). However, at this juncture, no studies about the effect of osteoblast-derived MMPs or MMPs derived from other cellular sources on osteoblast behavior in the pathologic context of bone metastasis have been documented.

In the tumor microenvironment, MMPs are often induced in the host compartment in response to the cancer cells (3, 8). In previous studies, roles for tumor derived

Authors' Affiliations: [1]Department of Cell Biology, State University of Campinas (UNICAMP), Campinas, Sao Paulo, Brazil; [2]VUIIS and [3]Department of Orthopaedics and Rehabilitation, Vanderbilt University, Nashville, Tennessee; and [4]Department of Urology, University of Washington, Seattle, Washington

Note: Supplementary data for this article are available at Molecular Cancer Research Online (http://mcr.aacrjournals.org/).

Corresponding Author: Conor C. Lynch, Department Of Orthopaedics and Rehabilitation, Vanderbilt University Medical Center East, South Tower, Suite 4200, Nashville, TN, 37232-8774. Phone: 615-343-5729. Fax: 615-343-1028. E-mail: conor.lynch@vanderbilt.edu

doi: 10.1158/1541-7786.MCR-09-0445

Published OnlineFirst March 23, 2010; DOI:10.1158/1541-7786.MCR-09-0445

MMPs in the prostate tumor–bone microenvironment have been described (9, 10). However, little is known about the contribution of host-derived MMPs to tumor growth or tumor-induced osteolytic/osteogenic changes. The analysis of MMP expression in human samples of prostate to bone metastasis and in an animal model that recapitulates the human clinical scenario of prostate tumor–induced osteolytic and osteogenic change (4) revealed that osteoclasts are a major source of MMP-9. In the current *in vivo* study, we addressed whether host-derived MMP-9 affects prostate tumor growth or prostate tumor–induced osteolytic or osteogenic changes. Although MMP-9 contributed to prostate tumor growth, we found that this observation was not due to an effect on tumor-induced osteolysis or osteogenic response. In pursuing the mechanism, we observed that osteoclast-derived MMP-9 could contribute to tumor growth by promoting angiogenesis in the tumor-bone microenvironment.

Materials and Methods

All experiments involving animals were conducted after review and approval by the office of animal welfare at Vanderbilt University. Double null immunocompromised recombinase activating gene-2 and MMP-9 mice (c57BL/6 background) were generated as previously described (11, 12). Rat prostate adenocarcinoma tissue was provided by Dr. Mitsuru Futakuchi, Nagoya Medical School, Nagoya, Japan (13). Human samples of prostate to bone metastasis were provided by Dr. Robert L. Vessella, University of Washington, Seattle, WA. All reagents were obtained from Sigma-Aldrich except where specified.

Surgical Procedure and Measurement of Tumor Growth

Six-week-old immunocompromised wild-type (WT; n = 9) and MMP-9 null (n = 9) mice were anesthetized, and using a pair of scissors, a small incision between the ears was made in the dermis of the scalp. The subcutaneous tissue was separated from the underlying calvaria using a blunt-ended scissors to form a pocket. To promote tumor-bone interaction, the periosteum was removed from the calvaria to expose the calvarial bone. Equal volumes of rat prostate adenocarcinoma tissue (0.1 mm^3) was inserted into the pocket, which was closed with wound clips. Tumor measurements with calipers (Fine Science Tools) were made on a weekly basis. The length, width, and height of the tumor were used to calculate the tumor volume. All animal studies were repeated on three independent occasions with similar sized groups.

In vivo Imaging of Tumor-Induced Osteolysis and Osteogenesis

To assess extent of tumor-induced osteolysis in three-dimensions, microcomputed tomography scanning (Siemens Preclinical) was used. Mice were imaged using X-ray tube settings of 80 kVp and 0.5 mA for 300 ms per projection, 360 projections at weeks 1, 2, and 3 posttumor transplantation. Data were reconstructed into three-dimensional images with voxel sizes of 0.1 × 0.1 × 0.1 mm.

With a different set of mice, microsingle-photon emission computed tomography (Micro-SPECT) imaging was also done to measure changes in bone formation at weeks 1, 2, and 3 posttumor transplantation. Each animal received 1 mCi of ^{99m}Technetium-Methylene DiPhosphonate through tail vein injection and 1.5 h later were subjected to micro-SPECT imaging on the NanoSPECT/CT system (Bioscan, Inc.). Subsequently, 24 projection views were acquired in a helical scan mode using a nine-pinhole (1.4 mm diameter) collimator on each of the four camera heads—a total of six scanner positions with 60-s acquisition per position. Tomographic images were reconstructed from the projection data using an ordered subsets expectation maximization algorithm provided with the scanner at an isotropic voxel size of 0.3 mm. To aid in interpretation of the micro-SPECT images, low-dose microcomputed tomography images were acquired along with each micro-SPECT image on the same scanner without moving the subject. X-ray tube settings were 45 kVp and 0.17 mA, and the data were reconstructed into images with 0.2 mm isotropic voxel size that were inherently registered with the micro-SPECT images based on the geometric calibration of the system.

For the quantitative analysis of bone formation and bone destruction in individual tumor-bearing WT and MMP-9 null animals over time, we took the following approach. The serial scans of individual animals at different time points were coregistered with each other, a process that was achievable due to the rigid structures of the skull such as the eye orbits and upper teeth staying constant over time. Using the Amira software (Visage Imaging), the images taken with micro-SPECT and microcomputed tomography were superimposed using an isosurface thresholding method, allowing for the visualization of the changes in the calvarial bone at each time point. Using a smaller region of interest in the registered images, bone volumes were determined by calculating the number of image voxels exceeding a chosen threshold. This threshold was kept constant from mouse to mouse allowing for comparative analysis. Individual micro-SPECT images were converted to percentage injected dose per gram body weight by dividing voxel values by the injected dose for that study, thus facilitating comparisons between animals. These radiotracer uptake ratios were used to normalize the data pertaining to bone formation between time points in individual animals and the animals in each group being studied.

Immunohistochemistry, Cytochemistry, and Histomorphometry

After sacrifice, rodent tissues were fixed overnight in 10% buffered formalin and decalcified for 3 wk in 14% EDTA at pH 7.4 at 4°C with changes every 48 to 72 h. Tissues were embedded in paraffin and 5-μm-thick sections were cut. Human prostate to bone metastasis samples (n = 10) were provided by Dr. Vessella. For MMP-9 and tartrate resistant acid phosphatase (TRAcP) localization,

Published OnlineFirst March 23, 2010; DOI:10.1158/1541-7786.MCR-09-0445

the following technique was used. Sections were rehydrated through a series of ethanols and then rinsed in TBST (10 mmol/L Tris at pH 7.4, 150 mmol/L NaCl) with 0.05% Tween 20. For antigen retrieval, slides were immersed in a 20-μg/mL solution of proteinase K (Sigma-Aldrich) according to the manufacturer's instructions for 10 min at room temperature. Following washing in TBS, tissue sections were blocked using standard blocking criteria for 1 h at room temperature. MMP-9 (Oncogene) antibodies at a dilution of 1:100 were added in blocking solution overnight at 4°C. Slides were washed extensively in TBST (TBS with 0.05% Tween-20) before the addition of a species-specific fluorescently labeled secondary antibody (Alexafluor 568 nm, Invitrogen) diluted 1:1,000 in blocking solution for 1 h at room temperature. Slides were washed in TBS and then equilibrated in an acetate buffer as described (14). The ELF97 TRAcP stain (Invitrogen) was diluted 1:1,000 in acetate buffer and slides were incubated for 15 min at room temperature. Following washing, slides were aqueously mounted in media (Biomeda Corp) containing 2 μmol/L 4′,6-diamidino-2-phenylindole for nuclear localization. Angiogenesis in the tumor microenvironment was assessed by CD-31 (BD Pharmingen) immunohistochemistry using a standard immunohistochemistry protocol as previously described (4).

For histomorphometry, at least three nonserial sections from multiple animals in each group were stained with H&E using standard protocols or TRAcP staining as described to assess osteoclast/osteoblast number per ×20 field at the tumor-bone interface using Metamorph. The extent of osteolysis was calculated in multiple sections from each animal using a "bone destruction index," which refers to the length of osteolysis per length of cranial bone beneath the transplanted tumors, and was determined using Metamorph. The chaotic and woven nature of pathologic bone was easily distinguished from the remaining laminar calvarial bone by H&E. The area of pathologic bone at the tumor-bone interface was calculated using Metamorph.

Osteoclastogenesis and Aortic Ring Assays

CD11b-positive myeloid precursors were isolated from the bone marrow of 6-wk-old immunocompromised mice that were WT or null for MMP-9 using the MACS separation system as per manufacturer's instructions (Miltyni Biotec). After isolation, 1×10^6 myeloid cells/osteoclast precursors were resuspended in 1 mL of αMEM medium containing 10% FCS seeded into each well of a 48-well plate. The following day, WT and MMP-9 null groups were treated with osteoclast differentiation factors, 75 ng/mL recombinant receptor activator of nuclear κB ligand (R&D systems), and 25 ng/mL of macrophage colony–stimulating factor (R&D Systems). A separate group of WT and MMP-9 null cultures (n = 6 per group) were treated with 100 ng/mL recombinant active MMP-9 (Calbiochem). Osteoclast differentiation medium with or without MMP-9 was changed every 48 h. After 10 d of culture, cells were fixed with ice-cold methanol for 5 min, rinsed in 1xPBS, and then subjected to colorimetric staining for the osteoclast marker, TRAcP, as per manufacturer's instructions (Sigma-Aldrich). For the collection of conditioned media, the same procedure was used with the exception that on day 10, groups subjected to media alone or osteoclast differentiation media were carefully rinsed with 1xPBS. Serum-free αMEM (200 μL) was added to each well and the medium was allowed to condition for 24 h. Levels of vascular endothelial growth factor (VEGF)-A were quantitated by ELISA as per manufacturer's instructions (R&D Systems).

Aortic ring assays were done as described (15). After isolation and embedding of WT aortic rings in-type I collagen, the explants were treated with 2.5% mouse serum/αMEM including 20% conditioned media derived from WT or MMP-9 null osteoclast cultures or 10 ng/mL of VEGF-A_{164} (R&D Systems) as a positive control. The medium was changed daily for 9 d. Photomicrographs were also recorded on a daily basis and the distance of sprout outgrowth was determined by Metamorph.

Statistical Analysis

For *in vivo* data, statistical analysis was done using ANOVA and Bonferroni multiple comparison tests. A value of $P < 0.05$ was considered significant. Data are presented as mean ± SD.

Results

MMP-9 Is Primarily Localized to Osteoclasts in the Prostate Tumor–Bone Microenvironment

Previously, we identified that several MMPs including MMP-9 were highly expressed in the prostate tumor–bone microenvironment (4).[5] Because changes in MMP expression at the level of gene transcription often are not reflected at the level of the translated protein product, we addressed whether MMP-9 protein was detectable in the prostate tumor–bone microenvironment and what the cellular source of MMP-9 was. Our results indicate that MMP-9 was localized to the stromal compartment of the human (n = 10) and rodent (n = 25) prostate tumor–bone microenvironment, whereas the prostate cancer cells were largely negative (Supplementary Figs. S1 and S2; Fig. 1A-D). Analysis of ×40 photomicrographs (n = 10) of the rodent tumor–bone microenvironment revealed that 7.3% of the cell total (as assessed by counting 4′,6- diamidino-2-phenylindole–stained nuclei) was positive for MMP-9 by immunofluorescence. Using multinuclearity and TRAcP as markers for mature osteoclasts, we determined that within the population of MMP-9–positive cells, 58.7% (4.26% ± 1.99% SD) were osteoclasts. These results show that osteoclasts are a major source of MMP-9 in the tumor-bone microenvironment and are in keeping with our studies examining the localization of MMP-9 in human and murine breast/mammary osteolytic tumor–bone microenvironments (16).

[5] M. Futakuchi, unpublished observations.

Published OnlineFirst March 23, 2010; DOI:10.1158/1541-7786.MCR-09-0445

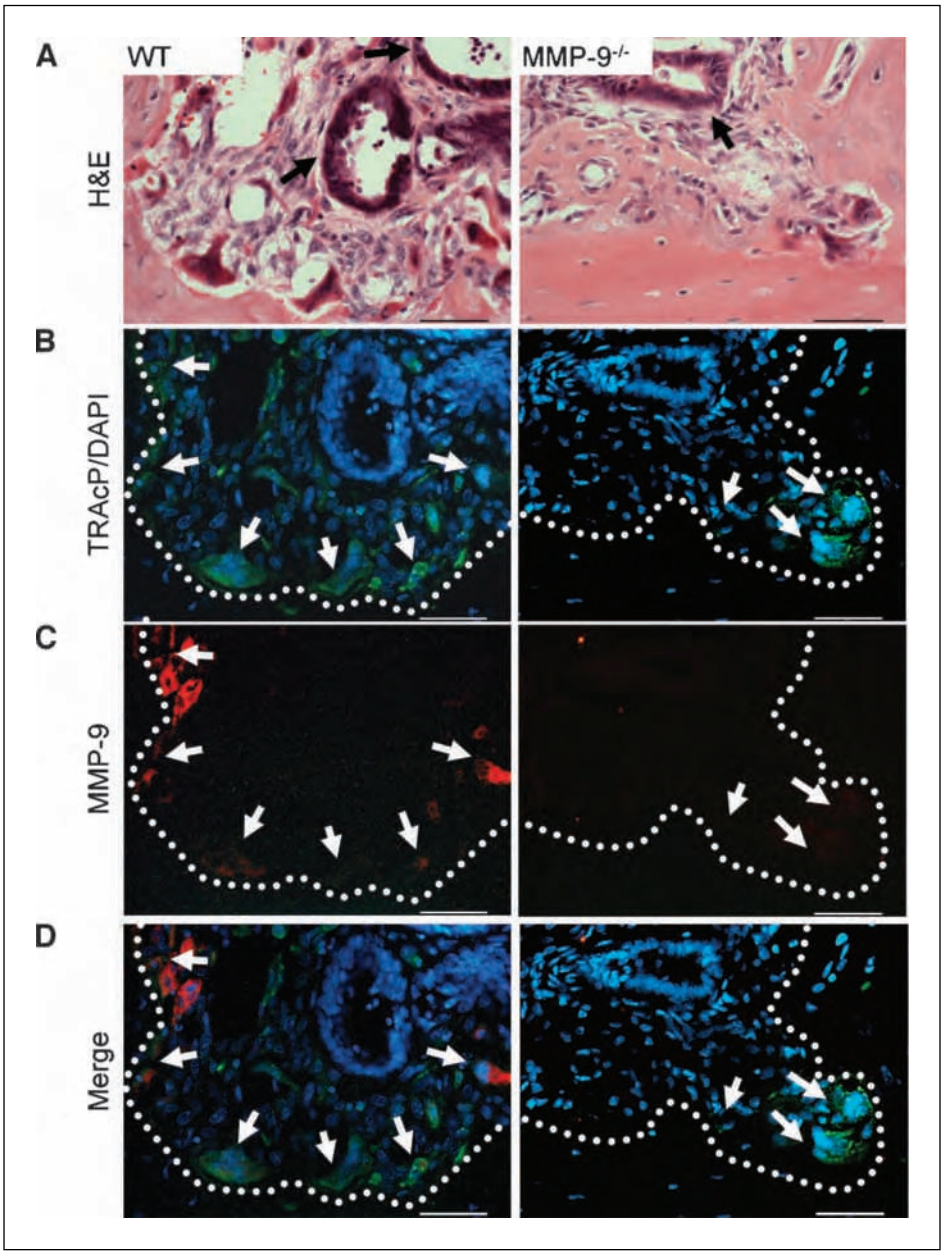

FIGURE 1. MMP-9 is largely localized to osteoclasts in the prostate tumor–bone microenvironment. The calvarias of 6-wk-old immunocompromised WT and MMP-9 null mice were transplanted with equal volumes of rat prostate adenocarcinoma tissue as described in Materials and Methods. A, representative photomicrograph of the rat prostate tumor–bone microenvironment in WT and MMP-9 null (MMP-9$^{-/-}$) mice. Arrows, rat prostate adenocarcinoma. B to D, fluorescent TRAcP staining (green) was used to localize osteoclasts (arrows; B), whereas immunofluorescence was used to localize MMP-9 (red; C). 4′,6-Diamidino-2-phenylindole (blue) was used as a nuclear stain. D, merged image. Dashed line, tumor-bone interface. Scale bars, 50 μm.

Host MMP-9 Promotes Tumor Growth in the Bone Microenvironment

Because osteoclasts are primarily responsible for bone resorption, we next determined whether the ablation of host MMP-9 would affect prostate tumor progression in a bone microenvironment. To this end, equal volumes of rat prostate adenocarcinoma tissue were transplanted to the calvaria of immunocompromised 6-week-old mice that were either WT (n = 9 per time point) or null for MMP-9 (n = 9 per time point). Tumor volumes were measured on a weekly basis for 3 weeks using calipers. Our results show that the tumor volume in the WT animals was significantly higher compared with the MMP-9 null animals at the week 3 time point [1,746 ± 250.2 mm^3 (WT) versus 1,262 ± 207.6 (MMP-9$^{-/-}$) mm^3; $P < 0.05$; Fig. 2], suggesting that host-derived MMP-9 contributes to prostate tumor growth in the bone microenvironment. This effect was consistently observed in three independently repeated experiments.

Host MMP-9 Does Not Affect Prostate Tumor–Induced Osteolysis

Next, we determined the effect of host MMP-9 on prostate tumor–induced osteolysis because we observed that osteoclasts are a major source of MMP-9 in the prostate tumor–bone microenvironment; the concept of the vicious

Published OnlineFirst March 23, 2010; DOI:10.1158/1541-7786.MCR-09-0445

cycle dictates that osteoclast-mediated bone resorption is critical for tumor growth (2); and MMP-9 null mice have been shown to have a delay in osteoclast recruitment to centers of ossification during bone development (17, 18). Using *in vivo* microcomputer tomography imaging, prostate tumor–induced osteolysis was imaged over a 3-week time period and segmentation analysis using the Amira software allowed for the quantitation of osteolysis. The results from three independent experiments with small numbers of animals in each group (n = 3) revealed the presence of more bone in the MMP-9 null animals at the week 3 time point, i.e., less osteolysis, but this difference was not statistically significant [5,617 ± 208.2 mm^3 (WT) versus 7,057 ± 1,443 mm^3 (MMP-$9^{-/-}$); $P > 0.05$; Fig. 3A].

Histomorphometry analysis of the bone destruction index at the week 3 time point also revealed no difference in the extent of osteolysis between the WT (n = 9) and MMP-9 null (n = 9) groups [0.4398 ± 0.1331 (WT) versus 0.34833 ± 0.0752 (MMP-$9^{-/-}$) bone destruction index; $P > 0.05$; Fig. 3B]. Furthermore, no difference in the number of multinucleated TRAcP-positive osteoclasts was observed between the WT and MMP-9 null groups [5.67 ± 2.236 (WT) versus, 8.02 ± 2.693 osteoclasts per ×20 field (MMP-$9^{-/-}$); $P > 0.05$; Fig. 3C]. Taken together, these *in vivo* and histologic analyses show that host MMP-9 does not contribute to prostate tumor–induced osteolysis.

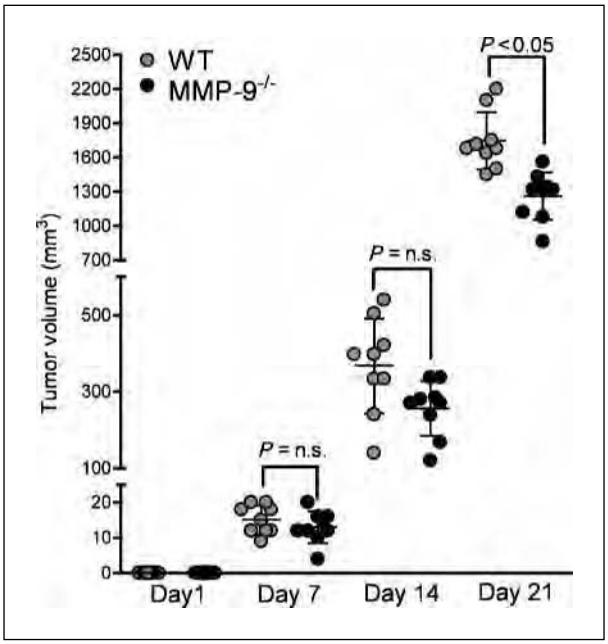

FIGURE 2. Host-derived MMP-9 promotes prostate tumor growth in the bone microenvironment. Tumor volume was recorded on a weekly basis after the transplantation of the rat prostate tumor tissue to WT (n = 9) and MMP-9 null (MMP-$9^{-/-}$; n = 9) calvarias. N.s., nonsignificant ($P > 0.05$) P values.

Host MMP-9 Does Not Affect Prostate Tumor–Induced Osteogenic Response

Our data show that osteoblasts are not a major source of MMP-9 in the *in vivo* tumor-bone microenvironment (Fig. 1). However, given the interdependency between osteoblasts and osteoclasts with respect to the bone remodeling process, we next determined whether the ablation of host MMP-9 could affect prostate tumor–induced osteogenic changes

Before and at weekly intervals after transplantation of the prostate tumor tissue, WT and MMP-9 null mice were injected with ^{99m}TC-MDP, which selectively concentrates in areas of active bone remodeling (19). Using *in vivo* micro-SPECT imaging, the osteogenic responses were measured in individual animals in each group over time and whereas lower values were obtained in the MMP-9 null group compared with WT control, these differences did not reach statistical significance [$2.9 \times 10^{-5} \pm 1.5 \times 10^{-5}$ (WT) versus $1.9 \times 10^{-5} \pm 0.94 \times 10^{-5}$ (MMP-$9^{-/-}$) micro-SPECT activity ratio; $P > 0.05$; Fig. 4A]. Similarly, histomorphometry examining the extent of pathologic bone formation, which was discerned by H&E staining (Fig. 4B) of multiple sections from multiple animals (n = 9 per group), revealed no differences in prostate tumor–induced osteogenesis [$5.4 \times 10^4 \pm 2.3 \times 10^4$ μm^2 (WT) versus $5.4 \times 10^4 \pm 2.4 \times 10^4$ μm^2 (MMP-$9^{-/-}$); $P > 0.05$; Fig. 4C]. Furthermore, the number of osteoblasts rimming the pathologic bone also showed no difference between the WT and MMP-9 null mice [83.9 ± 28.9 (WT) versus 126.3 ± 21.23 (MMP-$9^{-/-}$) osteoblasts per ×20 field; $P > 0.05$; Fig. 4D]. Collectively, these data show that host MMP-9 does not affect prostate tumor–induced osteogenic change.

Host MMP-9 Contributes to Angiogenesis in the Prostate Tumor–Bone Microenvironment

Our studies indicate that host MMP-9 contributed to tumor growth. But it seemed that this observation was independent of prostate tumor–induced osteolytic and osteogenic change because neither were significantly attenuated in the MMP-9 null mice compared with the WT controls. Several studies have shown that osteoclasts are important mediators of angiogenesis (17, 20), whereas MMP-9 has been identified as playing a key role in regulating the bioavailability of the angiogenic factor VEGF-A_{164} in the developing bone and in various tumor microenvironments (18, 21). Therefore, we next examined whether differences in angiogenesis existed within the WT and MMP-9 null prostate tumor–bone microenvironments.

Immunohistochemical staining for CD-31, a widely used marker for tumor vasculature (Fig. 5A), revealed a significantly lower number of blood vessels in the prostate tumor–bone microenvironment of the MMP-9 null mice (n = 17) compared with the WT (n = 25) controls [4.5 ± 0.91 (WT) versus 2.94 ± 1.14 (MMP-$9^{-/-}$) CD-31–positive blood vessels per ×20 field; $P < 0.05$; Fig. 5B]. Furthermore, we observed that the diameter of the blood vessels within each tissue section was also significantly

Published OnlineFirst March 23, 2010; DOI:10.1158/1541-7786.MCR-09-0445

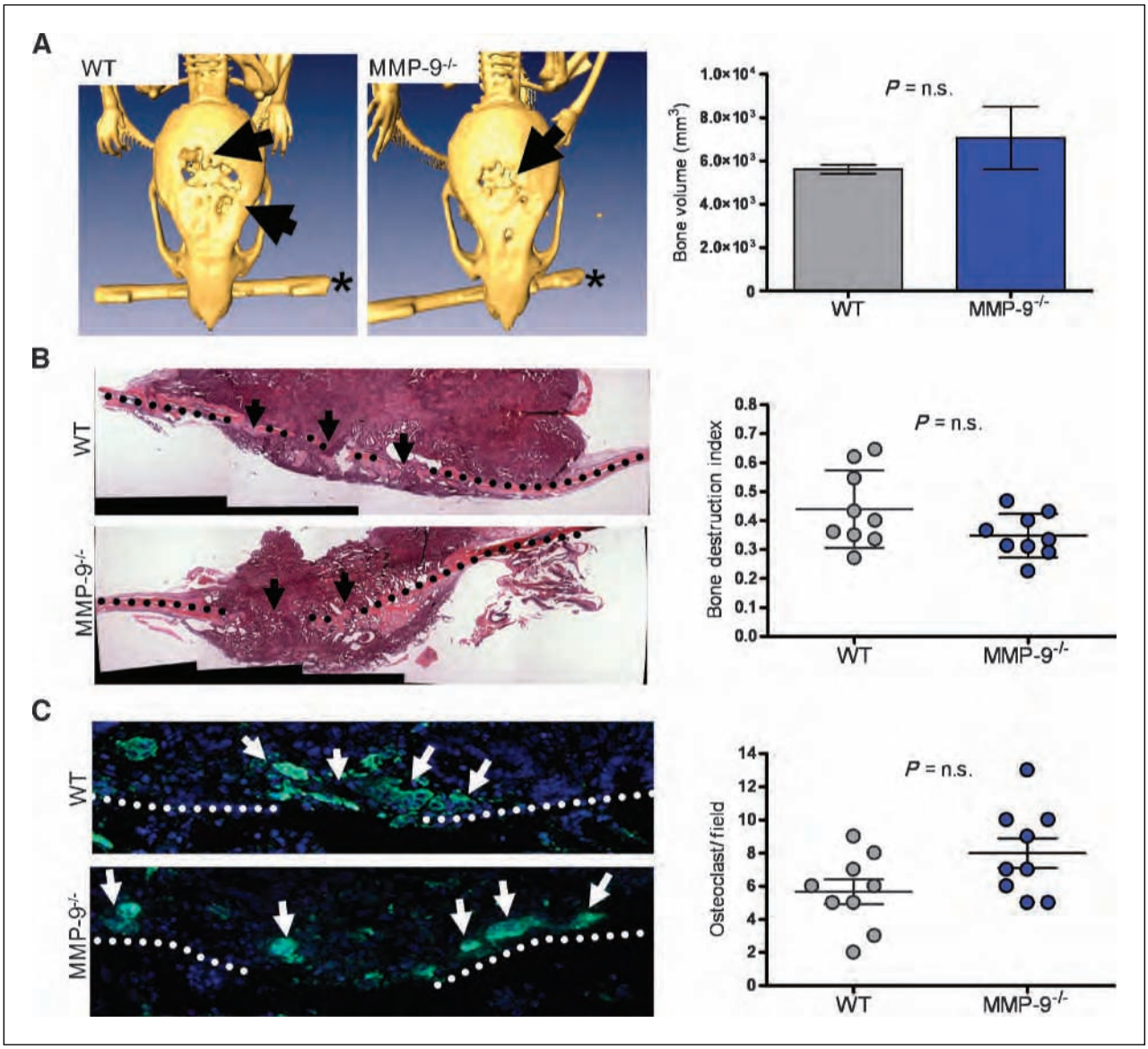

FIGURE 3. Host-derived MMP-9 does not affect prostate tumor–induced bone destruction in WT and MMP-9$^{-/-}$ tumor-bearing animals. A, representative *in vivo* microcomputed tomography images of the extent of bone destruction (arrow) induced by the rat prostate tumor in the calvaria of WT (n = 3) and MMP-9$^{-/-}$ (n = 3) animals at the 3-wk time point. *, stabilization bar used to prevent movement of skull during imaging. Segmentation analysis of the reconstructed three-dimensional images was used to calculate the bone volume. B, representative montage of H&E photomicrographs derived from WT and MMP-9 null tumor-bearing mice at 3 wk. Arrow, areas of bone destruction; dashed line, the remaining calvaria. The bone destruction index was calculated by dividing the length of the osteolytic lesion by the total length of calvarial bone underlying the tumor in WT (n = 9) and MMP-9 null animals (n = 9). C, representative photomicrograph of TRAcP-positive (green) multinucleated (blue) osteoclasts (arrows) at the tumor-bone interface (dashed line) in WT and MMP-9 null animals. The number of osteoclasts per ×20 field in multiple WT (n = 9) and MMP-9 null (n = 9) animals was determined. N.s., nonsignificant (P > 0.05) P values.

smaller in the MMP-9 null group [124 ± 72.22 μm (WT) versus 89.33 ± 58.33 μm (MMP-9$^{-/-}$); P < 0.05; Fig. 5C]. Because MMP-9 can potentially be derived from other cellular sources in the prostate tumor–bone microenvironment, we tested whether MMP-9 affected the ability of osteoclasts to directly influence angiogenesis. Initially, we observed that MMP-9 ablation (n = 7) did not affect the ability of osteoclast precursors to undergo osteoclastogenesis compared with WT (n = 6) controls [153.8 ± 19.45 (WT) versus 173.9 ± 24.2 (MMP-9$^{-/-}$) TRAcP-positive multinucleated osteoclasts per 48-well chamber; P > 0.05, *6A* and *B*]. However, analysis of the conditioned media by ELISA revealed that MMP-9 was critical for mediating VEGF-A$_{164}$ bioavailability because MMP-9 null osteoclast conditioned media (n = 7) had significantly lower levels of VEGF-A$_{164}$

Published OnlineFirst March 23, 2010; DOI:10.1158/1541-7786.MCR-09-0445

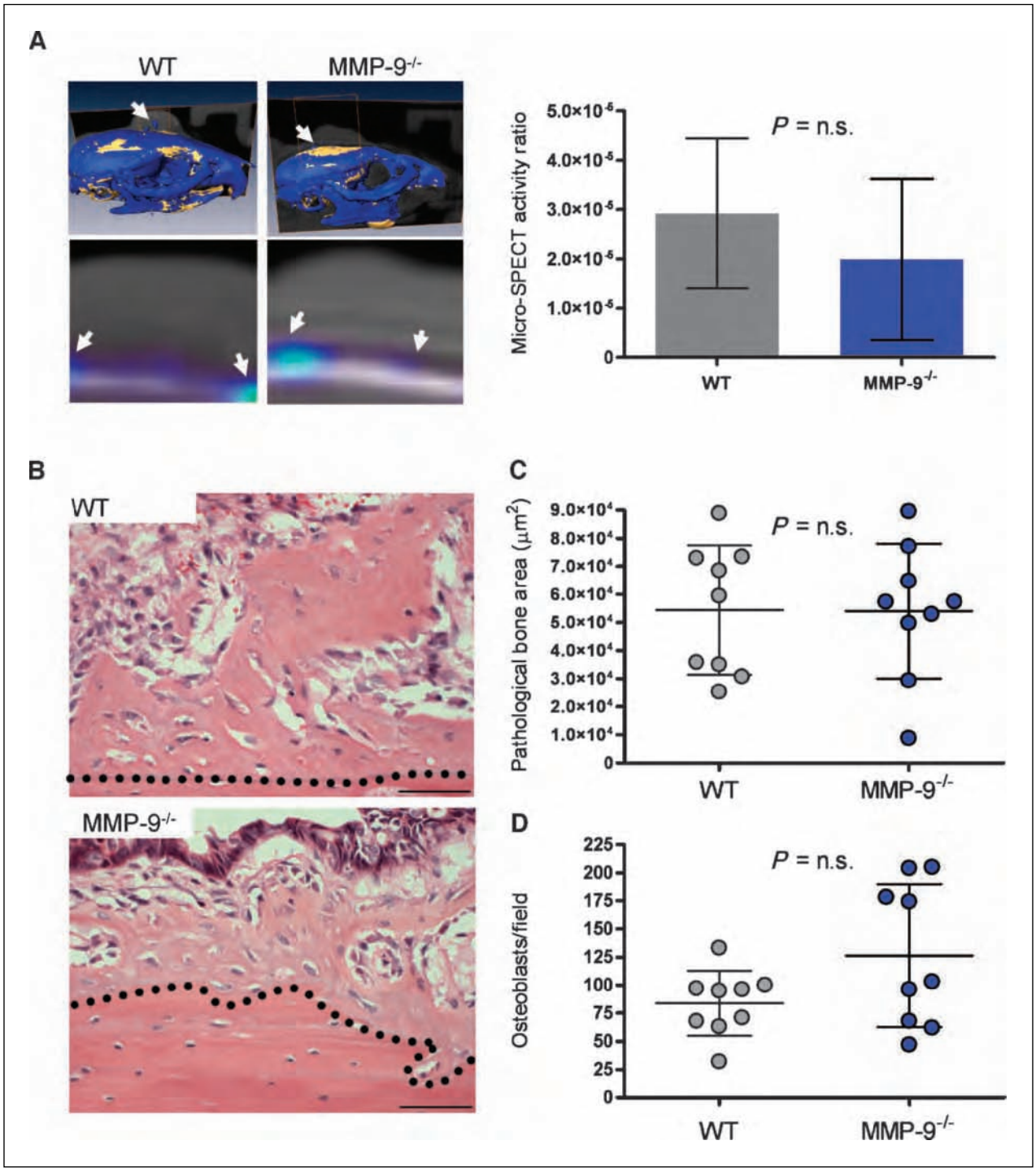

FIGURE 4. Pathologic bone formation in the prostate tumor–bone microenvironment is not affected by MMP-9. A, representative coregistered micro-SPECT images of changes in bone from week 1 (yellow) to week 3 (blue) in the same WT and MMP-9$^{-/-}$ animals (top). Arrows, areas of new bone in the three-dimensional rat prostate tumor–bone microenvironment. Bottom, a representative axial micro-SPECT slice of the tumor bone interface from WT and MMP-9$^{-/-}$ mice at the 3-wk time point. Colors (dark to light blue) indicated by arrows are areas of high micro-SPECT activity. The micro-SPECT activity ratio from multiple slices from individual animals in the WT and MMP-9$^{-/-}$ group was calculated by dividing the micro-SPECT activity per slice by the whole animal dose of ^{99}TC-MDP. B, representative photomicrographs of H&E-stained pathologic bone in WT (n = 9) and MMP-9 null (MMP-9$^{-/-}$; n = 9) mice, 3 wk posttumor implantation. Dashed line, normal calvarial bone. The chaotic woven bone above this line was considered pathologic bone. Scale bar, 50 μm. C, the area of pathologic bone formation in WT (n = 9) and MMP-9$^{-/-}$ (n = 9) mice was determined in multiple sections derived from each animal using MetaMorph imaging software. D, the number of osteoblasts rimming pathologic bone per ×20 field in multiple sections derived from WT (n = 9) and MMP-9$^{-/-}$ (n = 9) null mice. N.s., nonsignificant (P > 0.05) P values. Scale bars, 50 μm.

Published OnlineFirst March 23, 2010; DOI:10.1158/1541-7786.MCR-09-0445

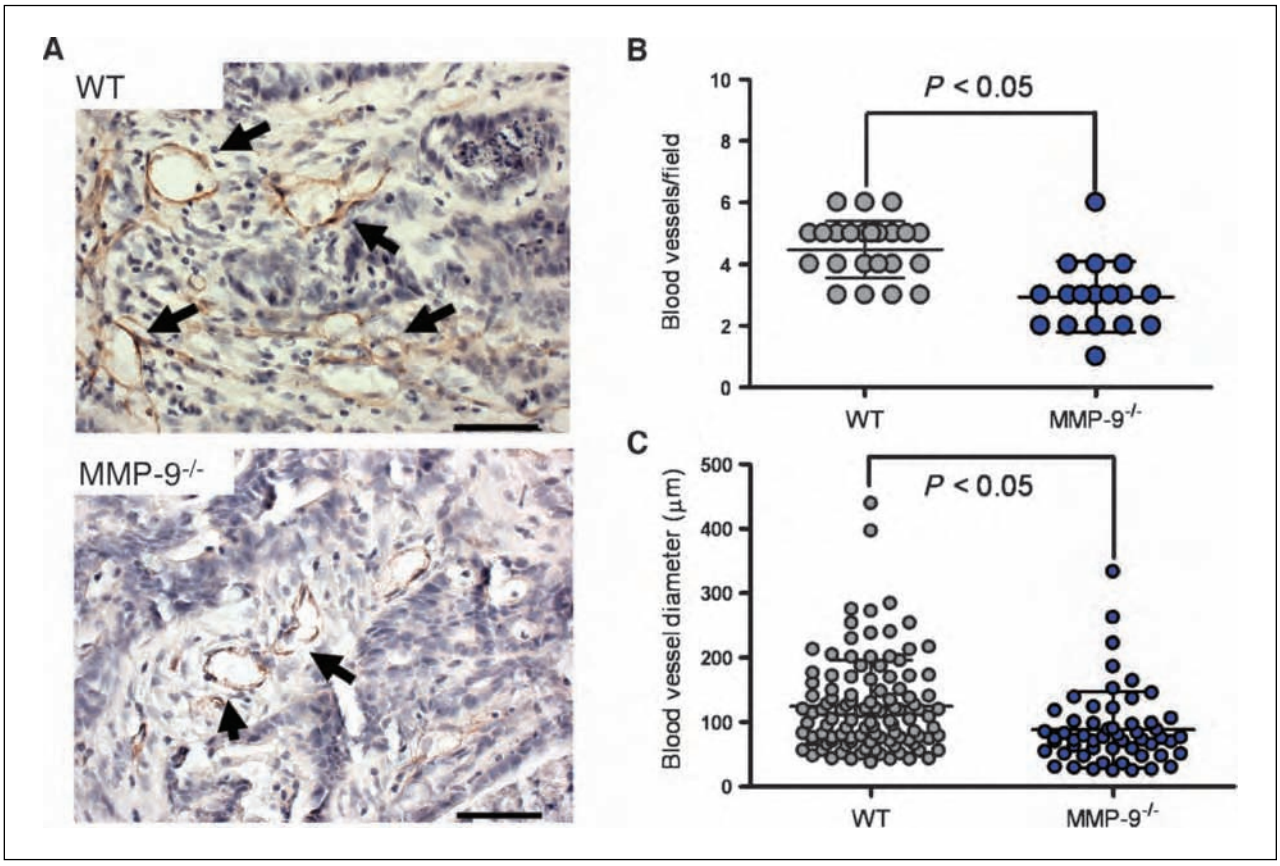

FIGURE 5. Host MMP-9 contributes to vascularization in the tumor-bone microenvironment. A, representative photomicrographs of CD-31 blood vessel staining (arrows) staining in the rat prostate tumor–bone microenvironment of WT and MMP-9 null (MMP-9$^{-/-}$) mice, 3 wk posttumor implantation. Hematoxylin was used as a nuclear counter stain. Scale bar, 50 μm. B, the number of CD-31–positive blood vessels in each section derived from WT (n = 25) and MMP-9$^{-/-}$ (n = 17) null mice was determined. C, the diameter of each of the CD-31 blood vessels within each section derived from WT (n = 25) and MMP-9$^{-/-}$ (n = 17) null animals was determined using the MetaMorph imaging software.

compared with WT (n = 6) controls [185 ± 17.5 pg/mL VEGF-A_{164} (WT OCL) versus 123.5 ± 17.56 pg/mL VEGF-A_{164} (MMP-9$^{-/-}$ OCL); P < 0.05; Fig. 6C]. Furthermore, the addition of recombinant MMP-9 to the MMP-9 null osteoclast cultures significantly enhanced the amount of bioavailable VEGF-A_{164} [123.5 ± 17.6 pg/mL VEGF-A_{164} (MMP-9$^{-/-}$ OCL) versus 219 ± 15.6 pg/mL VEGF-A_{164} (MMP-9$^{-/-}$ OCL plus rMMP-9); P < 0.05, Fig. 6C]. Reverse transcription-PCR analysis of VEGF-A_{164} isoform expression revealed no significant difference between WT and MMP-9 osteoclasts (data not shown), thus indicating that osteoclast-derived MMP-9 can regulate the bioavailability of VEGF-A_{164}. This conclusion was further supported by the observation that conditioned media derived from the MMP-9 null osteoclast cultures was not as efficient as conditioned media derived from WT osteoclasts in promoting angiogenic sprouting using an aortic ring assay [1,654 ± 81.75 μm (WT) versus 1,087 ± 175.9 μm (MMP-9$^{-/-}$) distance of sprout invasion at day 7; P < 0.05; Fig. 6D]. These observations agree with published roles for MMP-9 controlling angiogenesis and we suggest that a defect in osteoclast-mediated vascularization of the prostate tumor–bone microenvironment is the mechanism underlying the observed decrease in tumor volume in the MMP-9 null animals at week 3.

Discussion

In human and rodent samples of the prostate tumor–bone microenvironment, we identified that osteoclasts are a rich source of the proteinase, MMP-9. Given that MMPs are involved in matrix remodeling and skeletal development, the observation that MMPs are expressed by osteoclasts in the prostate tumor–bone microenvironment is perhaps not surprising. However, the major novelty and conclusions of the current study are coherent with a theme that has been emerging from the MMP field of research over the past decade, i.e., that MMPs can have a profound effect on multiple aspects of tumor-host communication by regulating the bioactivity and bioavailability of growth factors and cytokines, in this case, VEGF-A_{164} and angiogenesis.

Our data show that MMP-9 is primarily localized to osteoclasts in a model of prostate tumor–induced osteolytic

Published OnlineFirst March 23, 2010; DOI:10.1158/1541-7786.MCR-09-0445

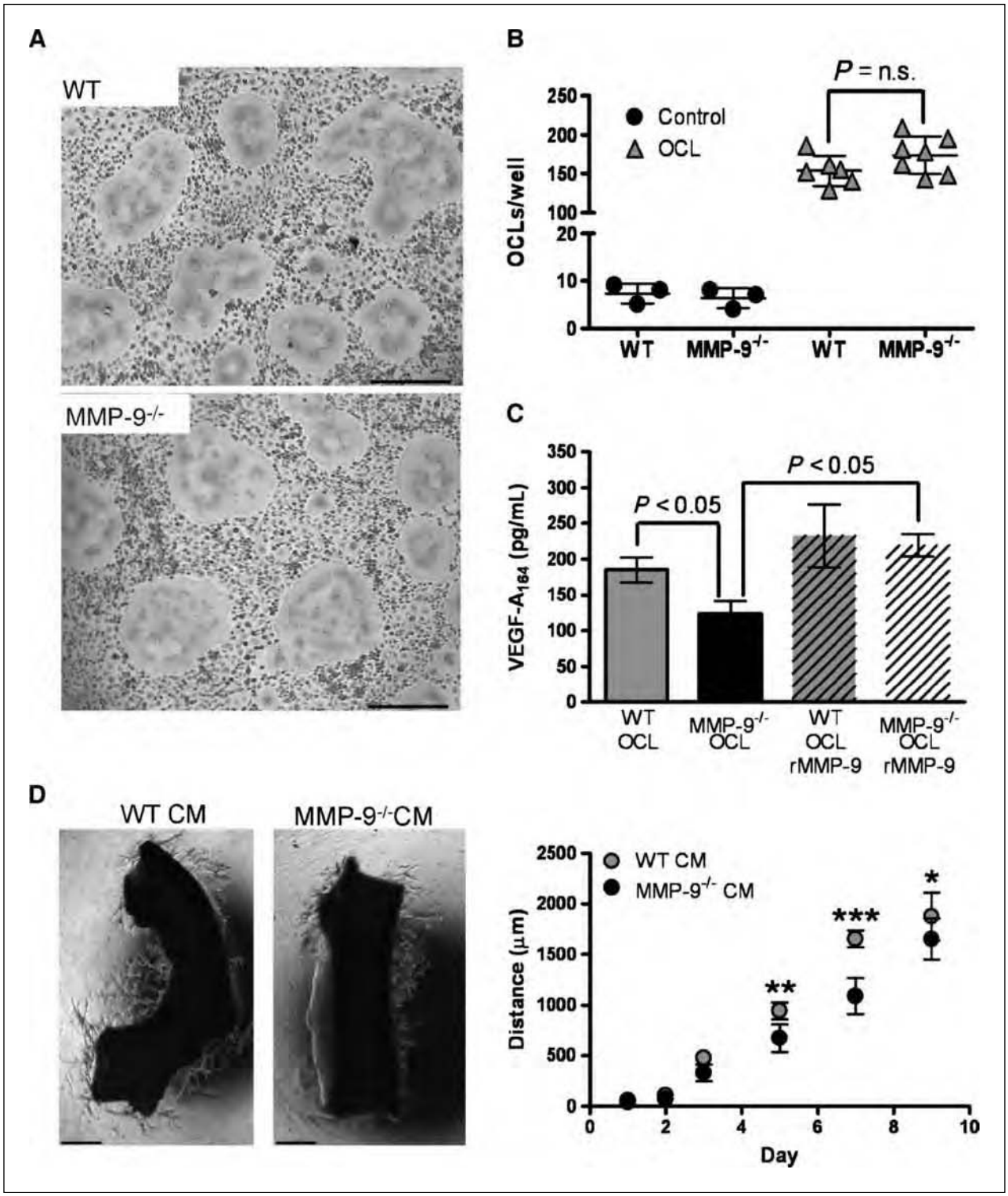

FIGURE 6. Osteoclast-derived MMP-9 regulates VEGF-A_{164} bioavailability and angiogenesis. A, representative photomicrographs of mature multinucleated osteoclasts generated from $CD11b^{+ve}$ myeloid precursor cells isolated from WT or MMP-$9^{-/-}$ mice after 10 d of culture in osteoclast differentiation media. Scale bars, 50 μm. B, quantitation of the number of osteoclasts generated by treatment with control or osteoclast (OCL) differentiation media. Only multinucleated (>3 per cell) TRAcP-positive cells were counted. C, quantitation of VEGF-A_{164} levels in conditioned media derived from WT or MMP-$9^{-/-}$ osteoclast cultures in the presence or absence of 100 ng/mL recombinant MMP-9. D, representative photomicrographs of mouse thoracic aortas stimulated with WT or MMP-$9^{-/-}$ osteoclast culture conditioned media (CM) at day 7. The average distance of sprout migration was calculated from photomicrographs on a daily basis. Scale bar, 1 mm. N.s., nonsignificant ($P > 0.05$) P values. *, $P < 0.05$; **, $P < 0.01$; ***, $P < 0.001$.

Published OnlineFirst March 23, 2010; DOI:10.1158/1541-7786.MCR-09-0445

and osteogenic response (Fig. 1). We observed that the ablation of host MMP-9 significantly reduced tumor growth. Bone is a rich source of growth factors such as transforming growth factor-β and insulin-like growth factors, and the concept of the vicious cycle of tumor-bone interaction dictates that the resorption of the mineralized bone matrix by osteoclasts is critical for the release of these growth factors, thereby resulting in the stimulation of tumor growth (2). However, analysis of the amount of bone destruction between the WT and MMP-9 null groups revealed no difference, nor in the number of osteoclasts present at the tumor-bone interface. These results are consistent with previous reports from our group and others showing that host/osteoclast-derived MMP-9 does not seem to affect the extent of tumor-induced osteolysis (16, 22). Importantly, these studies do not rule out roles for MMP-9 in other types of cancer-induced bone disease. For example, in a recent study examining multiple myeloma progression, we observed that host MMP-9 significantly contributed to myeloma-induced bone destruction (23). These findings underscore the rationale for examining the contribution of individual MMPs in specific disease contexts, a conclusion that is consistent with reports examining the roles for MMPs in other diseases. For example, epithelial expression of MMP-3 is capable of initiating mammary gland tumorigenesis but in the context of skin cancer progression, leukocyte-derived MMP-3 has a protective effect (24, 25).

Osteoblasts are essential mediators of the vicious cycle and human to prostate to bone metastases are hallmarked by extensive areas of osteogenesis. Despite osteoblasts expressing a wide variety of proteinases including MMP-2 and MMP-14 that are important for normal osteoblast function (26, 27), it seemed that in our model system and in human samples of prostate to bone metastasis, that osteoblasts do not express MMP-9 *in vivo*. However, given the close relationship between osteoblasts and osteoclasts, we assessed if osteoclast-derived MMP-9 could affect the prostate tumor–induced osteogenic response. This is the first report to test the contribution of a host-derived MMP to tumor-induced osteogenesis. Although micro-SPECT and histomorphometry did not reveal a significant difference in prostate tumor–induced osteogenesis, our study shows the feasibility of examining the role of tumor or host-derived MMPs in osteogenic bone remodeling using micro-SPECT.

We acknowledge that the model used in the current study has limitations in that it is not reflective of the process of metastasis, true intraosseous growth, or an anatomic site that metastatic human prostate cancer cells typically metastasize to. However, the model does have several advantages including (*a*) the generation of a mixed osteogenic/osteolytic lesion that is more reflective of human prostate to bone metastases compared with the solely lytic type lesions generated by human prostate cancer cell lines such as PC-3; (*b*) its use of a straight forward surgical technique, and (*c*) it allows for the rapid interrogation of hypotheses *in vivo* (~3 weeks). Furthermore, our studies with this model are complemented by Cher and colleagues (22) examining the contribution of host MMP-9 to prostate tumor–induced tibial osteolysis with the human PC-3 prostate cancer cell line. Given the caveats of the model used in the current study, it is possible that MMP-9 can contribute to other steps of metastasis that are not taken into account in the current study such as extravasation and survival/establishment, the latter of which is an important role for host-derived MMP-9 in early lung metastasis (12). Therefore, roles for host MMP-9 in other aspects of the metastatic cascade cannot be ruled out.

Although MMP-9 did not affect prostate tumor–induced osteolysis or osteogenesis, we did observe that osteoclast-derived MMP-9 significantly contributed to prostate tumor growth in the bone microenvironment. Although studies in the breast tumor–bone microenvironment have shown that MMP-9 may facilitate this process by transforming growth factor-β (28), our data identify that osteoclast-derived MMP-9 can affect angiogenesis in the prostate tumor–bone microenvironment. Recently, reports have indicated proangiogenic roles for osteoclasts based on findings that (*a*) osteoclasts express several proangiogenic factors such as VEGF-A (29); (*b*) the close proximity between osteoclasts and endothelial cells in areas of bone remodeling (30); (*c*) evidence that osteoclasts can directly stimulate angiogenesis *in vitro* (31); and (*d*) clinical data showing that bisphosphonates, potent antiosteoclast therapies, also significantly halt angiogenesis in pathologic bone diseases such as bone metastasis (32). MMP-9 has also been shown to be important in mediating the "angiogenic switch" by controlling the bioavailability of VEGF-A_{164} (21). Analysis of the developing bone in MMP-9 null mice showed a delay in osteoclast invasion and angiogenesis in primary ossification centers (18). Our data show that MMP-9 null osteoclast cultures generate significantly less bioavailable VEGF-A_{164} compared with WT controls. Analysis of VEGF-A_{164} expression at a mRNA level revealed that MMP-9 null osteoclast cultures expressed similar levels of VEGF-A_{164} (data not shown). Therefore, it seems that MMP-9 is important in regulating the bioavailability of VEGF-A_{164} that is generated by the osteoclast cultures and we suggest that the decreased angiogenesis observed in the MMP-9 null tumor–bone microenvironment is, in part, due to an inefficiency of MMP-9 null osteoclasts to generate bioavailable VEGF-A_{164}.

Although osteoclasts are a major source of MMP-9 in the prostate tumor–bone microenvironment as observed by immunofluorescent localization, other cells throughout the stromal compartment also stained positively for MMP-9. Although we did not investigate the identity of the cellular sources, we posit based on the literature that these cell types are most likely composed of macrophages and neutrophils that are potent mediators of the angiogenic process (12, 33-36). Therefore, although we suspect that osteoclast-derived MMP-9 is important in mediating angiogenesis, roles for other MMP-9–positive host cells cannot be excluded. Surprisingly, it appeared that in our model and in human samples of prostate to bone metastasis

Published OnlineFirst March 23, 2010; DOI:10.1158/1541-7786.MCR-09-0445

(n = 10) that tumor cells were largely negative for MMP-9, but given the small sample size, roles for tumor-derived MMP-9 cannot be excluded at this juncture. Collectively however, our data point toward MMP-9 as being a clinically relevant target for the inhibition of angiogenesis in the tumor-bone microenvironment.

The rationale for the use of selective MMP inhibitors for the treatment of lytic breast and prostate to bone metastases is supported by several independently performed preclinical studies obtained with animal models of the disease. The treatment of mice bearing lytic breast or prostate bone metastases with the broad spectrum MMP inhibitors BB-94 or GM6001 could prevent tumor growth and tumor-induced osteolysis (37-39). Thus far, no studies have examined the affect of MMP inhibitors on osteogenic bone metastases. To translate MMP inhibitors for human clinical use, selective inhibition of metalloproteinases is a prerequisite to avoid the described drawbacks of the original MMP inhibitors (40). To this end, SB-3CT, an MMP inhibitor with heightened selectivity for MMP-2 and MMP-9 is effective in preventing PC-3 prostate tumor progression with decreased tumor growth, vascularization, and osteolysis being reported (41). Based on our findings, these data suggest that SB-3CT–mediated MMP-9 inhibition prevents tumor and host-mediated angiogenesis and points toward a potentially important role for MMP-2 in controlling osteolysis, which has thus far not been investigated. Therefore, fine-tuning the specificity of MMP inhibitors may be a relevant approach for the development of therapies for the treatment of bone metastases.

In conclusion, we have identified that osteoclasts are a major source of MMP-9 in the human and rodent prostate tumor–bone microenvironment. However, we have shown that host MMP-9 does not affect tumor-induced osteolytic or osteogenic responses in our animal model but does contribute to tumor growth in the prostate tumor–bone microenvironment by mediating angiogenesis through regulating the bioavailability of matrix-sequestered VEGF-A_{164}. These observations are in keeping with the growing studies that show differential roles for host MMPs in mediating tumor-host interaction.

Disclosure of Potential Conflicts of Interest

No potential conflicts of interest were disclosed.

Acknowledgments

Views and opinions of, and endorsements by the author(s), do not reflect those of the U.S. Army or the Department of Defense. We thank Kathy J. Carter for assistance with the aortic ring assay.

Grant Support

Department of Defense under award number W81XWH-07-1-0208 (C.C. Lynch). Partial support was also provided by the NIH under grants R25-CA136440 (L.C. Johnson), S10-RR23784, P30-CA068485, and U24-CA126588 (T.E. Peterson). Human samples of prostate to bone metastases were collected under award number PO1-CA85859 and P50-CA097186 (R.L. Vessella).

The costs of publication of this article were defrayed in part by the payment of page charges. This article must therefore be hereby marked *advertisement* in accordance with 18 U.S.C. Section 1734 solely to indicate this fact.

Received 10/08/2009; revised 01/25/2010; accepted 02/18/2010; published OnlineFirst 03/23/2010.

References

1. Keller ET, Brown J. Prostate cancer bone metastases promote both osteolytic and osteoblastic activity. J Cell Biochem 2004;91:718–29.
2. Mundy GR. Metastasis to bone: causes, consequences and therapeutic opportunities. Nat Rev Cancer 2002;2:584–93.
3. Lynch CC, Matrisian LM. Matrix metalloproteinases in tumor-host cell communication. Differentiation 2002;70:561–73.
4. Lynch CC, Hikosaka A, Acuff HB, et al. MMP-7 promotes prostate cancer-induced osteolysis via the solubilization of RANKL. Cancer Cell 2005;7:485–96.
5. Heissig B, Hattori K, Dias S, et al. Recruitment of stem and progenitor cells from the bone marrow niche requires mmp-9 mediated release of kit-ligand. Cell 2002;109:625–37.
6. Holmbeck K, Bianco P, Caterina J, et al. MT1-MMP-deficient mice develop dwarfism, osteopenia, arthritis, and connective tissue disease due to inadequate collagen turnover. Cell 1999;99:81–92.
7. Mosig RA, Dowling O, DiFeo A, et al. Loss of MMP-2 disrupts skeletal and craniofacial development and results in decreased bone mineralization, joint erosion and defects in osteoblast and osteoclast growth. Hum Mol Genet 2007;16:1113–23.
8. Egeblad M, Werb Z. New functions for the matrix metalloproteinases in cancer progression. Nat Rev Cancer 2002;2:161–74.
9. Chinni SR, Sivalogan S, Dong Z, et al. CXCL12/CXCR4 signaling activates Akt-1 and MMP-9 expression in prostate cancer cells: the role of bone microenvironment-associated CXCL12. Prostate 2006;66:32–48.
10. Nabha SM, dos Santos EB, Yamamoto HA, et al. Bone marrow stromal cells enhance prostate cancer cell invasion through type I collagen in an MMP-12 dependent manner. Int J Cancer 2008;122:2482–90.
11. Shinkai Y, Rathbun G, Lam KP, et al. RAG-2-deficient mice lack mature lymphocytes owing to inability to initiate V(D)J rearrangement. Cell 1992;68:855.
12. Acuff HB, Carter KJ, Fingleton B, Gorden DL, Matrisian LM. Matrix metalloproteinase-9 from bone marrow-derived cells contributes to survival but not growth of tumor cells in the lung microenvironment. Cancer Res 2006;66:259–66.
13. Shirai T, Cui L, Takahashi S, et al. Carcinogenicity of 2-amino-1-methyl-6-phenylimidazo [4,5-b]pyridine (PhIP) in the rat prostate and induction of invasive carcinomas by subsequent treatment with testosterone propionate. Cancer Lett 1999;143:217–21.
14. Filgueira L. Fluorescence-based staining for tartrate-resistant acidic phosphatase (TRAP) in osteoclasts combined with other fluorescent dyes and protocols. J Histochem Cytochem 2004;52:411–4.
15. Masson VV, Devy L, Grignet-Debrus C, et al. Mouse aortic ring assay: a new approach of the molecular genetics of angiogenesis. Biol Proced Online 2002;4:24–31.
16. Thiolloy S, Halpern J, Holt GE, et al. Osteoclast-derived matrix metalloproteinase-7, but not matrix metalloproteinase-9, contributes to tumor-induced osteolysis. Cancer Res 2009;69:6747–55.
17. Vu TH, Shipley JM, Bergers G, et al. MMP-9/Gelatinase B is a key regulator of growth plate angiogenesis and apoptosis of hypertrophic chondrocytes. Cell 1998;93:411.
18. Engsig MT, Chen QJ, Vu TH, et al. Matrix metalloproteinase 9 and vascular endothelial growth factor are essential for osteoclast recruitment into developing long bones. J Cell Biol 2000;151:879–90.
19. Uematsu T, Yuen S, Yukisawa S, et al. Comparison of FDG PET and

Published OnlineFirst March 23, 2010; DOI:10.1158/1541-7786.MCR-09-0445

SPECT for detection of bone metastases in breast cancer. AJR Am J Roentgenol 2005;184:1266–73.
20. Cackowski FC, Roodman GD. Perspective on the osteoclast: an angiogenic cell? Ann N Y Acad Sci 2007;1117:12–25.
21. Bergers G, Brekken R, McMahon G, et al. Matrix metalloproteinase-9 triggers the angiogenic switch during carcinogenesis. Nat Cell Biol 2000;2:737–44.
22. Nabha SM, Bonfil RD, Yamamoto HA, et al. Host matrix metalloproteinase-9 contributes to tumor vascularization without affecting tumor growth in a model of prostate cancer bone metastasis. Clin Exp Metastasis 2006;23:335–44.
23. Fowler JA, Mundy GR, Lwin ST, Lynch CC, Edwards CM. A murine model of myeloma that allows genetic manipulation of the host microenvironment. Dis Model Mech 2009;2:604–11.
24. Radisky DC, Levy DD, Littlepage LE, et al. Rac1b and reactive oxygen species mediate MMP-3-induced EMT and genomic instability. Nature 2005;436:123–7.
25. McCawley LJ, Crawford HC, King LE, Jr., Mudgett J, Matrisian LM. A protective role for matrix metalloproteinase-3 in squamous cell carcinoma. Cancer Res 2004;64:6965–72.
26. Holmbeck K, Bianco P, Pidoux I, et al. The metalloproteinase MT1-MMP is required for normal development and maintenance of osteocyte processes in bone. J Cell Sci 2005;118:147–56.
27. Inoue K, Mikuni-Takagaki Y, Oikawa K, et al. A crucial role for matrix metalloproteinase 2 in osteocytic canalicular formation and bone metabolism. J Biol Chem 2006;281:33814–24.
28. Wilson TJ, Nannuru KC, Singh RK. Cathepsin G-mediated activation of pro-matrix metalloproteinase 9 at the tumor-bone interface promotes transforming growth factor-β signaling and bone destruction. Mol Cancer Res 2009;7:1224–33.
29. Tombran-Tink J, Barnstable CJ. Osteoblasts and osteoclasts express PEDF, VEGF-A isoforms, and VEGF receptors: possible mediators of angiogenesis and matrix remodeling in the bone. Biochem Biophys Res Commun 2004;316:573–9.
30. Andersen TL, Sondergaard TE, Skorzynska KE, et al. A physical mechanism for coupling bone resorption and formation in adult human bone. Am J Pathol 2009;174:239–47.
31. Tanaka Y, Abe M, Hiasa M, et al. Myeloma cell-osteoclast interaction enhances angiogenesis together with bone resorption: a role for vascular endothelial cell growth factor and osteopontin. Clin Cancer Res 2007;13:816–23.
32. Croucher PI, De Hendrik R, Perry MJ, et al. Zoledronic acid treatment of 5T2MM-bearing mice inhibits the development of myeloma bone disease: evidence for decreased osteolysis, tumor burden and angiogenesis, and increased survival. J Bone Miner Res 2003;18:482–92.
33. Nakamura T, Kuwai T, Kim JS, Fan D, Kim SJ, Fidler IJ. Stromal metalloproteinase-9 is essential to angiogenesis and progressive growth of orthotopic human pancreatic cancer in parabiont nude mice. Neoplasia 2007;9:979–86.
34. Du R, Lu KV, Petritsch C, et al. HIF1α induces the recruitment of bone marrow-derived vascular modulatory cells to regulate tumor angiogenesis and invasion. Cancer Cell 2008;13:206–20.
35. Pahler JC, Tazzyman S, Erez N, et al. Plasticity in tumor-promoting inflammation: impairment of macrophage recruitment evokes a compensatory neutrophil response. Neoplasia 2008;10:329–40.
36. Ardi VC, Kupriyanova TA, Deryugina EI, Quigley JP. Human neutrophils uniquely release TIMP-free MMP-9 to provide a potent catalytic stimulator of angiogenesis. Proc Natl Acad Sci U S A 2007;104:20262–7.
37. Lee J, Weber M, Mejia S, Bone E, Watson P, Orr W. A matrix metalloproteinase inhibitor, batimastat, retards the development of osteolytic bone metastases by MDA-MB-231 human breast cancer cells in Balb C *nu/nu* mice. Eur J Cancer 2001;37:106–13.
38. Winding B, NicAmhlaoibh R, Misander H, et al. Synthetic matrix metalloproteinase inhibitors inhibit growth of established breast cancer osteolytic lesions and prolong survival in mice. Clin Cancer Res 2002;8:1932–9.
39. Nemeth JA, Yousif R, Herzog M, et al. Matrix metalloproteinase activity, bone matrix turnover, and tumor cell proliferation in prostate cancer bone metastasis. J Natl Cancer Inst 2002;94:17–25.
40. Coussens LM, Fingleton B, Matrisian LM. Matrix metalloproteinase inhibitors and cancer: trials and tribulations. Science 2002;295:2387–92.
41. Bonfil RD, Sabbota A, Nabha S, et al. Inhibition of human prostate cancer growth, osteolysis and angiogenesis in a bone metastasis model by a novel mechanism-based selective gelatinase inhibitor. Int J Cancer 2006;118:2721–6.

RESEARCH REPORT

Disease Models & Mechanisms 2, 604-611 (2009) doi:10.1242/dmm.003160
Published by The Company of Biologists 2009

A murine model of myeloma that allows genetic manipulation of the host microenvironment

Jessica A. Fowler[1], Gregory R. Mundy[2], Seint T. Lwin[2], Conor C. Lynch[1,3] and Claire M. Edwards[1,*]

SUMMARY

Multiple myeloma, and the associated osteolytic bone disease, is highly dependent upon cellular interactions within the bone marrow microenvironment. A major limitation of existing myeloma models is the requirement for a specific host strain of mouse, preventing molecular examination of the bone marrow microenvironment. The aim of the current study was to develop a model of myeloma in which the host microenvironment could be modified genetically. The Radl 5T murine model of myeloma is well characterized and closely mimics human myeloma. In the current study, we demonstrate 5T myeloma establishment in recombination activating gene 2 (RAG-2)-deficient mice, which have improper B- and T-cell development. Importantly, these mice can be easily bred with genetically modified mice to generate double knockout mice, allowing manipulation of the host microenvironment at a molecular level. Inoculation of 5TGM1 myeloma cells into RAG-2$^{-/-}$ mice resulted in myeloma development, which was associated with tumor growth within bone and an osteolytic bone disease, as assessed by microcomputed tomography (microCT), histology and histomorphometry. Myeloma-bearing RAG-2$^{-/-}$ mice displayed many features that were similar to both human myeloma and the original Radl 5T model. To demonstrate the use of this model, we have examined the effect of host-derived matrix metalloproteinase 9 (MMP-9) in the development of myeloma in vivo. Inoculation of 5TGM1 myeloma cells into mice that are deficient in RAG-2 and MMP-9 resulted in a reduction in both tumor burden and osteolytic bone disease when compared with RAG-2-deficient wild-type myeloma-bearing mice. The establishment of myeloma in RAG-2$^{-/-}$ mice permits molecular examination of the host contribution to myeloma pathogenesis in vivo.

INTRODUCTION

Multiple myeloma is one of the most common hematological malignancies in the USA (Jemal et al., 2004). Myeloma is characterized by the clonal expansion of malignant plasma cells within the bone marrow, which is associated with the development of a destructive osteolytic bone disease, anemia and immune suppression. The mechanisms involved in the development of myeloma are not well understood; therefore, despite many advances in the treatment of multiple myeloma, it remains an incurable and fatal malignancy. Myeloma progression and the development of osteolytic bone disease are inextricably linked and are dependent upon cellular interactions within the bone marrow microenvironment. Therefore, the study of the bone marrow microenvironment in myeloma is crucial for both our understanding of mechanisms involved in disease progression, and the identification of novel therapeutic targets.

The advances in the treatment of myeloma are limited owing to the number of clinically relevant animal models that allow for the in vivo study of myeloma development in the context of a bone marrow microenvironment. The current animal models for myeloma include the severe combined immunodeficiency (SCID)-hu/rab xenograft model, a conditional mouse model that is dependent upon Myc activation in germinal center B cells, and the Radl 5T model. The SCID-hu/rab xenograft model provides a system where primary human myeloma cells can be injected into either a fetal human bone or rabbit bone that is implanted subcutaneously into an immunocompromised mouse (Yaccoby et al., 1998; Yaccoby et al., 2007). The Radl model uses 5T myeloma cells that arose spontaneously in aged, inbred C57BL/KaLwRijHsd mice and is propagated by the inoculation of these myeloma cells into syngeneic mice (Radl et al., 1979; Radl et al., 1988; Garrett et al., 1997). Both of these models allow the study of tumor growth and myeloma bone disease, and have proven to be effective preclinical models to test novel therapeutic approaches for the treatment of myeloma bone disease (Dallas et al., 1999; Croucher et al., 2001; Croucher et al., 2003; Oyajobi et al., 2003; Yaccoby et al., 2004; Edwards et al., 2007; Yaccoby et al., 2007; Edwards et al., 2008). Activation of Myc under the control of the kappa light chain regulatory elements results in the development of myeloma with features that are similar to human multiple myeloma (Chesi et al., 2008). A major limitation of all existing models is that manipulation of the bone marrow microenvironment, independent of the tumor, is limited to systemic pharmacological reagents, rendering it impossible to elucidate specific cellular and molecular mechanisms of myeloma bone disease within the bone marrow microenvironment. Current research has demonstrated the crucial role that the tumor microenvironment plays in disease progression, but the existing animal models for the study of the tumor microenvironment in myeloma severely impair both clinical and basic research in this field.

The aim of the current study was to develop a murine model of myeloma in which the host microenvironment could subsequently be modified genetically, thus enabling molecular studies of the host contribution to multiple myeloma progression to be conducted in vivo. The Radl 5T murine model of myeloma was originally identified to occur spontaneously in aging mice of the C57BL/KaLwRij strain. Several 5T cell lines have been

[1]Vanderbilt Center for Bone Biology, Department of Cancer Biology and
[2]Vanderbilt Center for Bone Biology, Department of Medicine/Clinical Pharmacology, Vanderbilt University, Nashville, TN 37232, USA
[3]Department of Orthopedics and Rehabilitation, Vanderbilt University, Nashville, TN 37235, USA
*Author for correspondence (e-mail: claire.edwards@vanderbilt.edu)

developed from this model, including 5T2 and 5TGM1, which result in tumor growth within bone and osteolytic bone disease when cells are inoculated into either syngeneic C57BL/KaLwRij mice or bg/nu/Xid mice (Garrett et al., 1997; Asosingh et al., 2000). By contrast, myeloma does not develop when cells are inoculated into C57BL/6 mice. The genetic mutation that defines C57BL/KaLwRij mice is unknown, and the deleterious effects of the bg/nu/Xid mutation on breeding and life span mean that neither of these strains can be crossed with genetically modified mice in order to modify the host microenvironment in mice which are permissive to myeloma growth. In the current study, we investigated the establishment of 5TGM1 myeloma cells in immunocompromised recombination activating gene 2 (RAG-2)-deficient mice on a C57BL/6 background. These mice have a targeted disruption of the *Rag2* gene, which results in the absence of functional recombinases, leading to improper B- and T-cell development (Shinkai et al., 1992). Importantly, these mice can be easily bred with genetically modified mice to generate double knockout mice, therefore greatly improving our ability to genetically manipulate the host microenvironment.

RESULTS

RAG-2$^{-/-}$ mice develop a characteristic myeloma tumor burden

RAG-2-deficient mice on a C57BL/6 background were inoculated with 10^6 green fluorescent protein (GFP)-tagged 5TGM1 myeloma cells by intravenous tail vein injection. Tumor burden was measured by serum IgG2bk ELISA, histomorphometric analysis of tumor burden in bone, and flow cytometric analysis of tumor burden in the bone marrow and spleen. Myeloma development in RAG-2-deficient mice was compared with the rate of development in syngeneic C57BL/KaLwRij mice, C57BL/6 mice, bg/nu/Xid mice, and T-cell-deficient athymic nude mice.

Following intravenous inoculation of 5TGM1 myeloma cells, the RAG-2-deficient mice developed myeloma at the same rate as that observed with the syngeneic C57BL/KaLwRij mice from the 5T model. The tumor burden of the RAG-2-deficient mice increased over time, as determined by measuring the serum levels of the myeloma-specific immunoglobulin IgG2b (Fig. 1A). The increase of IgG2b levels in the RAG-2-deficient mice was comparable to the tumor burden found in the myeloma-bearing C57BL/KaLwRij mice (Fig. 1A). Inoculation of 5TGM1 cells into immune-competent C57BL/6 mice did not result in myeloma development. Tumor burden was also assessed by measuring the percentage of GFP-positive myeloma cells present in the bone marrow and spleen. The myeloma-bearing RAG-2-deficient mice showed a significant accumulation of GFP-positive myeloma cells in both the bone marrow and spleen (Fig. 1B), and this burden was comparable to that observed in the C57BL/KaLwRij mice. Therefore, the development of multiple myeloma in RAG-2-deficient mice occurs in an identical manner to C57BL/KaLwRij mice, both with respect to the time for tumor development and the extent of tumor burden.

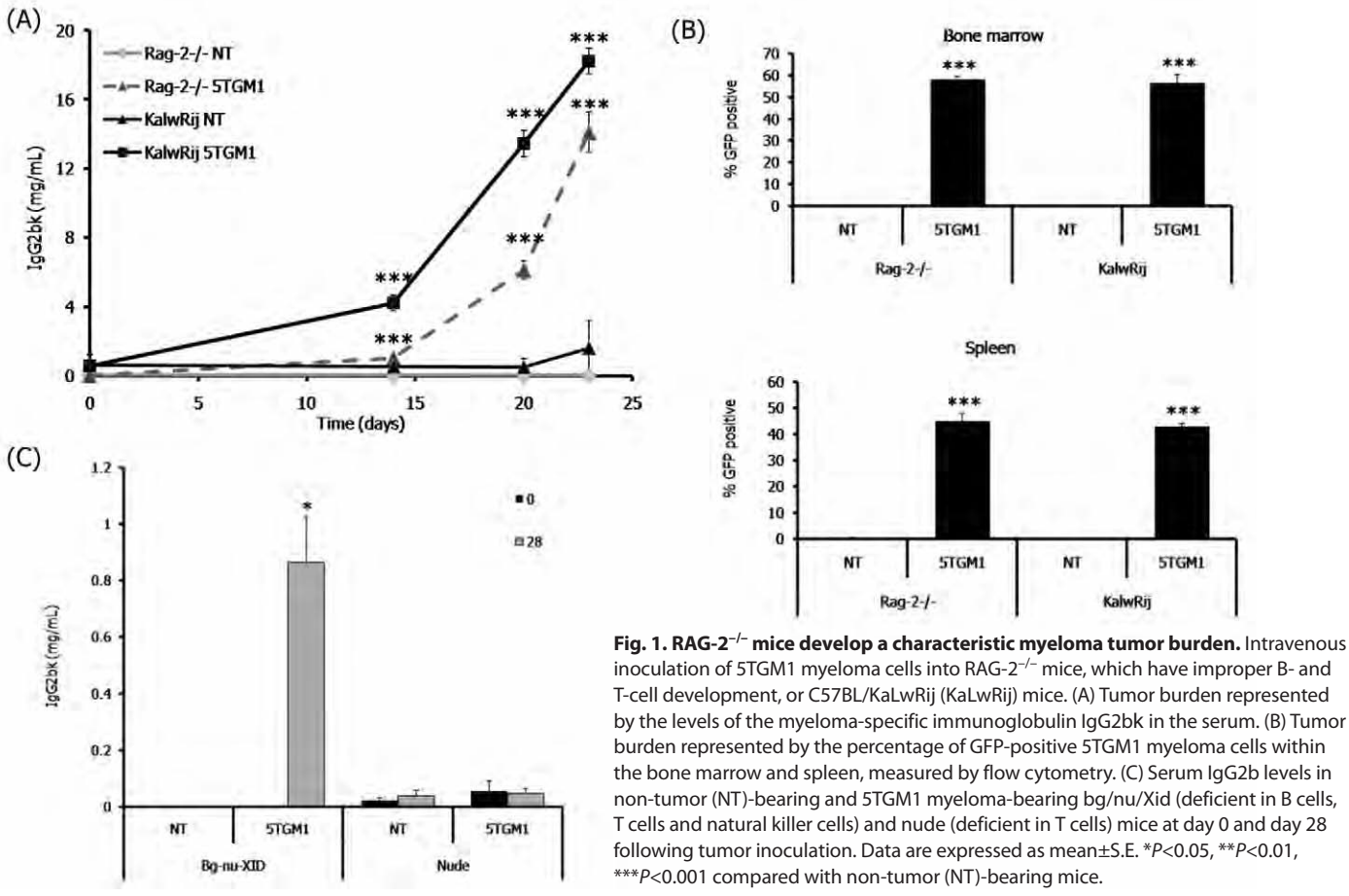

Fig. 1. RAG-2$^{-/-}$ mice develop a characteristic myeloma tumor burden. Intravenous inoculation of 5TGM1 myeloma cells into RAG-2$^{-/-}$ mice, which have improper B- and T-cell development, or C57BL/KaLwRij (KaLwRij) mice. (A) Tumor burden represented by the levels of the myeloma-specific immunoglobulin IgG2bk in the serum. (B) Tumor burden represented by the percentage of GFP-positive 5TGM1 myeloma cells within the bone marrow and spleen, measured by flow cytometry. (C) Serum IgG2b levels in non-tumor (NT)-bearing and 5TGM1 myeloma-bearing bg/nu/Xid (deficient in B cells, T cells and natural killer cells) and nude (deficient in T cells) mice at day 0 and day 28 following tumor inoculation. Data are expressed as mean±S.E. **P*<0.05, ***P*<0.01, ****P*<0.001 compared with non-tumor (NT)-bearing mice.

In contrast to the accumulation of myeloma cells that was observed in RAG-2-deficient mice and bg/nu/Xid mice, when 5TGM1 myeloma cells were inoculated into T-cell-deficient athymic nude mice, the measurements of myeloma-specific immunoglobulin levels in the serum demonstrated that there was no increase in IgG2b levels in 5TGM1-bearing athymic nude mice (Fig. 1C). This demonstrates that a lack of T cells is not sufficient to permit myeloma development in vivo.

RAG-2$^{-/-}$ mice develop myeloma-associated bone disease

In addition to indices of tumor burden, we also evaluated the myeloma-associated osteolytic bone disease in RAG-2-deficient mice in comparison to the well-characterized bone disease of the C57BL/KaLwRij mice. Trabecular bone volume and osteolytic lesions were analyzed by microcomputed tomography (microCT), and osteoclast and osteoblast numbers were determined by bone histomorphometry. Myeloma-bearing RAG-2-deficient mice were found to have characteristic features of myeloma bone disease, which were identical to those seen in C57BL/KaLwRij mice and strikingly similar to human multiple myeloma. The myeloma-bearing RAG-2-deficient mice had a significant number of osteolytic lesions within the cortical bone, whereas the non-tumor mice had no lesions (Fig. 2A,B). Histological analysis confirmed areas where the cortical bone had been destroyed, with tumor cells expanding through the cortices, leading to the development of discrete osteolytic lesions (Fig. 3). We found that the myeloma-bearing RAG-2-deficient mice had a significant decrease in the overall trabecular bone volume when compared with the non-tumor control mice (Fig. 2C; Fig. 3). Histomorphometric analysis of the RAG-2-deficient myeloma-bearing mice demonstrated other features that are characteristic of myeloma-associated bone disease, such as an increase in bone-resorbing osteoclasts and a decrease in bone-forming osteoblasts (Fig. 2D; Fig. 3). Histological analysis demonstrated a striking similarity between 5TGM1 myeloma-bearing RAG-2$^{-/-}$ mice and myeloma-bearing syngeneic KaLwRij mice in terms of both tumor expansion within the bone marrow cavity and development of myeloma bone disease (Fig. 3).

Deficiency in matrix metalloproteinase 9 (MMP-9) decreases both tumor burden and the severity of the associated osteolytic bone disease

The MMP family of proteolytic enzymes has been studied extensively for their role in extracellular matrix degradation, which can result in cancer progression in various tumor cell types including myeloma (Barille et al., 1997; Vacca et al., 1998; Barille et al., 1999; Vacca et al., 1999). Previous studies have demonstrated a role for tumor-

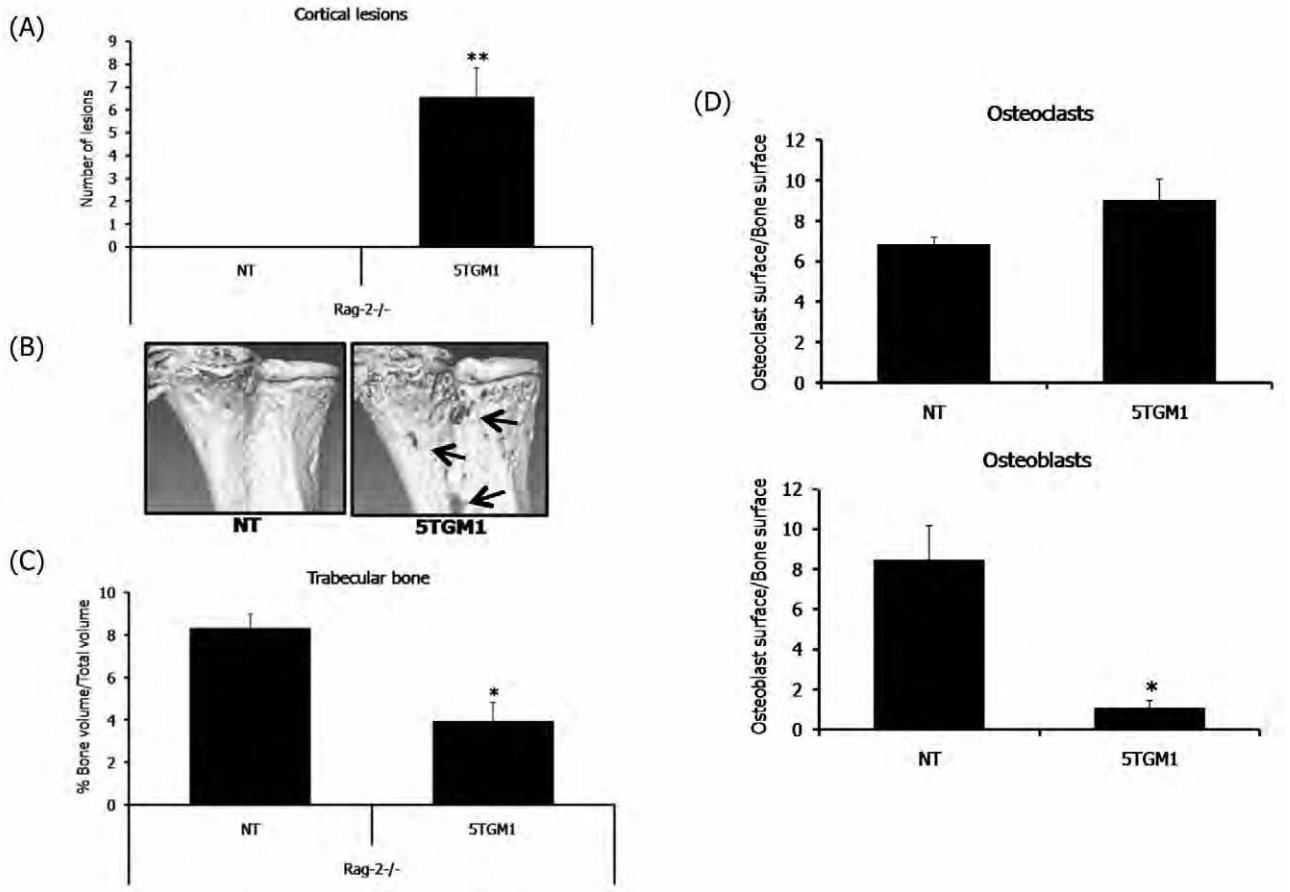

Fig. 2. RAG-2$^{-/-}$ mice develop myeloma-associated bone disease. Myeloma-associated bone disease assessed by microCT analysis, histomorphometry and histology. (A) MicroCT analysis of osteolytic bone lesions through the cortical bone. (B) Representative microCT images of cortical bone lesions. (C) MicroCT analysis of trabecular bone volume. (D) Histomorphometric analysis of the osteoclast and osteoblast surface area (mm^2) to trabecular bone surface area (mm^3) in RAG-2$^{-/-}$ mice. Data are expressed as mean±S.E. *P<0.05, **P<0.01, ***P<0.001 compared with non-tumor (NT)-bearing mice.

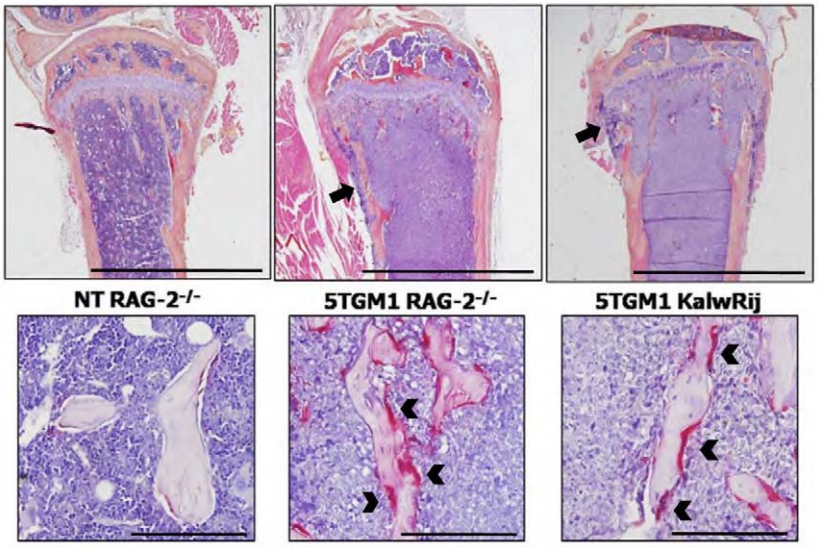

Fig. 3. RAG-2$^{-/-}$ mice develop characteristic pathology that is typical of clinical myeloma. The pathology present in myeloma-bearing RAG-2-deficient mice is similar to that seen in the well-established Radl 5T murine model of myeloma in C57BL/KaLwRij mice. (Top row) Myeloma cell growth within the bone marrow cavity, and osteolytic lesions through the cortical bone (black arrows). Bars, 2 mm. (Bottom row) Myeloma-bearing mice display a characteristic increase in TRAP-positive osteoclasts (black arrowheads). NT=non-tumor bearing. Bars, 200 μm.

derived MMP-9 in myeloma progression, but also revealed the presence of host-derived MMP-9 within the bone marrow microenvironment (Van Valckenborgh et al., 2005). In order to demonstrate the use of this RAG-2$^{-/-}$ model of myeloma, we chose to investigate myeloma development in mice that were deficient in MMP-9. MMP-9 expression in the bone marrow of C57BL/KaLwRij mice was demonstrated by immunohistochemistry in tartrate-resistant acid phosphatase (TRAP)-positive multi-nucleated osteoclasts on the surface of trabecular bone (Fig. 4A). A similar level of expression was observed in RAG-2-deficient mice (data not shown). Mice that were deficient in both RAG-2 and MMP-9, in addition to mice that were deficient in RAG-2 alone, were inoculated intravenously with 5TGM1 myeloma cells to determine how MMP-9 deficiency would affect tumor burden and the associated bone disease. When compared with myeloma-bearing mice that were deficient in only RAG-2, the tumor burden, as indicated by IgG2b serum levels, in mice that were deficient in both RAG-2 and MMP-9 was decreased significantly at 14 and 21 days following tumor inoculation (Fig. 4B). Mice that were deficient in both RAG-2 and MMP-9 showed a significant decrease in the proportion of GFP-positive 5TGM1 myeloma cells that were present in the bone marrow when compared with myeloma-bearing RAG-2-deficient mice; however, there was no significant difference in the proportion of GFP-positive myeloma cells in the spleens of these mice (Fig. 4C). The contribution of host-derived MMP-9 from the osteoclasts within the bone marrow microenvironment also had significant effects on myeloma bone disease. The number of lesions present through the cortical bone of myeloma-bearing mice that were deficient in both RAG-2 and MMP-9 was significantly decreased when compared with myeloma-bearing RAG-2-deficient mice (Fig. 4D). Additionally, the overall bone loss in myeloma-bearing double-deficient mice was significantly less when compared with the control RAG-2-deficient mice, as indicated by microCT analysis of trabecular bone volume (Fig. 4E). Histomorphometric analysis demonstrated a trend towards a reduction in osteoclasts in myeloma-bearing double-deficient mice when compared with myeloma-bearing RAG-2-deficient mice (Fig. 4F). No significant difference in osteoblast number was observed (data not shown).

DISCUSSION

The present study demonstrates a new in vivo system for the examination of the host tumor microenvironment and the contributions of this specialized niche to myeloma development. Despite many therapeutic advancements in the treatment of myeloma using existing mouse models, the field of myeloma research has long been limited by the inability of these models to permit specific investigation of the tumor microenvironment. The results from the current study demonstrate that myeloma development in RAG-2-deficient mice shares many of the clinical and histological features of human myeloma and the associated osteolytic bone disease that is also demonstrated in the established Radl 5T model. Myeloma-bearing RAG-2-deficient mice displayed extensive tumor burden within the bone marrow, an increase in osteoclasts, a decrease in osteoblasts, and the development of destructive lytic lesions and overall bone loss. In the 5TGM1 model of myeloma, inoculation of myeloma cells results in them homing to both the bone marrow and spleen, with homing to the spleen being a result of the hematopoietic nature of this organ in mice. The growth of myeloma cells in bone and non-bone sites is a useful tool for elucidating the role of the bone marrow microenvironment; this important feature was also observed in myeloma-bearing RAG-2-deficient mice, with an accumulation of myeloma cells within the bone marrow and spleen. The use of RAG-2-deficient mice in a myeloma model is an extremely important advancement for myeloma research, as gene expression in the host compartment of the tumor microenvironment can be more specifically manipulated.

The results from this study also provide compelling evidence that the bone marrow microenvironment is crucial for myeloma development. We are able to demonstrate crucial differences between 5TGM1 myeloma-permissive and non-permissive strains of mice. We found significant differences in myeloma establishment and progression in various strains of mice despite their similar genetic backgrounds. The most interesting example is the difference between tumor establishment in the C57BL/KaLwRij mice that are used in the Radl model and the lack of tumor take and growth in the C57BL/6 mice of the same

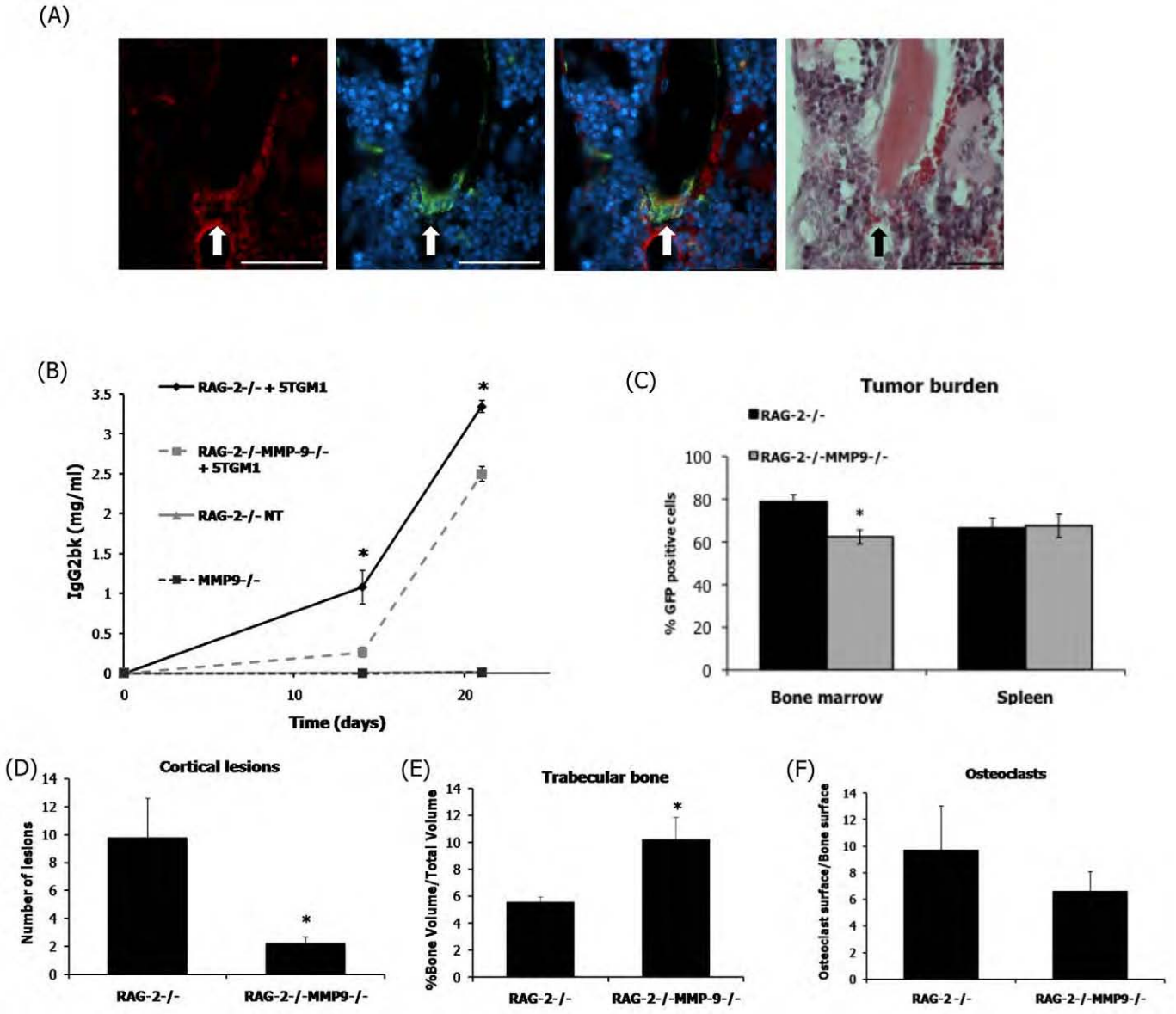

Fig. 4. A lack of host-derived MMP-9 significantly reduces tumor burden and myeloma bone disease in vivo. Intravenous inoculation of 5TGM1 cells into either RAG-2$^{-/-}$ mice or mice that were deficient in both RAG-2 and MMP-9 was followed by an assessment of tumor burden. (A) MMP-9 localization in KaLwRij bone marrow. Fluorescent TRAP staining (green) was used to localize osteoclasts (arrows), whereas immunofluorescence was used to localize MMP-9 (red). Non-specific staining was observed in red blood cells. DAPI (blue) was used as a nuclear stain. Murine IgG was used as a negative control. Bars, 50 μM. (B) Tumor burden represented by the IgG2bk levels present in the serum. (C) Tumor burden represented by the percentage of GFP-positive 5TGM1 myeloma cells within the bone marrow and spleen, measured by flow cytometry. Myeloma bone disease was assessed by microCT analysis, histomorphometry and histology. (D) MicroCT analysis of osteolytic bone lesions through the cortical bone. (E) MicroCT analysis of trabecular bone volume. (F) Histomorphometric analysis of osteoclast number. Data are expressed as mean±S.E. *P<0.05 compared with tumor-bearing RAG-2$^{-/-}$ mice.

genetic background. Of additional interest is the difference in tumor establishment between two immunocompromised strains of mice: athymic nude mice do not develop characteristics of myeloma, whereas RAG-2-deficient mice develop a pathology that is identical to the Radl C57BL/KaLwRij mice. Although the use of RAG-2-deficient mice will not allow for the investigation of the immune system, specifically B and T cells, in myeloma, our results demonstrates that a lack of T cells is not sufficient to permit myeloma development in vivo. Since the major difference between RAG-2-deficient mice and nude mice is the absence of mature B cells, it raises the intriguing possibility that the development of 5T myeloma in RAG-2-deficient mice may not simply be the result of immunodeficiency, but may in part be dependent on specific B-cell regulation. Nude mice are also known to have increased natural killer cell and macrophage activity, and it is possible that theses differences may also contribute to their inability to permit myeloma development (Budzynski and Radzikowski, 1994).

The use of the RAG-2-deficient mice in a model of multiple myeloma creates many opportunities to improve current therapies by increasing our understanding of specific mechanisms within the host tumor microenvironment. The use of this animal model will allow specific manipulation of the host tumor microenvironment through genetic mutation; for example, this model system allowed for the specific examination of host-derived MMP-9 and its contribution to myeloma progression. MMPs are known to have important roles in tumor progression; however, it is impossible to discern their specific contributions owing to the lack of specificity of MMP inhibitors. The ability to inhibit specific MMP expression in the host microenvironment using MMP-deficient mice permits the investigation of the specific roles of individual MMPs in myeloma pathogenesis. In a previous study by Van Valckenborgh et al., in which an MMP-9 pro-drug was used to specifically target tumor cells within the bone marrow microenvironment, MMP-9 activity was higher in myeloma-bearing mice compared with non-tumor-bearing mice (Van Valckenborgh et al., 2005). However, cells in the bone marrow of non-tumor mice still showed elevated levels of MMP-9 expression, suggesting that MMP-9 was present in the bone marrow of C57BL/KaLwRij mice. Our studies confirmed this by using immunofluorescence to demonstrate MMP-9 expression in osteoclasts within both C57BL/KaLwRij and RAG-2$^{-/-}$ bone marrow. By investigating the development of 5TGM1 myeloma in mice that were deficient in both RAG-2 and MMP-9, we were able to demonstrate a significant reduction in both tumor burden and the associated osteolytic bone disease in MMP-9-deficient mice. This both identifies a role for host-derived MMP-9 in myeloma pathogenesis, and illustrates the potential for this model in studies of the host microenvironment in myeloma.

There are many important questions in myeloma research regarding the relative contribution of host-derived factors versus tumor-derived factors, such as receptor activator of nuclear factor-kB ligand (RANKL) and Dickkopf homolog 1 (DKK1), which are known to be expressed by both tumor cells and other cells within the bone marrow microenvironment, including stromal cells. The study of myeloma growth in vivo combined with genetic modification of the host microenvironment offers a novel molecular approach to elucidate the specific host-tumor interactions. Overall, the establishment of multiple myeloma in RAG-2-deficient mice, and the resulting ability to study myeloma growth and the associated bone disease in a genetically modified host microenvironment, is a major advancement in myeloma research and a highly important tool for the myeloma research community.

TRANSLATIONAL IMPACT

Clinical issue

Multiple myeloma is a hematological malignancy that affects approximately 100,000 patients in the USA, with nearly 20,000 new cases diagnosed each year. Myeloma is characterized by the clonal expansion of malignant plasma cells within the bone marrow and the development of a destructive osteolytic bone disease. Despite many advances in the treatment of multiple myeloma, it remains an incurable and fatal malignancy. Myeloma progression and the development of osteolytic bone disease are linked inextricably and depend on cellular interactions within the bone marrow microenvironment. Understanding the bone marrow microenvironment in myeloma is crucial to elucidate the mechanisms involved in disease progression and to identify novel therapeutic targets.

Results

In this study, the authors describe a new murine model of myeloma in which the host microenvironment can be modified genetically. They induced myeloma by inoculating myeloma cells into mice with compromised B- and T-cell development that results from their lack of recombination activating gene 2 (RAG-2). Myeloma-bearing RAG-2$^{-/-}$ mice exhibit tumor growth within the bone marrow and develop osteolytic bone disease. These features are consistent with both human myeloma and an original Radl 5T model for the disease, suggesting that these mice accurately model myeloma. RAG2$^{-/-}$ mice are easily bred with other genetically modified mice to generate myeloma models with genetic modifications to the host microenvironment. The authors use this mouse model to show that deletion of host matrix metalloproteinase 9 reduces the tumor burden and osteolytic bone disease that are associated with myeloma.

Implications and future directions

A major limitation of the current murine models of myeloma is that manipulation of the bone marrow microenvironment, independent of the tumor, is limited to systemic pharmacological reagents. The establishment of myeloma in RAG-2$^{-/-}$ mice permits molecular examination of the host contribution to myeloma pathogenesis in vivo. This sophisticated model should allow for investigation of important questions in myeloma research regarding the relative contribution of host-derived versus tumor-derived factors.

doi:10.1242/dmm.004382

METHODS

Cell culture

The 5TGM1-GFP myeloma cell line was cultured as described previously (Dallas et al., 1999; Oyajobi et al., 2007).

In vivo 5TGM1 myeloma studies

Studies were performed using 8–10-week-old female RAG-2$^{-/-}$, C57BL/6 (Harlan U.S., Indianapolis, IN), C57BL/KaLwRijHsd (Harlan Netherlands, Horst, The Netherlands), or RAG-2$^{-/-}$/MMP-9$^{-/-}$ mice. Studies were approved by the Institution of Animal Care and Use Committee at Vanderbilt University and were conducted in accordance with the National Institutes of Health (NIH) Guide for the Care and Use of Laboratory Animals. Myeloma was propagated in these animals by the intravenous inoculation of 10^6 5TGM1-GFP-tagged myeloma cells in 100 μl of phosphate-buffered saline (PBS). Tumor burden was assessed by serum analysis of the myeloma-specific immunoglobulin IgG2bk, as described previously (Dallas et al., 1999).

Bone histomorphometric analysis

Histomorphometric analysis was performed to quantify bone volume; osteoclast and osteoblast surface area to bone surface area; trabecular number; and trabecular spacing. Tibias and femurs were formalin-fixed, decalcified in 14% EDTA, paraffin-embedded, and sectioned along the mid-sagittal plane in 4 μm-thick sections. To visualize osteoclasts, sections were stained with hematoxylin and eosin, and for TRAP activity. Three non-consecutive sections were evaluated using Osteomeasure histomorphometry software, as described previously (Edwards et al., 2008).

Immunohistochemistry

For MMP-9 and TRAP localization, the following technique was employed: sections were rehydrated through a series of ethanol

solutions and then rinsed in Tris-buffered saline (TBS; 10 mM Tris at pH 7.4, 150 mM NaCl) with Tween 20 (0.05%). For antigen retrieval, slides were immersed in a 20 μg/ml solution of proteinase K, according to the manufacturer's instructions, for 10 minutes at room temperature. Following washing in TBS, tissue sections were blocked using standard blocking criteria for 1 hour at room temperature. MMP-9 antibodies (Oncogene) were added as part of a blocking solution overnight at 4°C at a dilution of 1:100. Slides were washed extensively in TBS with Tween 20 before the addition of a species-specific fluorescently labeled secondary antibody (Alexa Fluor 568 nm, Invitrogen), diluted 1:1000 in blocking solution, for 1 hour at room temperature. Slides were washed in TBS and then equilibrated in an acetate buffer, as described (Filgueira, 2004). The ELF97 TRAP stain (Invitrogen) was diluted 1:1000 in acetate buffer, and slides were incubated for 15 minutes at room temperature. Following washing, slides were aqueously mounted in media (Biomeda Corp.) containing 2 mM DAPI (4′,6-diamidino-2-phenylindole) for nuclear localization.

MicroCT analysis

Cortical bone lesions were measured using microCT analysis on the proximal tibia. Bones were fixed in formalin and scanned at an isotropic voxel size of 12 μm using a microCT40 (SCANCO Medical, Bassersdorf, Switzerland). For analysis of cortical bone lesions, cross-sectional images of the entire metaphysis including the cortices and extending 0.25 mm from the growth plate were imported into Amira 3D graphics software (Mercury Computer Systems, Chelmsford, MA). The Amira software generated a 3D reconstruction of the metaphyses using a consistent threshold. The number of osteolytic lesions that completely penetrated the cortical bone, as seen in the virtual reconstruction, were counted. MicroCT analysis was also performed on the trabecular bone to assess the overall volume and structural characteristics of the trabeculae. Contours were drawn within the cortices of the proximal tibia using the microCT40. The analysis provided a ratio measurement of bone volume to total tissue volume within the cortical bone.

Flow cytometry

Bone marrow was flushed from the tibia and femur of 5TGM1 myeloma-bearing mice. Splenic cells from myeloma-bearing mice were obtained by homogenization in tissue culture media. Cell suspensions from both organs were filtered through a 70 μm filter followed by analysis for GFP fluorescence using a 3-laser BD LSRII (Becton Dickinson, San Jose, CA).

ACKNOWLEDGEMENTS

We thank Kathy Carter from the Department of Cancer Biology for help with the intravenous injections. This work was supported by NCI through P01 CA-40035 (G.R.M.). C.M.E. is supported by the International Myeloma Foundation and the Elsa U. Pardee Foundation. We gratefully acknowledge support from the Vanderbilt University Institute of Imaging Science. We are grateful to Kevin P. Weller and David K. Flaherty for their assistance with flow cytometry. Flow cytometry experiments were performed in the Vanderbilt Medical Center (VMC) Flow Cytometry Shared Resource. The VMC Flow Cytometry Shared Resource is supported by the Vanderbilt Ingram Cancer Center (P30 CA68485) and the Vanderbilt Digestive Disease Research Center (DK058404). Deposited in PMC for release after 12 months.

COMPETING INTERESTS

The authors declare no competing financial interests.

AUTHOR CONTRIBUTIONS

J.A.F., G.R.M., C.C.L. and C.M.E. conceived and designed the experiments; J.A.F., C.C.L. and S.T.L. performed the experiments; J.A.F. analyzed the data; C.C.L. contributed reagents/animals; J.A.F. and C.M.E. wrote the paper.

Received 6 March 2009; Accepted 2 July 2009.

REFERENCES

Asosingh, K., Radl, J., Van Riet, I., Van Camp, B. and Vanderkerken, K. (2000). The 5TMM seies: a useful *in vivo* mouse model of human multiple myeloma. *Hematol. J.* **1**, 351-356.

Barille, S., Akhoundi, C., Collette, M., Mellerin, M. P., Rapp, M. J., Harousseau, J. L., Bataille, R. and Amiot, M. (1997). Metalloproteinases in multiple myeloma: production of matrix metalloproteinase-9 (MMP-9), activation of proMMP-2, and induction of MMP-1 by myeloma cells. *Blood* **90**, 1649-1655.

Barille, S., Bataille, R., Rapp, M. J., Harousseau, J. L. and Amiot, M. (1999). Production of metalloproteinase-7 (matrilysin) by human myeloma cells and its potential involvement in metalloproteinase-2 activation. *J. Immunol.* **163**, 5723-5728.

Budzynski, W. and Radzikowski, C. (1994). Cytotoxic cells in immunodeficient athymic mice. *Immunopharmacol. Immunotoxicol.* **16**, 319-346.

Chesi, M., Robbiani, D. F., Sebag, M., Chng, W. J., Affer, M., Tiedemann, R., Valdez, R., Palmer, S. E., Haas, S. S., Stewart, A. K. et al. (2008). AID-dependent activation of a MYC transgene induces multiple myeloma in a conditional mouse model of post-germinal center malignancies. *Cancer Cell* **13**, 167-180.

Croucher, P. I., Shipman, C. M., Lippitt, J., Perry, M., Asosingh, K., Hijzen, A., Brabbs, A. C., van Beek, E. J., Holen, I., Skerry, T. M. et al. (2001). Osteoprotegerin inhibits the development of osteolytic bone disease in multiple myeloma. *Blood* **98**, 3534-3540.

Croucher, P. I., De Hendrik, R., Perry, M. J., Hijzen, A., Shipman, C. M., Lippitt, J., Green, J., Van Marck, E., Van Camp, B. and Vanderkerken, K. (2003). Zoledronic acid treatment of 5T2MM-bearing mice inhibits the development of myeloma bone disease: evidence for decreased osteolysis, tumor burden and angiogenesis, and increased survival. *J. Bone Miner. Res.* **18**, 482-492.

Dallas, S. L., Garrett, I. R., Oyayobi, B. O., Dallas, M. R., Boyce, B. F., Bauss, F., Radl, J. and Mundy, G. R. (1999). Ibandronate reduces osteolytic lesions but not tumour burden in a murine model of myeloma bone disease. *Blood* **93**, 1697-1706.

Edwards, C. M., Mueller, G., Roelofs, A. J., Chantry, A., Perry, M., Russell, R. G., Van Camp, B., Guyon-Gellin, Y., Niesor, E. J., Bentzen, C. L. et al. (2007). Apomine, an inhibitor of HMG-CoA-reductase, promotes apoptosis of myeloma cells in vitro and is associated with a modulation of myeloma in vivo. *Int. J. Cancer* **120**, 1657-1663.

Edwards, C. M., Edwards, J. R., Lwin, S. T., Esparza, J., Oyajobi, B. O., McCluskey, B., Munoz, S., Grubbs, B. and Mundy, G. R. (2008). Increasing Wnt signaling in the bone marrow microenvironment inhibits the development of myeloma bone disease and reduces tumor burden in bone in vivo. *Blood* **111**, 2833-2842.

Filgueira, L. (2004). Fluorescence-based staining for tartrate-resistant acidic phosphatase (TRAP) in osteoclasts combined with other fluorescent dyes and protocols. *J. Histochem. Cytochem.* **52**, 411-414.

Garrett, I. R., Dallas, S., Radl, J. and Mundy, G. R. (1997). A murine model of human myeloma bone disease. *Bone* **20**, 515-520.

Jemal, A., Tiwari, R. C., Murray, T., Ghafoor, A., Samuels, A., Ward, E. and Feuer Thun, M. J. (2004). Cancer Statistics, 2004. *CA Cancer J. Clin.* **54**, 8-29.

Oyajobi, B. O., Franchin, G., Williams, P. J., Pulkrabek, D., Gupta, A., Munoz, S., Grubbs, B., Zhao, M., Chen, D., Sherry, B. et al. (2003). Dual effects of macrophage inflammatory protein-1alpha on osteolysis and tumor burden in the murine 5TGM1 model of myeloma bone disease. *Blood* **102**, 311-319.

Oyajobi, B. O., Munoz, S., Kakonen, R., Williams, P. J., Gupta, A., Wideman, C. L., Story, B., Grubbs, B., Armstrong, A., Dougall, W. C. et al. (2007). Detection of myeloma in skeleton of mice by whole-body optical fluorescence imaging. *Mol. Cancer Ther.* **6**, 1701-1708.

Radl, J., de Glopper, E., Schuit, H. E. R. and Zurcher, C. (1979). Idiopathic paraprotienemia II. Transplantation of the paraprotein-producing clone from old to young C587Bl/KaLwRij mice. *J. Immunol.* **122**, 609-613.

Radl, J., Croese, J. W., Zurcher, C., Van Den Enden-Vieveen, M. H. M. and Margreet de Leeuw, A. (1988). Animal model of human disease; multiple myeloma. *Am. J. Pathol.* **132**, 593-597.

Shinkai, Y., Rathbun, G., Lam, K. P., Oltz, E. M., Stewart, V., Mendelsohn, M., Charron, J., Datta, M., Young, F., Stall, A. M. et al. (1992). RAG-2-deficient mice lack mature lymphocytes owing to inability to initiate V(D)J rearrangement. *Cell* **68**, 855-867.

Vacca, A., Ribatti, D., Iurlaro, M., Albini, A., Minischetti, M., Bussolino, F., Pellegrino, A., Ria, R., Rusnati, M., Presta, M. et al. (1998). Human lymphoblastoid cells produce extracellular matrix-degrading enzymes and induce endothelial cell proliferation, migration, morphogenesis, and angiogenesis. *Int. J. Clin. Lab. Res.* **28**, 55-68.

Vacca, A., Ribatti, D., Presta, M., Minischetti, M., Iurlaro, M., Ria, R., Albini, A., Bussolino, F. and Dammacco, F. (1999). Bone marrow neovascularization, plasma cell angiogenic potential, and matrix metalloproteinase-2 secretion parallel progression of human multiple myeloma. *Blood* **93**, 3064-3073.

Van Valckenborgh, E., Mincher, D., Di Salvo, A., Van Riet, I., Young, L., Van Camp, B. and Vanderkerken, K. (2005). Targeting an MMP-9-activated prodrug to multiple myeloma-diseased bone marrow: a proof of principle in the 5T33MM mouse model. *Leukemia* **19**, 1628-1633.

Yaccoby, S., Barlogie, B. and Epstein, J. (1998). Primary myeloma cells growing in SCID-hu mice: a model for studying the biology and treatment of myeloma and its manifestations. *Blood* **92**, 2908-2913.

Yaccoby, S., Wezeman, M. J., Henderson, A., Cottler-Fox, M., Yi, Q., Barlogie, B. and Epstein, J. (2004). Cancer and the microenvironment:Myeloma-osteoclast interactions as a model. *Cancer Res.* **64**, 2016-2023.

Yaccoby, S., Ling, W., Zhan, F., Walker, R., Barlogie, B. and Shaughnessy, J. D., Jr (2007). Antibody-based inhibition of DKK1 suppresses tumor-induced bone resorption and multiple myeloma growth in vivo. *Blood* **109**, 2106-2111.

Bone 48 (2011) 44–53

Contents lists available at ScienceDirect

Bone

journal homepage: www.elsevier.com/locate/bone

Review

Matrix metalloproteinases as master regulators of the vicious cycle of bone metastasis

Conor C. Lynch *

Department of Orthopaedics and Rehabilitation, Vanderbilt University, Nashville, TN, 37232, USA

ARTICLE INFO

Article history:
Received 10 May 2010
Revised 7 June 2010
Accepted 9 June 2010
Available online 16 June 2010

Edited by: T. Jack Martin

Keywords:
Bone metastasis
Osteoblast
Osteoclast
MMPs
Vicious cycle
Prostate cancer
Breast cancer
Tumor–host microenvironment
PTHrP
RANKL
TGFβ
VEGF

ABSTRACT

Bone remodeling is a delicate balancing act between the bone matrix synthesizing osteoblasts and bone resorbing osteoclasts. Active bone metastases typically subvert this process to generate lesions that are comprised of extensive areas of pathological osteogenesis and osteolysis. The resultant increase in bone matrix remodeling enhances cytokine/growth factor bioavailability thus creating a vicious cycle that stimulates tumor progression. Given the extent of matrix remodeling occurring in the tumor–bone microenvironment, the expression of matrix metalloproteinases (MMPs) would be expected, since collectively they have the ability to degrade all components of the extracellular matrix (ECM). However, in addition to being "matrix bulldozers", MMPs control the bioavailability and bioactivity of factors such as RANKL and TGFβ that have been described as crucial for tumor–bone interaction, thus implicating MMPs as key regulators of the vicious cycle of bone metastases.

Contents

Introduction . . . 45
The "vicious cycle" . . . 45
Cellular sources of MMPs in the metastatic tumor–bone microenvironment . . . 45
MMPs derived from cancer metastases . . . 45
Osteoblast-derived MMPs . . . 46
Osteoclast derived MMPs . . . 46
Other cellular sources of MMPs in the tumor–bone microenvironment . . . 46
MMP regulation of the vicious cycle . . . 46
PTHrP . . . 46
ET-1 . . . 47
EGFR ligands . . . 47
Wnts . . . 48
Interleukins . . . 48
RANKL . . . 48
TGFβ . . . 48
IGFs . . . 49
VEGF-A . . . 49

* Department Of Orthopaedics and Rehabilitation, Vanderbilt University Medical Center East, South Tower, Suite 4200, Nashville, TN, 37232-8774, USA. Fax: +1 615 343 1028.
E-mail address: conor.lynch@vanderbilt.edu.

8756-3282/$ – see front matter © 2010 Elsevier Inc. All rights reserved.
doi:10.1016/j.bone.2010.06.007

Post-translational modification by MMPs—a delicate balancing act . . . 49
MMP inhibitors—a clinically relevant approach for the treatment of bone metastases? . . . 50
Summary . . . 51
Acknowledgments . . . 51
References . . . 51

Introduction

Bone is a frequent site of metastasis for several cancers. For example, in 2010, the American Cancer Society predicts that approximately 65,000 men and women combined will succumb to breast and prostate cancer and studies predict that 80–90% of these patients will have evidence of bone metastasis at the time of their death [1–3]. Bone metastases are often termed as either osteolytic or osteogenic but in reality, the lesions contain areas of extensive bone formation and resorption with the balance on the whole tipped toward osteolysis or osteogenesis. Bone metastases cause skeletal related events for the patient including hypercalcemia and spontaneous pathologic bone fracture that can cause intense pain and greatly impact the patient's quality of life [4,5]. Currently, the treatment options for these patients are mainly palliative and limited to surgery, radiation and chemotherapies such as bisphosphonates [6]. While bisphosphonates have been successful in "caging" the metastases by targeting the osteoclasts, bone metastases remain incurable and only by understanding the factors that regulate and facilitate tumor–bone interaction can new, more efficient therapies be generated.

The "vicious cycle"

The model that best describes our understanding of tumor–bone interaction is the 'vicious cycle' and was conceptualized by pioneers in the tumor–bone microenvironment field by researchers such as Dr. Gregory Mundy [7]. The cycle is commonly described as containing the following elements; (a) metastasis derived signals stimulate bone lining osteoblasts to proliferate and/or differentiate. Parathyroid hormone related protein (PTHrP) derived from the cancer metastases, has been traditionally identified as a mediator of this process [8,9]. Wnts, bone morphogenetic proteins (BMPs), fibroblast growth factors such as FGF-9, endothelins, interleukins (ILs) such as IL-1, IL-6 and IL-8, and epidermal growth factor receptor (EGFR) ligands such as transforming growth factor alpha (TGF-α) have also been implicated in the initiation of osteolytic and osteogenic lesions [10–16]. (b) In response to signals derived from the metastases the bone lining osteoblasts express osteoclastogenic factors such as receptor activator of nuclear kappa B ligand (RANKL) [17]. The presentation of membrane bound RANKL is a critical step for the recruitment and activation of osteoclast precursors [18]. (c) RANKL in turn promotes the maturation of those precursors into active multinucleated osteoclasts. The osteoclast subsequently forms a resorptive seal on the mineralized matrix surface and, via acidification and the secretion of acidophilic proteases such as cathepsin-K (cat-K), mediates the process of bone resorption [19,20]. (d) Since bone is rich in matrix sequestered growth factors such as transforming growth factor β (TGFβ) and insulin like growth factor-I (IGF-I), resorption by the osteoclasts results in the increased bioavailability of TGFβ and IGF-I. The osteoclast is also a major mediator of angiogenesis in the bone microenvironment via the regulation of vascular endothelial growth factor-A (VEGF-A) bioavailability. Taken together, these osteoclast generated factors facilitate the growth and expansion of the metastases thus completing the vicious cycle [7,21].

While the stepwise pattern of the vicious cycle paradigm is a straightforward interpretation of cellular interactions in the tumor–bone microenvironment, clearly many other cell types can influence tumor–osteoblast–osteoclast interaction. For example, tumor cells can often act as surrogate osteoblasts in directly inducing osteoclastogenesis and bone resorption; the cyclical process can be multidirectional in that the factors released from the bone matrix cannot only stimulate tumor growth but can also have profound effects on the osteoblast compartment and; in reciprocal interactions, the osteoblasts undoubtedly can also impact the cancer cell behavior in the bone microenvironment. Regardless of autonomous, juxtacrine and paracrine signaling, the factors that control the vicious cycle are obvious therapeutic targets. However, despite recent advances in the identification of the complex controls that govern tumor–bone interaction, we are still at the beginning of our understanding. Furthermore, exactly how these factors are regulated at a post translational level remains largely unexplored but new studies point to proteinases such as the MMPs as being key regulators of the bioavailability and bioactivity of factors that drive osteolytic and osteogenic bone metastases.

Cellular sources of MMPs in the metastatic tumor–bone microenvironment

In order to accommodate the expansion of the metastases, remodeling of the bone matrix is required and unsurprisingly, proteinases including the matrix metalloproteinases (MMPs) are highly expressed in the tumor–bone microenvironment. The MMPs are a family of 23 extracellular, zinc-dependent proteinases that collectively can degrade all components of the extracellular matrix (ECM) [22]. MMPs are a subset of the metazincin family of proteases that include metalloproteinases such as a disintegrin and metalloproteinases (ADAMs), ADAMS with thrombospondin motifs (ADAMTS) and others such as neprilysin. MMP activity is regulated by endogenous inhibitors of MMPs known as tissue inhibitor of metalloproteinases (TIMPs) of which there are four [23].

MMPs are expressed in numerous tumor–microenvironments and pioneering work from Liotta and other groups in the early 1970s implicated roles for MMPs in cancer invasion and metastasis due to their ability to degrade the ECM. Logically, MMPs can play a role in the processing of type I collagen-rich osteoid and other bone matrix components since several have type I collagenase activity including but not limited to, MMP-1, MMP-2 and MMP-14. Osteoclasts, which are the principal cells involved in the resorption of the bone matrix, primarily use the acidophilic cat-K to process the type I collagen. Given the pH activity profile of the MMPs, i.e. close to neutrality, it is thought that MMPs may not function directly in the resorption lacunae of the osteoclast but may assist in the polishing of the resorbed bone and in the degradation of non-mineralized osteoid after the exit of the osteoclasts. The role of MMPs in direct bone matrix resorption has been elegantly discussed by Delaisse and colleagues [20,24,25].

MMPs derived from cancer metastases

MMPs can be derived from a number of cellular sources in the tumor–bone microenvironment, in particular the main cellular players involved in the vicious cycle, i.e. the metastatic cancer cells, the osteoblasts and osteoclasts. In animal models and humans, several MMPs have been noted as being expressed by the cancer cells. The

expression of MMP-2, -3, -9, -12, -13 and -14 has been noted in the prostate tumor–bone microenvironment [26–29] while MMP-2 and MMP-13 have also been identified as being expressed by breast cancer cells in bone [30,31]. Moreover, MMP-1 and the metalloproteinase, ADAMTS1 have been shown to be expressed by osteotropic human breast cancer cell lines [32]. Many of these studies have identified causal roles for tumor derived MMPs in the bone microenvironment, but as we shall discuss, these roles are often not dependent on the matrix degrading ability of the MMP in question.

Osteoblast-derived MMPs

Bone is primarily comprised of type I collagen (>90%) which is mineralized via the deposition of apatite during its synthesis by osteoblasts. In addition to type I collagen, the osteoblasts also incorporate latent growth factors into the matrix, most notably TGFβ and IGF-I that subsequently serve as pivotal cellular cues during bone remodeling [33]. Given the role of osteoblasts in building the bone, it is somewhat counterintuitive that they also express a number of matrix degrading MMPs including MMP-2, MMP-3, MMP-8, MMP-9, MMP-13 and MMP-14 [34–40]. However, developmental studies of MMP null animals have defined important roles for osteoblast derived MMPs. For example, MMP-2 null mice have been shown to have impaired skeletogenesis during development leading to significant delays in bone formation. These unexpected findings can in part be explained by the necessity of MMP-2 for osteoblast differentiation [41]. While MMP-2 has type I collagenase activity, the exact mechanism through which osteoblast derived MMP-2 contributes to osteoblast function is unknown. MMP-14 is an important mediator of MMP-2 activation and therefore, skeletal abnormalities in MMP-14 null animals are consistent with those of the MMP-2 null mice [42,43]. MMP-13 is considered to be the human ortholog of human MMP-1. MMP-13 collagenase activity has been identified as rate limiting for organic bone matrix degradation during development since MMP-13 null animals have abnormalities in their growth plates and exhibit thickened trabecular bone compared to wild type controls [44,45].

Developmental studies in MMP-3 and MMP-8 and null animals have not indicated roles in bone development or in osteoblast biology although MMP-8 may be important in bone remodeling [46]. Surprisingly, many of the skeletal phenotypes noted in MMP null mice during development, with the exception of MMP-14, are transient and have resolved by young adulthood. The resolution or absence of a skeletal phenotype raises the important question whether these MMPs would then play a role in the pathology of the tumor–bone microenvironment. However, it is noteworthy that many MMP phenotypes only become manifest in injury or disease settings despite the presence of other MMPs that share a substrate overlap. As a case in point, our group has identified that osteoclasts are a primary source of MMP-7, yet MMP-7 null mice have no overt bone phenotype. However, in the breast and prostate tumor–bone microenvironment we have conclusively shown in two separate studies that host/osteoclast derived MMP-7 significantly contributes to tumor induced osteolysis [47,48]. Therefore, the absence of a persistent bone phenotype in the MMP null animals does not necessarily rule out that those MMPs play important roles in the tumor–bone microenvironment.

Osteoclast derived MMPs

Despite the important role for cat-K in osteoclast mediated bone resorption, osteoclasts express MMP-3, -7, -9, -10, -12 and -14 [47,49–51] and intuitively, one would surmise roles for these MMPs in direct osteoclast mediated bone matrix resorption. However, as discussed, the optimal pH for cathepsin K activity is pH 4, which is appropriate for the acidic environment of the sub-osteoclast zone undergoing resorption while many of the MMPs have optimal activities at a more neutral pH [52,53]. Presumably, MMPs are secreted to areas outside of the resorption lacuna and are active in the bone microenvironment since our studies and others have defined roles for MMPs in the bone using MMP null animals [41,44,47,48,54]. This raises the question as to what the exact functions for osteoclast derived MMPs are.

Other cellular sources of MMPs in the tumor–bone microenvironment

In addition to the cancer cells, osteoblasts and osteoclasts, the bone microenvironment contains a myriad of cell types that can express MMPs and factors that may modulate the vicious cycle. For example, macrophages that are derived from the same progenitors as osteoclasts express MMP-1, -2, -7, -9 and -12 while neutrophils are a noted source of inhibitor free MMP-9 [55–59]. Furthermore, recent studies have begun to highlight the importance of immune cells such as T-cells in the regulation of bone remodeling [60,61]. T-cells are often overlooked in the context of the tumor–bone microenvironment since the animal models utilized to study bone metastases are typically immunocompromised. However, cell lines such as 4 T1 and those derived from the polyoma virus middle T antigen of mammary tumorigenesis are now allowing researchers to begin studying the effects of T-cells using immunocompetent Balb/c and FVB mice respectively [48,62]. T-cells have been identified as potent producers of multiple cytokines and ligands that can control cell behavior and are a noted source of MMPs [63,64]. Collectively, these studies identify that MMPs can be derived from various cellular sources that can play a role in the vicious cycle.

MMP regulation of the vicious cycle

Traditionally, research on MMPs in cancer progression focused on steps relating to invasion and metastasis because of the described roles in ECM degradation. However, in the past decade and a half, MMPs have clearly been shown to impact many aspects of cancer progression such as initiation, proliferation and apoptosis by virtue of their ability to regulate the bioactivity and bioavailability of non-matrix molecules such as growth factors and cytokines [22]. However, in the context of the tumor–bone microenvironment, outside of roles in bone matrix remodeling, relatively little is known about whether MMP activity affects the vicious cycle by regulating the factors that drive it, but emerging evidence in the literature has shed light on the area (Fig. 1).

PTHrP

Arguably, one of the most well defined factors involved in initiating the vicious cycle is PTHrP [8,9]. PTHrP is often associated as being responsible for the induction of lytic bone metastases [7,65]. There is also evidence that PTHrP can play important roles in prostate cancer induced osteolytic and osteogenic changes [66–68]. PTHrP can promote osteoclastogenesis indirectly by stimulating osteoblasts to express RANKL [69]. The PTHrP gene gives rise to three splice variants that are 139, 141 and 173 amino acids in length and these variants mediate their effects through PTH receptor 1 (PTHR1) [70]. Interestingly, PTHrP can be proteolytically processed into numerous fragments that have putative biological effects. Surprisingly, no MMP has been identified as mediating PTHrP processing to date but the metalloproteinase member neprilysin, in addition to the serine proteases furin and prostate serum antigen (PSA)/kallikrien-3, can process PTHrP [71–75]. The action of these enzymes results in the generation of multiple PTHrP fragments including but not limited to $PTHrP_{1–26}$, $PTHrP_{27–36}$, $PTHrP_{1–36}$ and $PTHrP_{107–139}$. At this point it is not entirely clear how PTHrP derived fragments elicit their proposed effects. While some fragments may still bind to PTHR1 it is plausible that other, as yet unidentified receptors may also be targeted. For

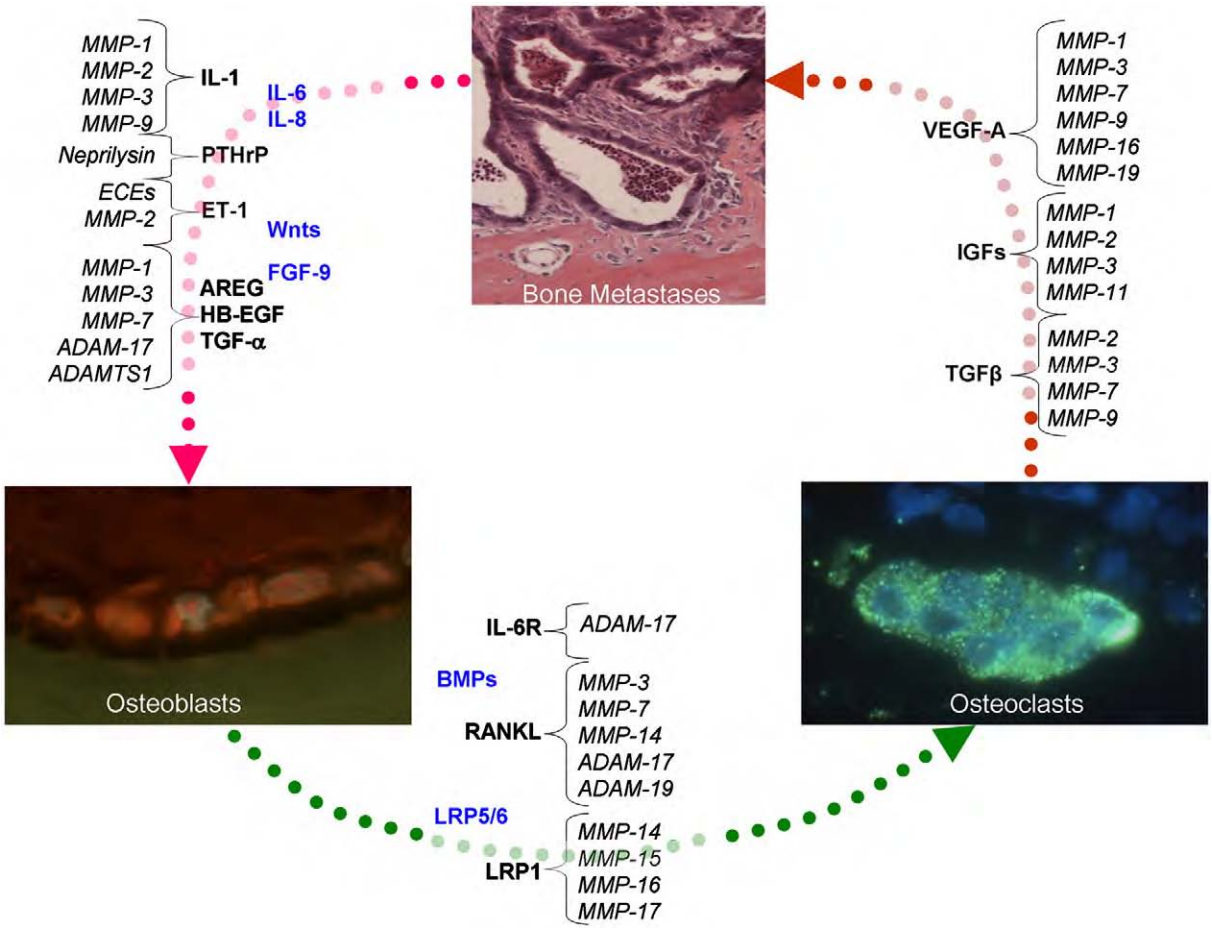

Fig. 1. MMPs as master regulators of the vicious cycle of bone metastases. MMP processing of factors that drive the vicious cycle often result in a bioactive molecule or an alteration in how the effects of the factor are executed. Importantly, the MMPs illustrated here can be derived from multiple cellular sources and only key factors are shown. Furthermore, the cell–cell signaling can work both in an auto-/bi-/poly-directional manner. Factors in blue have not been identified as MMP substrates to date. Unpublished micrographs courtesy of the author.

example, $PTHrP_{1-26}$ has sequence similarities to endothelin-1 (ET-1) and therefore $PTHrP_{1-26}$ may mediate cell signaling via the endothelin-A receptor (ET_A) [76]. Therefore, protease-mediated PTHrP processing has the potential to impact (positively and/or negatively) the behavior of osteoblasts and other cell types in the tumor–bone microenvironment.

ET-1

In a bid to determine tumor derived factors that stimulate osteogenic metastases, Guise and colleagues identified that a key difference in conditioned media derived from breast cancer cell lines (ZR-75-1, T47-D and MCF-7) known to induce osteogenic metastases in nude mice and breast cancer cells known to induce osteolytic metastases (MDA-MB-231) was the level of endothelin-1 (ET-1). Subsequently, ET-1 was found to stimulate osteogenic lesions via the activation of the ET_A receptor on the surface of osteoblasts and further, blocking ET_A activity with inhibitors was demonstrated to be efficacious in preventing tumor induced osteogenesis [12]. ET-1 is produced as Big Endothelin-1 (Big ET-1) and requires conversion to an active 21 amino acid form. The process of activation is controlled by the metalloproteinase members endothelin converting enzymes (ECEs) [77]. However, MMP-2 has also been described as generating functional ET-1 from Big ET-1, and ET-1 in turn can induce the expression of MMPs such as MMP-2 and MMP-9 [78,79]. Therefore, the expression of osteoblast or tumor derived MMP-2 can potentially contribute to the generation of active ET-1 in the tumor–bone microenvironment leading to the formation of osteogenic metastases.

EGFR ligands

Using isolated osteotropic MDA-MB-231 breast cancer clones, Kang and colleagues identified a subset of genes that were differentially expressed in comparison to the parental cell line [80]. These genes included MMP-1 and ADAMTS1 and the group explored the role of these proteinases in the process of breast to bone metastasis and, in particular, whether or not they played a causal role in tumor progression in the bone microenvironment. To this end silencing of MMP-1 and ADMATS1 expression significantly abrogated the ability of the cells to metastasize to bone and, of the tumors that did establish in the bone microenvironment, a dramatic decrease in the number of osteoclasts at the tumor bone interface was noted [32]. Since MMP-1 has the ability to process native fibrillar type I collagen, one would expect that tumor–derived MMP-1 may be important in the direct processing of the bone matrix. However, analysis of the conditioned media of the osteophilic cell lines demonstrated that MMP-1 and ADAMTS1 enhanced the solubilization of EGFR ligands such as amphiregulin (AREG), heparin bound EGF (HB-EGF) and TGF-α. Activation of the EGFR in osteoblasts leads to a suppression of the RANKL soluble inhibitor osteoprotegerin (OPG). The suppression of OPG tipped the ratio of RANKL:OPG in favor of RANKL thus leading to enhanced osteoclastogenesis and increased bone resorption. In addition, the ability of established EGFR inhibitors such as cetuximab

and gefitinib to reduce the ability of the MDA-MB-231 clones to form aggressive bone metastases was demonstrated [32]. These data illustrate how tumor-derived metalloproteinases such as MMP-1 and ADAMTS1 cannot only mediate homing to bone but also induce bone resorption through the production of soluble factors such as EGFR ligands. Interestingly, the impact of these metalloproteinases on tumor progression in the bone required the expression of both genes since individual silencing did not significantly affect the ability of the cells to metastasize or establish in the bone. Therefore, it is possible that although *in vitro*, these MMPs can mediate the shedding of EGFR ligands, they are also capable of activating other MMPs that can play a role in mediating tumor progression in bone. For example, MMP-1 has been identified as an activator of MMP-2 [81] and the forced overexpression of MMP-2 or the endogenous tissue inhibitor of metalloproteinase-2 (TIMP-2) in the cancer cells can promote or protect against tumor mediated bone destruction, respectively [31,82,83]. The exact mechanism through which MMP-2 mediates this effect is unknown but MMP-2 has been demonstrated to process numerous growth factors, cytokines and receptors [84]. In the *in vivo* microenvironment, EGFR ligands generated by the tumor cells may also be subject to direct proteolytic cleavage by other MMPs. For example, HB-EGF has been shown to be processed by MMP-3 and MMP-7 which are expressed by osteoblasts and osteoclasts respectively [85,86]. Therefore, while MMPs can directly mediate the solubilization of a substrate *in vitro*, it is possible that host derived MMPs *in vivo* can also regulate the bioavailability of EGF ligands.

Wnts

Wnt ligands and canonical wnt signaling pathways are key regulators of osteoblast behavior with respect to differentiation and bone development and play a particularly important role in osteogenic bone metastases [87]. Wnts mediate their effect via signaling through the co-receptors Frizzled and low-density lipoprotein receptor-related proteins (LRPs). Primary prostate and breast cancer and cell lines have been shown to express Wnts, and Wnt expressing bone metastases have the ability to control osteoblast behavior, hence bone formation [10]. Interestingly, inhibitors of Wnt signaling such as dickkopf-1 (DKK-1) prevent ligand interaction with the Frizzled/Lrp5/6 receptors and are expressed at high levels by prostate tumor cells in the bone [87]. Keller and colleagues posit that the expression of DKK-1 during early prostate tumor establishment in the bone prevents Wnt signaling but induces RANKL expression in osteoblasts resulting in enhanced osteoclast maturation and bone degradation. Subsequently as the prostate cancer cells grow in bone, levels of DKK-1 decrease allowing for Wnt mediated bone formation. MMP-2, -3, -7, -9, -13 and -14 have been identified as downstream targets of Wnts [88,89]. While MMPs have not been shown to directly modify the activity of Wnt ligands, there is evidence to suggest that MMPs can function in altering Wnt signaling. LRP1 can bind to Frizzled but, unlike LRP5/6, the interaction abrogates signaling via this pathway [90]. Furthermore, LRP1 can be processed by MMP-14, -15, -16, -17 and as a result, the expression of these MMPs on the surface of osteoblasts in the tumor–bone microenvironment may have a profound effect on Wnt signaling [91]. As research in this area continues it will be exciting to see whether other MMPs can affect the Wnt signaling axis, either by modifying the effects of the Wnt ligands or by docking with and/or processing the cognate Wnt receptors.

Interleukins

In vitro and *in vivo* analyses have identified interleukins (ILs) such as IL-1β, IL-6 and IL-8 as influencing the behavior of several cell types in the tumor–bone microenvironment [13,16,92]. Interleukins have long been known to stimulate MMP expression [39]. As is the case with Wnts, MMPs have not been show regulate the bioactivity of the majority of interleukins in the tumor–bone microenvironment but exceptions do exist. MMP-2, -3 and -9 process the proform of IL-1β into a soluble active form and this form mediates osteoclastogenesis in an IL-6 dependent manner [93]. IL-6 is a pleiotropic inflammatory cytokine involved in promoting tumor proliferation and angiogenesis, with its effects mediated via the IL-6 receptor (IL-6R) and the co-receptor molecule gp130. The IL-6R can be solubilized from the cell surface, a process that is dependent on ADAM-17 activity, and the sIL-6R amplifies the effect of IL-6 [92,94]. IL-8 can mediate osteoclastogenesis in a RANKL independent manner adding a layer of complexity to our understanding of how bone metastases elicit osteolytic responses [13]. While IL-8 can induce the expression of MMPs in various cell types, relatively little is know at this juncture as to whether the IL-8 signaling axis is subject to post-translational modification by MMPs.

RANKL

RANKL, a member of the tumor necrosis factor (TNF) family, is a type II transmembrane protein typically expressed by osteoblasts in the bone microenvironment [18]. RANKL is an essential mediator of osteoclast maturation since RANKL-null mice have thickened bones due to a lack of bone resorbing osteoclasts [18]. The effect of RANKL on osteoclast maturation is attenuated by a soluble decoy receptor known as osteoprotegerin (OPG) that prevents the interaction between RANKL and the receptor RANK on the osteoclast precursor cell surface [95]. In the metastatic tumor–bone microenvironment, tumor-derived factors such as PTHrP induce RANKL expression in osteoblasts thereby leading to the activation of osteoclasts and the induction of osteolysis [17,69]. Interestingly, RANKL can also be expressed by metastatic prostate tumors and has been demonstrated to mediate direct tumor induced osteoclastogenesis [96]. The direct interaction of membrane bound RANKL expressed by osteoblasts and/or tumor cells with RANK expressing osteoclast precursor cells is posited to be the principal mechanism of RANKL mediated osteoclast maturation.

RANKL exists as a trimeric molecule on the cell surface supported by a juxta-membrane stalk region. However, our group and others have documented that RANKL is sensitive to cleavage at variable sites within the juxtamembrane region by metalloproteinase family members, MMP-1, MMP-3, MMP-7, MMP-14 a disintegrin and metalloproteinase-17 (ADAM-17) and ADAM-19 [47,97–99]. In the host cells of the bone, these metalloproteinases with the exception of MMP-7 are typically expressed by osteoblasts while prostate cancer expression of MMP-14 can also mediate the solubilization of RANKL [28]. Therefore, osteoblast and osteoclast expression of MMPs in response to the metastatic prostate tumor cells in the bone by factors such as PTHrP may not only serve to induce RANKL but also the MMPs that are capable of solubilizing RANKL. While the potency of MMP solubilized RANKL may vary depending on the cleavage site, the exact role of soluble RANKL versus membrane bound RANKL remains controversial [47,100] but clearly MMP solubilized RANKL can (a) act as a chemotactic factor for osteoclast precursors and (b) circumvent the necessity for direct osteoblast/osteoclast precursor interaction in the prostate tumor–bone microenvironment. Obviously, the effects of full length and sRANKL are still dependent on the levels of OPG but as discussed earlier, the shedding of EGFR ligands by metalloproteinases can inhibit OPG expression thus allowing for full length or soluble RANKL to execute osteoclastogenesis.

TGFβ

TGFβ has been shown to have pleiotropic effects on metastatic cancer cells, osteoblasts and osteoclasts. During bone matrix synthesis by osteoblasts, TGFβ (primarily, isoform type 1) is co-expressed with a latency associated peptide (LAP) and is incorporated into the bone

matrix in an inactive state via latent TGFβ binding proteins (LTBPs) and decorin and as a result requires activation by proteolytic processing [101,102]. BMPs are members of the TGFβ superfamily that are potent regulators of osteoblast differentiation and are also thought to play a role in the "osteomimicry" noted in some bone metastases, particularly those of a prostate origin [103]. Surprisingly, BMPs are not subject to the same limitations with respect to the sequestration of their activity and it is not yet clear if MMPs play a role in regulating BMP bioactivity. However, the complex proteins that sequester TGFβ in a latent state are susceptible to processing by several MMPs [104]. MMP-2, MMP-3 and MMP-9 mediate the release of TGFβ from either LTBP molecules and/or the LAP molecule [105–108] while MMP-2, MMP-3 and MMP-7 can process decorin thus releasing sequestered TGFβ [109]. Active TGFβ has been shown to (a) support tumor growth by activating TGFβ receptors (TβR) on the tumor cell surface in multiple studies [110–113]; (b) mediate osteoblast retraction from the bone surface thereby providing the osteoclasts with access to the mineralized matrix [114]; (c) mediate osteoclast differentiation and activation [112,115,116]; and (d) modulate the expression of osteoblast like genes in the tumor cells such as RUNX2, RANKL, OPG and bone sialoprotein thereby rendering them "osteomimetic" [103,117]. These studies therefore imply that the MMPs responsible for the activation of TGFβ in the tumor–bone microenvironment are critical for the progression bone metastases.

IGFs

The bone matrix is also rich in insulin like growth factors and in a similar manner to TGFβ, the IGFs can be sequestered in a latent state by IGF binding proteins (IGF-BPs) that require processing in order to release the active ligand. In addition to promoting prostate cancer growth, IGF-I is an important regulator of osteoblast differentiation and osteoclastogenesis [118–120]. MMP-1, -2 and -3 process the major IGF-binding proteins, IGF-BP2, 3 and 5 [121–123] while IGF-BP1 has been identified as a substrate for MMP-11 [124]. IGF-BPs directly bind to IGFs and prevent the interaction of IGFs with the IGF receptor (IGF-R). Therefore, MMP processing of IGF-BPs can significantly alter the levels of bioavailable IGF-I and subsequently assist in driving tumor growth in bone.

VEGF-A

The VEGF family encompasses a number of ligands (VEGF-A, -B, -C, -D and -E as well as placental growth factor) [125]. VEGF-A has several isoforms with VEGF-A_{164} (VEGF-A_{165} in humans) being arguably the most studied. VEGF-A_{164} is a powerful stimulator of angiogenesis and is a critical component for the progression of many tumors including bone metastases [126]. In the bone microenvironment studies using a VEGF receptor inhibitor have identified that VEGF was important for osteoclast maturation both *in vitro* and *in vivo* [127]. Furthermore, BMP-7 has been shown to induce the expression of VEGF-A in the tumor cells and that VEGF-A subsequently contributed to osteoblast differentiation and mineralization [128].

VEGF-A_{164} is complexed to the extracellular matrix and requires proteolytic release in order to become bioavailable [129]. In the tumor–bone microenvironment, the osteoclast has recently come under scrutiny as a major facilitator of angiogenesis and a number of studies point to MMP-9 being critical for mediating the release of VEGF-A_{164} from the bone matrix [21,130–132]. In development, MMP-9 expression by osteoclasts is critical for their invasion into developing long bones, and MMP-9 mediated release of VEGF-A (presumably the VEGF-A_{164} isoform) is the principal molecular mechanism underlying this effect [54]. Recently, Roodman and colleagues have defined the osteoclast as being vital for angiogenesis in an MMP-9 dependent manner [132]. Treatment of metatarsal explants with RANKL and PTH stimulated an increase in blood vessel density in wild type controls but not in MMP-9 null explants. Again, MMP-9 was implicated in osteoclast migration, invasion and angiogenesis, presumably via an increase in the amount of bioavailable VEGF-A, as the mechanism mediating these effects. Our group has also defined osteoclast derived MMP-9 as mediating angiogenesis in the prostate tumor–bone microenvironment [130]. We observed that in human samples of prostate to bone metastasis, the osteoclasts are a major source of MMP-9 while surprisingly, the human cancer metastases were rarely positive for this MMP. Using wild type and MMP-9 null mice we observed that osteoclast derived MMP-9 did not contribute to prostate tumor induced osteolytic or osteogenic changes in our animal model, but did contribute to tumor growth by promoting angiogenesis. Wild type and MMP-9 null osteoclast cultures had significant differences in the amount of bioavailable VEGF-A_{164} and conditioned media from the MMP-9 null osteoclasts did not stimulate endothelial sprouting in an aortic ring assay to the same extent as those treated with conditioned media derived from wild type control osteoclast cultures. Important roles for host MMP-9 in mediating angiogenesis in bone have also been defined [131]. Therefore, it appears that osteoclast derived MMP-9 is a key mediator of angiogenesis in the tumor–bone microenvironment by regulating the bioavailability of VEGF-A_{164}. It is noteworthy that MMP-9 does not mediate the direct release of VEGF-A_{164} but does so by activating other proteinases and/or processing factors that sequester it in the matrix such as connective tissue growth factor (CTGF) and in addition, other MMPs can also impact the bioavailability of VEGF-A [133,134]. Vascularization of the tumor–bone microenvironment has rarely been studied and is a key requirement for the perpetuation of tumor growth in bone.

Post-translational modification by MMPs—a delicate balancing act

Collectively, these studies demonstrate the importance of MMPs in regulating the bioavailability and bioactivity of growth factors in the tumor–bone microenvironment that drive the vicious cycle of bone metastasis and the MMP substrates described herein most likely represent only the "tip of the iceberg." Caveats to the supposition that MMPs are master regulators of the vicious cycle exist (Fig 2). (a) A number of endogenous checks and balances are in place that dictate whether MMP processing of a particular substrate occurs and whether subsequently that the product generated by MMP processing can execute the desired biological effect. For example, although MMPs are highly expressed in the tumor–bone microenvironment, high levels of TIMPs may prevent the MMPs from mediating their biological effects. Furthermore, TIMPs have been shown to have biological effects other than MMP inhibition, and it remains unknown whether TIMPs can counteract MMP functions by stimulating the expression of inhibitors of MMP generated cytokine and growth factor products. It should also be noted that MMP processing of a cytokine/growth factor substrate can also lead to attenuation or inactivation of biological activity. For example, MMP-2 inactivates chemokine ligand 12/stromal derived factor 1 (CXCL12/SDF-1) thereby preventing the activation of the cognate receptor CXCR4 [135]. (b) Even if MMPs are able to increase the bioavailability of the growth factors and cytokines that control the vicious cycle, endogenous inhibitors of the factor, for example OPG, noggin or DKK-1 must be at a sufficiently low level in order for the cytokine/growth factor to mediate its biological effect. (c) The temporal and spatial expression of the MMPs is critical in mediating specific cellular effects. For example, it is not clear at this juncture whether a tumor-derived MMP can act as a surrogate for MMPs not expressed by host cells such as osteoblasts and osteoclasts. (d) MMPs share many similar substrates, and functional redundancy may exist, but the question remains whether the right MMP from the right cellular source is present at the right location in order to mediate a specific effect? Finally, just because we can demonstrate that a factor of interest is an MMP substrate *in vitro* and that the processed form has biological activity, we are still uncertain whether in the *in vivo* tumor–bone microenvironment, the putative mechanism is able to execute the proposed effect. These caveats reinforce the idea of

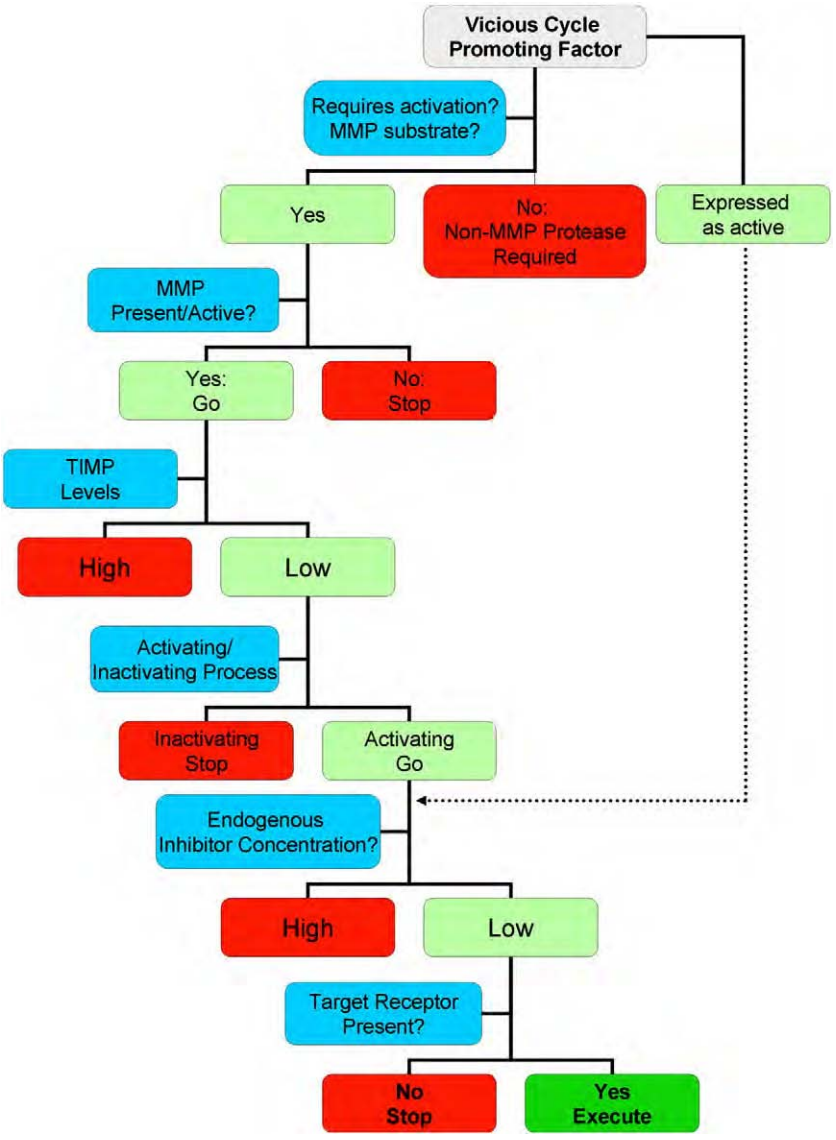

Fig. 2. Flow-chart of post-translational regulation of vicious cycle driving factors by MMPs. If the putative factor that initiates or drives the vicious cycle is in a latent form requiring activation and the factor is an MMP substrate, for example, TGFβ, a number of regulatory checkpoints must be overcome in order for the factor to execute an effect. The MMP equipped to perform the activation must be present and in an active form. The levels of the endogenous inhibitor (TIMP) of that MMP must be either absent or present at a low enough concentration so as to spare MMP enzymatic activity. If MMP processing results in an active form of the factor and endogenous inhibitors of the factor are low, the activated factor can mediate an effect on a target cell provided the cognate receptor is expressed. In the flowchart, the red and green boxes illustrate a "stop" or "go" checkpoint with respect to activation of the cytokine. Factors such as BMPs and Wnts are secreted in an active form and can bypass protease regulation (represented by dashed line) and elicit their effect.

multiple layers of complexity in the post-translational control of the factors that regulate the progression of the vicious cycle.

MMP inhibitors—a clinically relevant approach for the treatment of bone metastases?

MMP inhibitor trials were largely a failure [136]. In retrospect the reasons for the failure of the trials are multi-fold with perhaps the most important being that the precise functions of the metalloproteinase family were largely unknown, and naively at the time were thought to be limited mainly to ECM remodeling. The failure of the trials provided an almost permanent handicap for the field and it is difficult to convince the scientific community that understanding what these enzymes do in normal and pathological settings is worthwhile since the constant question that arises is "how can MMP inhibition be clinically translatable given the failure of the trials with the broad spectrum inhibitors?" While this is a valid question, research since the conclusion of the MMP inhibitor trials has begun asking what the role of individual MMPs are in various tumors, with the aim to (a) generate highly selective inhibitors that lack the deleterious effects noted with broad spectrum inhibitors and, (b) if an MMP of interest mediates an effect via a substrate that is previously unidentified then, this MMP generated product may be a potential target for therapeutic inhibition. This approach of defining the precise roles of individual MMPs is particularly relevant to bone metastases since pre-clinical experiments have reported the efficacy of broad spectrum and selective metalloproteinase inhibitors in preventing the progression of prostate and breast tumors in bone [137–139]. Recent studies have identified that individual metalloproteinases are key regulators of the vicious cycle such as MMP-1, MMP-2, MMP-7 and MMP-9 [31,32,47,48,130] and so, the selective inhibition of one or more of these proteinases should allow for the successful treatment of patients with debilitating bone metastases without the side effects noted with broad spectrum inhibitors. Whether selective MMP inhibitors would be more efficacious than current treatments such as bisphosphonates remains to be determined.

Summary

MMPs are often expressed in the rapidly remodeling metastatic tumor–bone microenvironment and can be derived from multiple cellular sources. In addition to their roles in ECM remodeling, MMPs should be considered as key for cell–cell communication in the tumor–bone microenvironment given their ability to regulate the bioactivity and bioavailability of the factors such as PTHrP, RANKL and TGFβ that traditionally are associated with driving the vicious cycle. Although we are only at the beginning of our understanding of the roles for MMPs in tumor–bone interaction, the data to date support the supposition that MMPs are master regulators of the vicious cycle. The definition of further mechanisms through which MMPs mediate their effects in the tumor–bone microenvironment will provide new insights into how the vicious cycle is perpetuated and assist in the design of selective metalloproteinase inhibitors that have the strong potential to be efficacious in the treatment of bone metastases.

Acknowledgments

This review is dedicated to my mentor, collaborator and friend, Dr. Greg Mundy whose insight, enthusiasm and support is missed daily. CCL is supported by the Department of Defense under award number W81XWH-07-1-0208. Views and opinions of, and endorsements by the author(s) do not reflect those of the US Army or the Department of Defense.

References

[1] www.cancer.org. Cancer Facts and Figures. American Cancer Society 2008.
[2] Ye XC, Choueiri M, Tu SM, Lin SH. Biology and clinical management of prostate cancer bone metastasis. Front Biosci 2007;12:3273–86.
[3] Bubendorf L, Schopfer A, Wagner U, Sauter G, Moch H, Willi N, et al. Metastatic patterns of prostate cancer: an autopsy study of 1, 589 patients. Hum Pathol 2000;31:578–83.
[4] Logothetis CJ, Lin SH. Osteoblasts in prostate cancer metastasis to bone. Nat Rev Cancer 2005;5:21–8.
[5] Keller ET, Brown J. Prostate cancer bone metastases promote both osteolytic and osteoblastic activity. J Cell Biochem 2004;91:718–29.
[6] Coleman RE, Guise TA, Lipton A, Roodman GD, Berenson JR, Body JJ, et al. Advancing treatment for metastatic bone cancer: consensus recommendations from the Second Cambridge Conference. Clin Cancer Res 2008;14:6387–95.
[7] Mundy GR. Metastasis to bone: causes, consequences and therapeutic opportunities. Nat Rev Cancer 2002;2:584–93.
[8] Bendre M, Gaddy D, Nicholas RW, Suva LJ . Breast cancer metastasis to bone: it is not all about PTHrP. Clin Orthop Relat Res 2003;2:S39–45.
[9] Suva LJ, Winslow GA, Wettenhall RE, Hammonds RG, Moseley JM, Diefenbach-Jagger H, et al. A parathyroid hormone-related protein implicated in malignant hypercalcemia: cloning and expression. Science 1987;237:893–6.
[10] Hall CL, Bafico A, Dai J, Aaronson SA, Keller ET. Prostate cancer cells promote osteoblastic bone metastases through Wnts. Cancer Res 2005;65:7554–60.
[11] Dai J, Hall CL, Escara-Wilke J, Mizokami A, Keller JM, Keller ET. Prostate cancer induces bone metastasis through Wnt-induced bone morphogenetic protein-dependent and independent mechanisms. Cancer Res 2008;68:5785–94.
[12] Yin JJ, Mohammad KS, Kakonen SM, Harris S, Wu-Wong JR, Wessale JL, et al. A causal role for endothelin-1 in the pathogenesis of osteoblastic bone metastases. Proc Natl Acad Sci USA 2003;100:10954–9.
[13] Bendre MS, Margulies AG, Walser B, Akel NS, Bhattacharrya S, Skinner RA, et al. Tumor-derived interleukin-8 stimulates osteolysis independent of the receptor activator of nuclear factor-kappaB ligand pathway. Cancer Res 2005;65:11001–9.
[14] Ibbotson KJ, Harrod J, Gowen M, D'Souza S, Smith DD, Winkler ME, et al. Human recombinant transforming growth factor alpha stimulates bone resorption and inhibits formation in vitro. Proc Natl Acad Sci USA 1986;83:2228–32.
[15] Takahashi N, MacDonald BR, Hon J, Winkler ME, Derynck R, Mundy GR, et al. Recombinant human transforming growth factor-alpha stimulates the formation of osteoclast-like cells in long-term human marrow cultures. J Clin Invest 1986;78:894–8.
[16] Guise TA, Garrett IR, Bonewald LF, Mundy GR. Interleukin-1 receptor antagonist inhibits the hypercalcemia mediated by interleukin-1. J Bone Miner Res 1993;8:583–7.
[17] Guise TA. Parathyroid hormone-related protein and bone metastases. Cancer 1997;80:1572–80.
[18] Kong YY, Yoshida H, Sarosi I, Tan HL, Timms E, Capparelli C, et al. OPGL is a key regulator of osteoclastogenesis, lymphocyte development and lymph-node organogenesis. Nature 1999;397:315–23.
[19] Blair HC, Teitelbaum SL, Ghiselli R, Gluck S. Osteoclastic bone resorption by a polarized vacuolar proton pump. Science 1989;245:855–7.
[20] Delaisse JM, Engsig MT, Everts V, del Carmen O, Ferreras M. Lund, Vu TH, Werb Z, Winding B, Lochter A, Karsdal MA, Troen T, Kirkegaard T, Lenhard T, Heegaard AM, Neff L, Baron R, Foged NT. Proteinases in bone resorption: obvious and less obvious roles. Clin Chim Acta 2000;291:223–34.
[21] Cackowski FC, Roodman GD. Perspective on the osteoclast: an angiogenic cell? Ann NY Acad Sci 2007;1117:12–25.
[22] Lynch CC, Matrisian LM. Matrix metalloproteinases in tumor–host cell communication. Differentiation 2002;70:561–73.
[23] Brew K, Nagase H. The tissue inhibitors of metalloproteinases (TIMPs): an ancient family with structural and functional diversity. Biochim Biophys Acta 2010;1803:55–71.
[24] Delaisse JM, Andersen TL, Engsig MT, Henriksen K, Troen T, Blavier L. Matrix metalloproteinases (MMP) and cathepsin K contribute differently to osteoclastic activities. Microsc Res Tech 2003;61:504–13.
[25] Garnero P, Ferreras M, Karsdal MA, Nicamhlaoibh R, Risteli J, Borel O, et al. The type I collagen fragments ICTP and CTX reveal distinct enzymatic pathways of bone collagen degradation. J Bone Miner Res 2003;18:859–67.
[26] Nemeth JA, Yousif R, Herzog M, Che M, Upadhyay J, Shekarriz B, et al. Matrix metalloproteinase activity, bone matrix turnover, and tumor cell proliferation in prostate cancer bone metastasis. J Natl Cancer Inst 2002;94:17–25.
[27] Chinni SR, Sivalogan S, Dong Z, Filho JC, Deng X, Bonfil RD, et al. CXCL12/CXCR4 signaling activates Akt-1 and MMP-9 expression in prostate cancer cells: the role of bone microenvironment-associated CXCL12. Prostate 2006;66:32–48.
[28] Bonfil RD, Dong Z. Trindade Filho JC, Sabbota A, Osenkowski P, Nabha S, Yamamoto H, Chinni SR, Zhao H, Mobashery S, Vessella RL, Fridman R, Cher ML. Prostate cancer-associated membrane type 1-matrix metalloproteinase: a pivotal role in bone response and intraosseous tumor growth. Am J Pathol 2007;170:2100–11.
[29] Nabha SM, dos Santos EB, Yamamoto HA, Belizi A, Dong Z, Meng H, et al. Bone marrow stromal cells enhance prostate cancer cell invasion through type I collagen in an MMP-12 dependent manner. Int J Cancer 2008;122:2482–90.
[30] Nannuru KC, Futakuchi M, Sadanandam A, Wilson TJ, Varney ML, Myers KJ, et al. Enhanced expression and shedding of receptor activator of NF-kappaB ligand during tumor–bone interaction potentiates mammary tumor-induced osteolysis. Clin Exp Metastasis 2009;26:797–808.
[31] Tester AM, Waltham M, Oh SJ, Bae SN, Bills MM, Walker EC, et al. Pro-matrix metalloproteinase-2 transfection increases orthotopic primary growth and experimental metastasis of MDA-MB-231 human breast cancer cells in nude mice. Cancer Res 2004;64:652–8.
[32] Lu X, Wang Q, Hu G, Van Poznak C, Fleisher M, Reiss M, et al. ADAMTS1 and MMP1 proteolytically engage EGF-like ligands in an osteolytic signaling cascade for bone metastasis. Genes Dev 2009;23:1882–94.
[33] Chirgwin JM, Guise TA. Molecular mechanisms of tumor–bone interactions in osteolytic metastases. Crit Rev Eukaryot Gene Expr 2000;10:159–78.
[34] Bord S, Horner A, Hembry RM, Compston JE. Stromelysin-1 (MMP-3) and stromelysin-2 (MMP-10) expression in developing human bone: potential roles in skeletal development. Bone 1998;23:7–12.
[35] Breckon JJ, Papaioannou S, Kon LW, Tumber A, Hembry RM, Murphy G, et al. Stromelysin (MMP-3) synthesis is up-regulated in estrogen-deficient mouse osteoblasts in vivo and in vitro. J Bone Miner Res 1999;14:1880–90.
[36] Bord S, Horner A, Hembry RM, Reynolds JJ, Compston JE. Production of collagenase by human osteoblasts and osteoclasts in vivo. Bone 1996;19:35–40.
[37] Holmbeck K, Bianco P, Caterina J, Yamada S, Kromer M, Kuznetsov SA, et al. MT1-MMP-deficient mice develop dwarfism, osteopenia, arthritis, and connective tissue disease due to inadequate collagen turnover. Cell 1999;99:81–92.
[38] Dew G, Murphy G, Stanton H, Vallon R, Angel P, Reynolds JJ, et al. Localisation of matrix metalloproteinases and TIMP-2 in resorbing mouse bone. Cell Tissue Res 2000;299:385–94.
[39] Kusano K, Miyaura C, Inada M, Tamura T, Ito A, Nagase H, et al. Regulation of matrix metalloproteinases (MMP-2, -3, -9, and -13) by interleukin-1 and interleukin-6 in mouse calvaria: association of MMP induction with bone resorption. Endocrinology 1998;139:1338–45.
[40] Parikka V, Vaananen A, Risteli J, Salo T, Sorsa T, Vaananen HK, et al. Human mesenchymal stem cell derived osteoblasts degrade organic bone matrix in vitro by matrix metalloproteinases. Matrix Biol 2005;24:438–47.
[41] Inoue K, Mikuni-Takagaki Y, Oikawa K, Itoh T, Inada M, Noguchi T, et al. A crucial role for matrix metalloproteinase 2 in osteocytic canalicular formation and bone metabolism. J Biol Chem 2006;281:33814–24.
[42] Sato H, Takino T, Okada Y, Cao J, Shinagawa A, Yamamoto E, et al. A matrix metalloproteinase expressed on the surface of invasive tumour cells. Nature 1994;370:61–4.
[43] Holmbeck K, Bianco P, Pidoux I, Inoue S, Billinghurst RC, Wu W, et al. The metalloproteinase MT1-MMP is required for normal development and maintenance of osteocyte processes in bone. J Cell Sci 2005;118:147–56.
[44] Inada M, Wang Y, Byrne MH, Rahman MU, Miyaura C, Lopez-Otin C, et al. Critical roles for collagenase-3 (Mmp13) in development of growth plate cartilage and in endochondral ossification. Proc Natl Acad Sci USA 2004;101:17192–7.
[45] Stickens D, Behonick DJ, Ortega N, Heyer B, Hartenstein B, Yu Y, et al. Altered endochondral bone development in matrix metalloproteinase 13-deficient mice 2. Development 2004;131:5883–95.
[46] Balbin M, Fueyo A, Tester AM, Pendas AM, Pitiot AS, Astudillo A, et al. Loss of collagenase-2 confers increased skin tumor susceptibility to male mice. Nat Genet 2003;35:252–7.
[47] Lynch CC, Hikosaka A, Acuff HB, Martin MD, Kawai N, Singh RK, et al. MMP-7 promotes prostate cancer-induced osteolysis via the solubilization of RANKL. Cancer Cell 2005;7:485–96.

[48] Thiolloy S, Halpern J, Holt GE, Schwartz HS, Mundy GR, Matrisian LM, et al. Osteoclast-derived matrix metalloproteinase-7, but not matrix metalloproteinase-9, contributes to tumor-induced osteolysis. Cancer Res 2009;69:6747–55.
[49] Andersen TL, del Carmen Ovejero M, Kirkegaard T, Lenhard T, Foged NT, Delaisse JM. A scrutiny of matrix metalloproteinases in osteoclasts: evidence for heterogeneity and for the presence of MMPs synthesized by other cells. Bone 2004;35:1107–19.
[50] Saftig P, Hunziker E, Wehmeyer O, Jones S, Boyde A, Rommerskirch W, et al. Impaired osteoclastic bone resorption leads to osteopetrosis in cathepsin-K-deficient mice. Proc Natl Acad Sci USA 1998;95:13453–8.
[51] Gowen M, Lazner F, Dodds R, Kapadia R, Feild J, Tavaria M, et al. Cathepsin K knockout mice develop osteopetrosis due to a deficit in matrix degradation but not demineralization. J Bone Miner Res 1999;14:1654–63.
[52] Delaisse JM, Ledent P, Vaes G. Collagenolytic cysteine proteinases of bone tissue. Cathepsin B, (pro)cathepsin L and a cathepsin L-like 70 kDa proteinase. Biochem J 1991;279(Pt 1):167–74.
[53] Nagase H, Woessner Jr JF. Matrix metalloproteinases. J Biol Chem 1999;274: 21491–4.
[54] Engsig MT, Chen QJ, Vu TH, Pedersen AC, Therkidsen B, Lund LR, et al. Matrix metalloproteinase 9 and vascular endothelial growth factor are essential for osteoclast recruitment into developing long bones. J Cell Biol 2000;151:879–90.
[55] Goetzl EJ, Banda MJ, Leppert D. Matrix metalloproteinases in immunity. J Immunol 1996;156:1–4.
[56] Burke B, Giannoudis A, Corke KP, Gill D, Wells M, Ziegler-Heitbrock L, et al. Hypoxia-induced gene expression in human macrophages: implications for ischemic tissues and hypoxia-regulated gene therapy. Am J Pathol 2003;163: 1233–43.
[57] Haro H, Crawford HC, Fingleton B, Shinomiya K, Spengler DM, Matrisian LM. Matrix metalloproteinase-7-dependent release of tumor necrosis factor-alpha in a model of herniated disc resorption. J Clin Investig 2000;105:143–50.
[58] Shapiro SD. Diverse roles of macrophage matrix metalloproteinases in tissue destruction and tumor growth. Thromb Haemost 1999;82:846–9.
[59] Ardi VC, Van den Steen PE, Opdenakker G, Schweighofer B, Deryugina EI, Quigley JP. Neutrophil MMP-9 proenzyme, unencumbered by TIMP-1, undergoes efficient activation in vivo and catalytically induces angiogenesis via a basic fibroblast growth factor (FGF-2)/FGFR-2 pathway. J Biol Chem 2009;284: 25854–66.
[60] Gao Y, Wu X, Terauchi M, Li JY, Grassi F, Galley S, et al. T cells potentiate PTH-induced cortical bone loss through CD40L signaling. Cell Metab 2008;8:132–45.
[61] Fournier PG, Chirgwin JM, Guise TA. New insights into the role of T cells in the vicious cycle of bone metastases. Curr Opin Rheumatol 2006;18:396–404.
[62] Eckhardt BL, Parker BS, van Laar RK, Restall CM, Natoli AL, Tavaria MD, et al. Genomic analysis of a spontaneous model of breast cancer metastasis to bone reveals a role for the extracellular matrix. Mol Cancer Res 2005;3:1–13.
[63] Owen JL, Iragavarapu-Charyulu V, Gunja-Smith Z, Herbert LM, Grosso JF, Lopez DM. Up-regulation of matrix metalloproteinase-9 in T lymphocytes of mammary tumor bearers: role of vascular endothelial growth factor. J Immunol 2003;171: 4340–51.
[64] Savinov AY, Strongin AY. Defining the roles of T cell membrane proteinase and CD44 in type 1 diabetes. IUBMB Life 2007;59:6–13.
[65] Liao J, McCauley LK. Skeletal metastasis: Established and emerging roles of parathyroid hormone related protein (PTHrP). Cancer Metastasis Rev 2006;25: 559–71.
[66] Liao J, Li X, Koh AJ, Berry JE, Thudi N, Rosol TJ, et al. Tumor expressed PTHrP facilitates prostate cancer-induced osteoblastic lesions. Int J Cancer 2008;123: 2267–78.
[67] Dougherty KM, Blomme EA, Koh AJ, Henderson JE, Pienta KJ, Rosol TJ, et al. Parathyroid hormone-related protein as a growth regulator of prostate carcinoma. Cancer Res 1999;59:6015–22.
[68] Deftos LJ, Barken I, Burton DW, Hoffman RM, Geller J. Direct evidence that PTHrP expression promotes prostate cancer progression in bone. Biochem Biophys Res Commun 2005;327:468–72.
[69] Thomas RJ, Guise TA, Yin JJ, Elliott J, Horwood NJ, Martin TJ, et al. Breast cancer cells interact with osteoblasts to support osteoclast formation. Endocrinology 1999;140:4451–8.
[70] Southby J, O'Keeffe LM, Martin TJ, Gillespie MT. Alternative promoter usage and mRNA splicing pathways for parathyroid hormone-related protein in normal tissues and tumours. Br J Cancer 1995;72:702–7.
[71] Cramer SD, Chen Z, Peehl DM. Prostate specific antigen cleaves parathyroid hormone-related protein in the PTH-like domain: inactivation of PTHrP-stimulated cAMP accumulation in mouse osteoblasts. J Urol 1996;156:526–31.
[72] Liu B, Goltzman D, Rabbani SA. Processing of pro-PTHRP by the prohormone convertase, furin: effect on biological activity. Am J Physiol 1995;268:E832–8.
[73] Smollich M, Gotte M, Yip GW, Yong ES, Kersting C, Fischgrabe J, et al. On the role of endothelin-converting enzyme-1 (ECE-1) and neprilysin in human breast cancer. Breast Cancer Res Treat 2007.
[74] Dall'Era MA, True LD, Siegel AF, Porter MP, Sherertz TM, Liu AY. Differential expression of CD10 in prostate cancer and its clinical implication. BMC Urol 2007;7:3.
[75] Ruchon AF, Marcinkiewicz M, Ellefsen K, Basak A, Aubin J, Crine P, et al. Cellular localization of neprilysin in mouse bone tissue and putative role in hydrolysis of osteogenic peptides. J Bone Miner Res 2000;15:1266–74.
[76] Schluter KD, Katzer C, Piper HM. A N-terminal PTHrP peptide fragment void of a PTH/PTHrP-receptor binding domain activates cardiac ET(A) receptors. Br J Pharmacol 2001;132:427–32.
[77] Macours N, Poels J, Hens K, Francis C, Huybrechts R. Structure, evolutionary conservation, and functions of angiotensin- and endothelin-converting enzymes. Int Rev Cytol 2004;239:47–97.
[78] Fernandez-Patron C, Radomski MW, Davidge ST. Vascular matrix metalloproteinase-2 cleaves big endothelin-1 yielding a novel vasoconstrictor. Circ Res 1999;85:906–11.
[79] Felx M, Guyot MC, Isler M, Turcotte RE, Doyon J, Khatib AM, et al. Endothelin-1 (ET-1) promotes MMP-2 and MMP-9 induction involving the transcription factor NF-kappaB in human osteosarcoma. Clin Sci (Lond) 2006;110:645–54.
[80] Kang Y, Siegel PM, Shu W, Drobnjak M, Kakonen SM, Cordon-Cardo C, et al. A multigenic program mediating breast cancer metastasis to bone. Cancer Cell 2003;3:537–49.
[81] Chakraborti S, Mandal M, Das S, Mandal A, Chakraborti T. Regulation of matrix metalloproteinases: an overview. Mol Cell Biochem 2003;253:269–85.
[82] Sternlicht MD, Werb Z. How matrix metalloproteinases regulate cell behavior. Annu Rev Cell Dev Biol 2001;17:463–516.
[83] Yoneda T, Sasaki A, Dunstan C, Williams PJ, Bauss F, DeClerck YA, et al. Inhibition of osteolytic bone metastasis of breast cancer by combined treatment with the bisphosphonate ibandronate and tissue inhibitor of the matrix metalloproteinase-2. J Clin Investig 1997;99:2509–17.
[84] Prudova A, Auf dem Keller U, Butler GS, Overall CM. Multiplex N-terminome analysis of MMP-2 and MMP-9 substrate degradomes by iTRAQ-TAILS quantitative proteomics. Mol Cell Proteomics 2010;9:894–911.
[85] Yu WH, Woessner Jr JF, McNeish JD, Stamenkovic I. CD44 anchors the assembly of matrilysin/MMP-7 with heparin-binding epidermal growth factor precursor and ErbB4 and regulates female reproductive organ remodeling. Genes Dev 2002;16: 307–23.
[86] Suzuki M, Raab G, Moses MA, Fernandez CA, Klagsbrun M. Matrix metalloproteinase-3 releases active heparin-binding EGF-like growth factor by cleavage at a specific juxtamembrane site. J Biol Chem 1997;272:31730–7.
[87] Hall CL, Keller ET. The role of Wnts in bone metastases. Cancer Metastasis Rev 2006;25:551–8.
[88] Blavier L, Lazaryev A, Dorey F, Shackleford GM, DeClerck YA. Matrix metalloproteinases play an active role in Wnt1-induced mammary tumorigenesis. Cancer Res 2006;66:2691–9.
[89] Crawford HC, Fingleton B, Gustavson MD, Kurpios N, Wagenaar RA, Hassell JA, et al. The PEA3 subfamily of Ets transcription factors synergizes with beta-catenin-LEF-1 to activate matrilysin transcription in intestinal tumors. Mol Cell Biol 2001;21:1370–83.
[90] Zilberberg A, Yaniv A, Gazit A. The low density lipoprotein receptor-1, LRP1, interacts with the human frizzled-1 (HFz1) and down-regulates the canonical Wnt signaling pathway. J Biol Chem 2004;279:17535–42.
[91] Rozanov DV, Hahn-Dantona E, Strickland DK, Strongin AY. The low density lipoprotein receptor-related protein LRP is regulated by membrane type-1 matrix metalloproteinase (MT1-MMP) proteolysis in malignant cells. J Biol Chem 2004;279:4260–8.
[92] T. Ara, Y.A. Declerck. Interleukin-6 in bone metastasis and cancer progression. Eur J Cancer 46: 1223-1231.
[93] Kurihara N, Bertolini D, Suda T, Akiyama Y, Roodman GD. IL-6 stimulates osteoclast-like multinucleated cell formation in long term human marrow cultures by inducing IL-1 release. J Immunol 1990;144:4226–30.
[94] Mullberg J, Durie FH, Otten-Evans C, Alderson MR, Rose-John S, Cosman D, et al. A metalloprotease inhibitor blocks shedding of the IL-6 receptor and the p60 TNF receptor. J Immunol 1995;155:5198–205.
[95] Simonet WS, Lacey DL, Dunstan CR, Kelley M, Chang MS, Luthy R, et al. Osteoprotegerin: a novel secreted protein involved in the regulation of bone density. Cell 1997;89:309–19.
[96] Zhang J, Dai J, Qi Y, Lin DL, Smith P, Strayhorn C, et al. Osteoprotegerin inhibits prostate cancer-induced osteoclastogenesis and prevents prostate tumor growth in the bone. J Clin Investig 2001;107:1235–44.
[97] Lum L, Wong BR, Josien R, Becherer JD, Erdjument-Bromage H, Schlondorff J, et al. Evidence for a role of a tumor necrosis factor-alpha (TNF-alpha)-converting enzyme-like protease in shedding of TRANCE, a TNF family member involved in osteoclastogenesis and dendritic cell survival. J Biol Chem 1999;274:13613–8.
[98] Schlondorff J, Lum L, Blobel CP. Biochemical and pharmacological criteria define two shedding activities for TRANCE/OPGL that are distinct from the tumor necrosis factor alpha convertase. J Biol Chem 2001;276:14665–74.
[99] Chesneau V, Becherer JD, Zheng Y, Erdjument-Bromage H, Tempst P, Blobel CP. Catalytic properties of ADAM19. J Biol Chem 2003;278:22331–40.
[100] Hikita A, Yana I, Wakeyama H, Nakamura M, Kadono Y, Oshima Y, et al. Negative regulation of osteoclastogenesis by ectodomain shedding of receptor activator of NF-kappaB ligand. J Biol Chem 2006;281:36846–55.
[101] Dallas SL, Zhao S, Cramer SD, Chen Z, Peehl DM, Bonewald LF. Preferential production of latent transforming growth factor beta-2 by primary prostatic epithelial cells and its activation by prostate-specific antigen. J Cell Physiol 2005;202:361–70.
[102] Bilezikian J, Raisz L. Martin T. Principles of Bone Biology: Academic Press; 2008.
[103] Chung LW, Baseman A, Assikis V, Zhau HE. Molecular insights into prostate cancer progression: the missing link of tumor microenvironment. J Urol 2005;173:10–20.
[104] Saharinen J, Hyytiainen M, Taipale J, Keski-Oja J. Latent transforming growth factor-beta binding proteins (LTBPs)—structural extracellular matrix proteins for targeting TGF-beta action. Cytokine Growth Factor Rev 1999;10:99–117.
[105] Dallas SL, Miyazono K, Skerry TM, Mundy GR, Bonewald LF. Dual role for the latent transforming growth factor-beta binding protein in storage of latent TGF-

beta in the extracellular matrix and as a structural matrix protein. J Cell Biol 1995;131:539–49.
[106] Yu Q, Stamenkovic I. Cell surface-localized matrix metalloproteinase-9 proteolytically activates TGF-beta and promotes tumor invasion and angiogenesis. Genes Dev 2000;14:163–76.
[107] Maeda S, Dean DD, Gay I, Schwartz Z, Boyan BD. Activation of latent transforming growth factor beta1 by stromelysin 1 in extracts of growth plate chondrocyte-derived matrix vesicles. J Bone Miner Res 2001;16:1281–90.
[108] Maeda S, Dean DD, Gomez R, Schwartz Z, Boyan BD. The first stage of transforming growth factor beta1 activation is release of the large latent complex from the extracellular matrix of growth plate chondrocytes by matrix vesicle stromelysin-1 (MMP-3). Calcif Tissue Int 2002;70:54–65.
[109] Imai K, Hiramatsu A, Fukushima D, Pierschbacher MD, Okada Y. Degradation of decorin by matrix metalloproteinases: identification of the cleavage sites, kinetic analyses and transforming growth factor-beta 1 release. Biochem J 1997;322: 809–14.
[110] Yoneda T, Sasaki A, Mundy GR. Osteolytic bone metastasis in breast cancer. Breast Cancer Res Treat 1994;32:73–84.
[111] Guise TA, Chirgwin JM. Transforming growth factor-beta in osteolytic breast cancer bone metastases. Clin Orthop Relat Res 2003:S32–8.
[112] Futakuchi M, Nannuru KC, Varney ML, Sadanandam A, Nakao K, Asai K, et al. Transforming growth factor-beta signaling at the tumor–bone interface promotes mammary tumor growth and osteoclast activation. Cancer Sci 2009;100:71–81.
[113] Kominsky SL, Doucet M, Brady K, Weber KL. TGF-beta promotes the establishment of renal cell carcinoma bone metastasis. J Bone Miner Res 2007;22:37–44.
[114] Perez-Amodio S, Beertsen W, Everts V. (Pre-)osteoclasts induce retraction of osteoblasts before their fusion to osteoclasts. J Bone Miner Res 2004;19:1722–31.
[115] Chambers TJ. Regulation of the differentiation and function of osteoclasts. J Pathol 2000;192:4–13.
[116] Fox SW, Haque SJ, Lovibond AC, Chambers TJ. The possible role of TGF-beta-induced suppressors of cytokine signaling expression in osteoclast/macrophage lineage commitment in vitro. J Immunol 2003;170:3679–87.
[117] Barnes GL, Javed A, Waller SM, Kamal MH, Hebert KE, Hassan MQ, et al. Osteoblast-related transcription factors Runx2 (Cbfa1/AML3) and MSX2 mediate the expression of bone sialoprotein in human metastatic breast cancer cells. Cancer Res 2003;63:2631–7.
[118] Canalis E, Centrella M, Burch W, McCarthy TL. Insulin-like growth factor I mediates selective anabolic effects of parathyroid hormone in bone cultures. J Clin Invest 1989;83:60–5.
[119] Jiang J, Lichtler AC, Gronowicz GA, Adams DJ, Clark SH, Rosen CJ, et al. Transgenic mice with osteoblast-targeted insulin-like growth factor-I show increased bone remodeling. Bone 2006;39:494–504.
[120] Gennigens C, Menetrier-Caux C, Droz JP. Insulin-Like Growth Factor (IGF) family and prostate cancer. Crit Rev Oncol Hematol 2006;58:124–45.
[121] Denley A, Cosgrove LJ, Booker GW, Wallace JC, Forbes BE. Molecular interactions of the IGF system. Cytokine Growth Factor Rev 2005;16:421–39.
[122] Fowlkes JL, Enghild JJ, Suzuki K, Nagase H. Matrix metalloproteinases degrade insulin-like growth factor-binding protein-3 in dermal fibroblast cultures. J Biol Chem 1994;269:25742–6.
[123] Thrailkill KM, Quarles LD, Nagase H, Suzuki K, Serra DM, Fowlkes JL. Characterization of insulin-like growth factor-binding protein 5-degrading proteases produced throughout murine osteoblast differentiation. Endocrinology 1995;136:3527–33.
[124] Manes S, Mira E, Barbacid MM, Cipres A, Fernandez-Resa P, Buesa JM, et al. Identification of insulin-like growth factor-binding protein-1 as a potential physiological substrate for human stromelysin-3. J Biol Chem 1997;272: 25706–12.
[125] Hicklin DJ, Ellis LM. Role of the vascular endothelial growth factor pathway in tumor growth and angiogenesis. J Clin Oncol 2005;23:1011–27.
[126] Fidler IJ. The organ microenvironment and cancer metastasis. Differentiation 2002;70:498–505.
[127] Mohamedali KA, Poblenz AT, Sikes CR, Navone NM, Thorpe PE, Darnay BG, et al. Inhibition of prostate tumor growth and bone remodeling by the vascular targeting agent VEGF121/rGel. Cancer Res 2006;66:10919–28.
[128] Dai J, Kitagawa Y, Zhang J, Yao Z, Mizokami A, Cheng S, et al. Vascular endothelial growth factor contributes to the prostate cancer-induced osteoblast differentiation mediated by bone morphogenetic protein. Cancer Res 2004;64:994–9.
[129] Bergers G, Brekken R, McMahon G, Vu TH, Itoh T, Tamaki K, et al. Matrix metalloproteinase-9 triggers the angiogenic switch during carcinogenesis. Nat Cell Biol 2000;2:737–44.
[130] Bruni-Cardoso A, Johnson LC, Vessella RL, Peterson TE, Lynch CC. Osteoclast-Derived Matrix Metalloproteinase-9 Directly Affects Angiogenesis in the Prostate Tumor–Bone Microenvironment. Mol Cancer Res 2010.
[131] Nabha SM, Bonfil RD, Yamamoto HA, Belizi A, Wiesner C, Dong Z, et al. Host matrix metalloproteinase-9 contributes to tumor vascularization without affecting tumor growth in a model of prostate cancer bone metastasis. Clin Exp Metastasis 2006;23:335–44.
[132] Cackowski FC, Anderson JL, Patrene KD, Choksi RJ, Shapiro SD, Windle JJ, et al. Osteoclasts are important for bone angiogenesis. Blood 2010;115:140–9.
[133] Lee S, Jilani SM, Nikolova GV, Carpizo D, Iruela-Arispe ML. Processing of VEGF-A by matrix metalloproteinases regulates bioavailability and vascular patterning in tumors. J Cell Biol 2005;169:681–91.
[134] Hashimoto G, Inoki I, Fujii Y, Aoki T, Ikeda E, Okada Y. Matrix metalloproteinases cleave connective tissue growth factor and reactivate angiogenic activity of vascular endothelial growth factor 165. J Biol Chem 2002;277:36288–95.
[135] McQuibban GA, Butler GS, Gong JH, Bendall L, Power C, Clark-Lewis I, et al. Matrix metalloproteinase activity inactivates the CXC chemokine stromal cell-derived factor-1. J Biol Chem 2001;276:43503–8.
[136] Coussens LM, Fingleton B, Matrisian LM. Matrix metalloproteinase inhibitors and cancer: trials and tribulations. Science 2002;295:2387–92.
[137] Lee J, Weber M, Mejia S, Bone E, Watson P, Orr W. A matrix metalloproteinase inhibitor, batimastat, retards the development of osteolytic bone metastases by MDA-MB-231 human breast cancer cells in Balb C nu/nu mice. Eur J Cancer 2001;37:106–13.
[138] Winding B, NicAmhlaoibh R, Misander H, Hoegh-Andersen P, Andersen TL, Holst-Hansen C, et al. Synthetic matrix metalloproteinase inhibitors inhibit growth of established breast cancer osteolytic lesions and prolong survival in mice. Clin Cancer Res 2002;8:1932–9.
[139] Bonfil RD, Sabbota A, Nabha S, Bernardo MM, Dong Z, Meng H, et al. Inhibition of human prostate cancer growth, osteolysis and angiogenesis in a bone metastasis model by a novel mechanism-based selective gelatinase inhibitor 1. Int J Cancer 2006;118:2721–6.

DOI:10.1158/0008-5472.CAN-08-3949

Cancer Research

Osteoclast-Derived Matrix Metalloproteinase-7, but Not Matrix Metalloproteinase-9, Contributes to Tumor-Induced Osteolysis

Sophie Thiolloy, Jennifer Halpern, Ginger E. Holt, et al.

Cancer Res 2009;69:6747-6755. Published online August 12, 2009.

DOI:10.1158/0008-5472.CAN-08-3949

Osteoclast-Derived Matrix Metalloproteinase-7, but Not Matrix Metalloproteinase-9, Contributes to Tumor-Induced Osteolysis

Sophie Thiolloy,[1] Jennifer Halpern,[2] Ginger E. Holt,[2] Herbert S. Schwartz,[2] Gregory R. Mundy,[3] Lynn M. Matrisian,[2] and Conor C. Lynch[1,2]

Departments of [1]Cancer Biology, [2]Orthopaedics and Rehabilitation, and [3]Vanderbilt Center for Bone Biology, Vanderbilt University, Nashville, Tennessee

Abstract

The matrix metalloproteinases MMP-2, MMP-3, MMP-7, MMP-9, and MMP-13 are highly expressed in the tumor-bone microenvironment, and, of these, MMP-7 and MMP-9 were found to be localized to bone-resorbing osteoclasts in human breast-to-bone metastases. In a bid to define the roles of host-derived MMP-7 and MMP-9 in the tumor-bone microenvironment, the tibias of MMP-7 and MMP-9 null mice were injected with osteolytic luciferase–tagged mammary tumor cell lines. Our data show that osteoclast-derived MMP-7 significantly contributes to tumor growth and tumor-induced osteolysis whereas osteoclast-derived MMP-9 had no effect on these processes. MMP-7 is capable of processing a number of nonmatrix molecules to soluble active forms that have profound effects on cell-cell communication, such as RANKL, a crucial mediator of osteoclast precursor recruitment and maturation. Therefore, the ability of osteoclast-derived MMP-7 to promote RANKL solubilization in the tumor-bone microenvironment was explored. Results revealed that levels of soluble RANKL were significantly lower in the MMP-7 null mice compared with wild-type (WT) controls. In keeping with this observation, MMP-7 null mice had significantly fewer osteoclast numbers at the tumor-bone interface compared with the WT controls. In summary, we propose that the solubilization of RANKL by MMP-7 is a potential mechanism through which MMP-7 mediates mammary tumor–induced osteolysis. Our studies indicate that the selective inhibition of MMP-7 in the tumor-bone microenvironment may be of benefit for the treatment of lytic breast-to-bone metastases. [Cancer Res 2009;69(16):6747–55]

Introduction

Bone metastasis is a common event during breast cancer progression with the resultant lesions often being osteolytic (1). In the bone microenvironment, metastatic breast cancer cells hijack the normal bone remodeling process to induce aberrant activation of bone-resorbing osteoclasts (2). Increased bone resorption results in the release of sequestered growth factors from the bone matrix, such as transforming growth factor-β (TGF-β) and insulin-like growth factors (IGF). These factors subsequently promote tumor survival and growth, thus completing what has aptly been described as the vicious cycle of tumor-induced osteolysis (3).

Osteoclasts are critical for the completion of the vicious cycle, because they are the principal cells involved in the direct resorption of the mineralized bone matrix. Therefore, understanding how osteoclast precursors are recruited to areas requiring bone remodeling and understanding the mechanisms involved in controlling their maturation and activation is the key for the development of new therapies that can effectively stop the vicious cycle. To resorb bone, the osteoclast forms a resorptive seal on the mineralized bone matrix after retraction of the osteoblast canopy (4). Acidification of the resorption zone, in combination with collagenolysis, leads to the demineralization and degradation of the bone matrix, respectively (5). Osteoclasts express a variety of proteases, including the cysteine protease, cathepsin-K, and matrix metalloproteinases (MMP; ref. 6). Whereas cathepsin-K activity is critical for bone resorption (7), the role of osteoclast-derived MMPs is less clear. The MMPs are a family of enzymatic proteins that are often overexpressed in the tumor microenvironment (8). Collectively, MMPs are capable of degrading the entire extracellular matrix, but more recently, MMPs have been implicated as important mediators of cell-cell communication by virtue of their ability to process multiple nonmatrix molecules such as cytokines and growth factors to soluble forms, resulting in either enhanced or attenuated activities (9).

In the context of the tumor-bone microenvironment, preclinical animal studies have shown the efficacy of broad spectrum MMP inhibitors (MMPI) in preventing tumor growth and tumor-induced osteolysis (10–12). However, the failure of MMPIs in human clinical trials prevents their application for the treatment of bone metastases (13). A main conclusion derived from these trials was the necessity for defining the precise roles of individual MMPs in disease processes that would allow for the generation of highly selective MMPIs. To this end, we have assessed the expression of MMPs in human clinical samples of osteolytic breast-to-bone metastasis. Whereas the expression of many MMPs was noted throughout the tumor/stroma, MMP-7 and MMP-9 were highly localized to bone-resorbing osteoclasts. Given the importance of the osteoclasts in driving the vicious cycle, the current study focused on determining if and how these osteoclast-derived MMPs affected tumor-induced osteolysis.

Materials and Methods

Reagents. All experiments involving animals were conducted after review and approval by the Office of Animal Welfare at Vanderbilt University. Deidentified human samples of frank osteolytic breast-to-bone metastasis (n = 11) were collected by curettage with institutional review board approval from Vanderbilt University from 2005 to 2008. Double null immunocompromised recombinase activating gene-2 (RAG-2) and MMP-7

Note: Supplementary data for this article are available at Cancer Research Online (http://cancerres.aacrjournals.org/).

Requests for reprints: Conor C. Lynch, Department of Orthopedics and Rehabilitation, Vanderbilt University Medical Center East, South Tower, Suite 4200, Nashville, TN 37232-8774. Phone: 615-343-5729; Fax: 615-343-1028; E-mail: conor.lynch@vanderbilt.edu.

doi:10.1158/0008-5472.CAN-08-3949

DOI:10.1158/0008-5472.CAN-08-3949

mice were generated as previously described (14). Wild-type (WT) and MMP-9 null mice in the FVB/N-Tg background were kindly provided by Dr. Lisa Coussens, Department of Pathology, University of California San Francisco. A luciferase expressing syngeneic FVB mammary tumor cell line derived from the polyoma virus middle T model of mammary tumorigenesis, designated PyMT-Luc, was isolated in our laboratory and maintained as previously described (15). A luciferase tagged 4T1 mammary tumor cell line (16) was kindly provided by Dr. Swati Biswas of Vanderbilt Center for Bone Biology. All reagents were obtained from Sigma-Aldrich, except where specified.

Intratibial injection and *in vivo* quantitation of tumor growth. PyMT-Luc and 4T1-Luc tumor cells (10^5) in a 10-μL volume of sterile PBS were injected into the tibias of anesthetized immunocompetent or immunocompromised 6-wk-old mice that were WT or null for MMP-7 or MMP-9. The contralateral limb was injected with 10 μL of PBS alone and acted as a sham-injected control. The IVIS system (Caliper Life Sciences) was used to detect luminescence from PyMT-Luc and 4T1-Luc cells after intratibial injection. Firefly luciferin (120 mg/kg in sterile PBS, Gold Biotechnology, Inc.) was delivered retro-orbitally 1 to 2 min prior imaging. Mice were imaged at 24 h and every 3 d after surgery until day 9, which was previously determined to be the time point before tumor breach of the cortical bone in WT control mice. Living Image software (Calipers Life Sciences) was used to quantify the luminescence intensity in the tumor-bearing limb over time. Mice were sacrificed at 9 d postsurgery, and both the tumor-injected and contralateral control tibias were harvested. All animal studies were independently repeated at least twice.

Histology. Fresh human breast-to-bone metastases and tumor and sham-injected mouse tibias were fixed overnight in 10% buffered formalin and decalcified for 3 wk in 14% EDTA at pH 7.4 with changes every 48 to 72 h. Tissues were embedded in paraffin, and 5-μm thick sections were cut. For MMP-7, MMP-9, and tartrate-resistant acid phosphatase (TRAcP) localization, the following technique was used. Sections were rehydrated through a series of ethanols and then rinsed in TBS (10 mmol/L Tris at pH 7.4, 150 mmol/L NaCl) with Tween 20 (0.05%). For antigen retrieval, slides were immersed in a 20 μg/mL solution of proteinase K according to the manufacturer's instructions for 10 min at room temperature. After washing in TBS, tissue sections were blocked using standard blocking criteria for 1 h at room temperature. MMP-7 (17) or MMP-9 (Oncogene) antibodies at a dilution of 1:100 were added in blocking solution overnight at 4°C. Slides were washed extensively in TBST before the addition of a species-specific fluorescently labeled secondary antibody (Alexafluor 568 nm, Invitrogen) diluted 1:1,000 in blocking solution for 1 h at room temperature. Slides were washed in TBS and then equilibrated in an acetate buffer as described (18). The ELF97 TRAcP stain (Invitrogen) was diluted 1:1,000 in acetate buffer, and slides were incubated for 15 min at room temperature. After washing, slides were aqueously mounted in media (Biomeda Corp.) containing 2 μmol/L 4′,6-diamidino-2-phenylindole (DAPI) for nuclear localization.

TRAcP was also detected using a traditional colorimetric kit according to the manufacturer's instructions (Sigma-Aldrich). Gross anatomy of the mouse tibias was assessed by H&E staining. Proliferation (anti–phosphorylated histone H3, Millipore) and apoptosis (anti–caspase-3, Cell Signaling) were assessed by immunohistochemistry as previously described (14).

Micro–computed tomography, X-ray, and histomorphometric analyses. For gross analysis of trabecular bone volume (BV), formalin-fixed tibias were scanned at an isotropic voxel size of 12 μm using a microCT40 (SCANCO Medical). The tissue volume (TV) was derived from generating a contour around the metaphyseal trabecular bone that excluded the cortices. The area of measurement began at least 0.2 mm below the growth plate and was extended by 0.12 mm. BV included all bone tissue that had a material density of >438.7 mgHA/cm^3. These analyses allowed for the calculation of the BV/TV ratio. The same threshold setting for bone tissue was used for all samples. Radiographic images (Faxitron X-ray Corp.) were obtained using an energy of 35 kV and an exposure time of 8 s. The tumor volume (TuV) was calculated as a function of the total TV of the tibial medullary canal using Metamorph software (Molecular Devices). For histomorphometry, three nonserial sections of tumor-bearing limbs were H&E stained to assess the

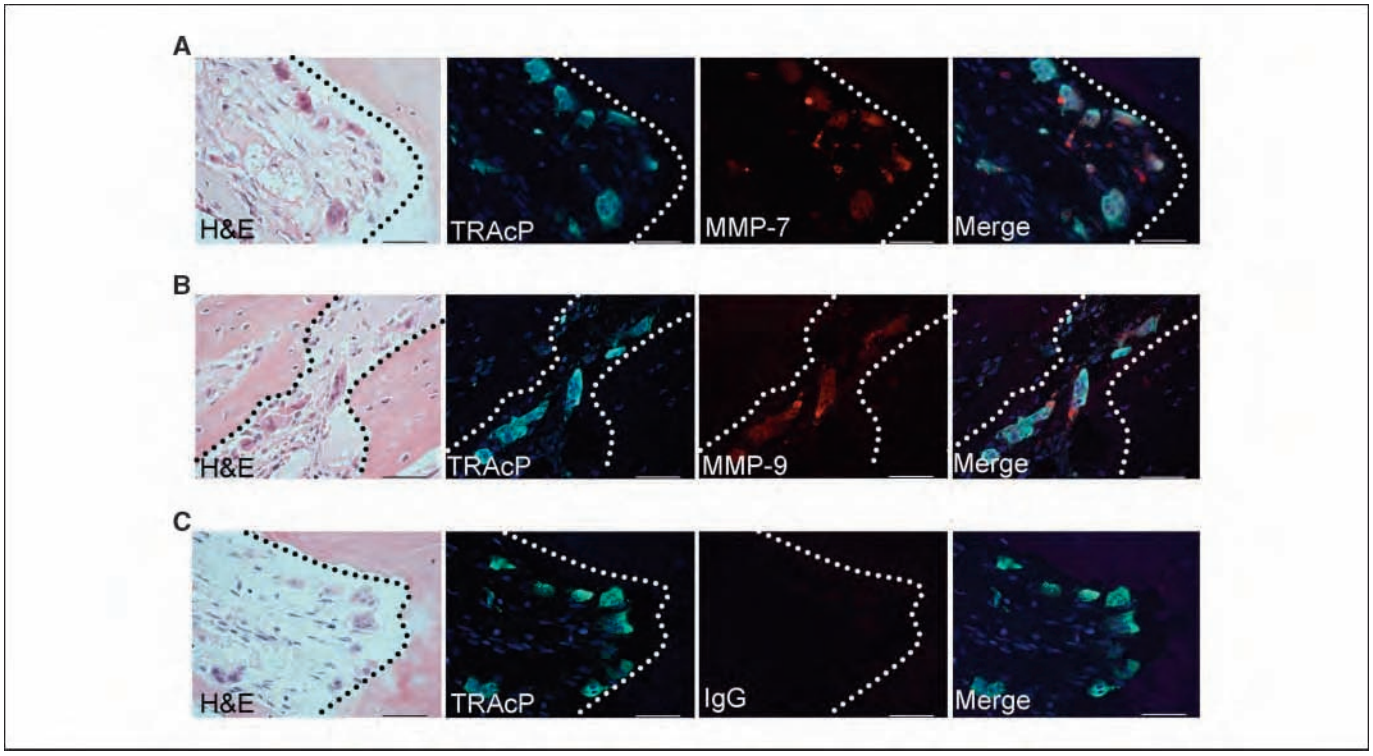

Figure 1. MMP-7 and MMP-9 localization in human breast-to-bone metastases (n = 11). *A-C,* fluorescent TRAcP staining (*green*) was used to localize osteoclasts, whereas immunofluorescence was used to localize MMP-7 and MMP-9 (*red*). DAPI (*blue*) was used as a nuclear stain. Murine or rat IgG was used as a negative control. Dashed lines represent the tumor-bone interface. *Scale bars,* 50 μm.

DOI:10.1158/0008-5472.CAN-08-3949

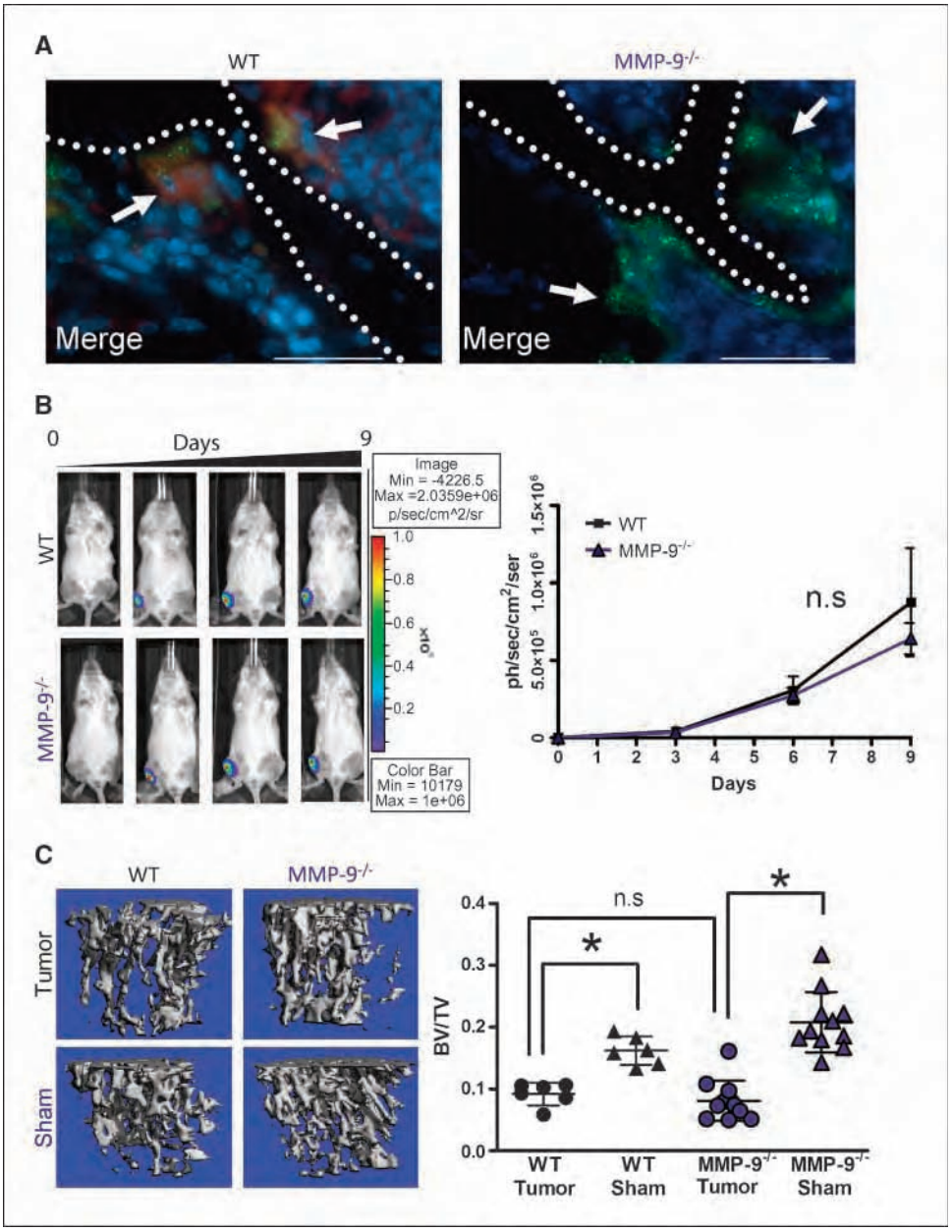

Figure 2. Host MMP-9 does not affect mammary tumor growth or osteolysis in the bone microenvironment. *A,* representative photomicrographs of MMP-9 (*red*) localization merged with TRAcP (*green*) localization in WT and MMP-9$^{-/-}$ animals. DAPI (*blue*) was used as a nuclear stain. *Arrows,* osteoclasts; *dashed line,* tumor-bone interface. *Scale bars,* 50 μm. *B,* PyMT-Luc cells were injected intratibially into syngeneic FVB WT (n = 6) or MMP-9 null (MMP-9$^{-/-}$; n = 11). The contralateral limb received a sham injection of saline. Luciferase activity was measured over a 9-d period and used to quantitate tumor growth. *C,* representative μCT scans of trabecular bone from tumor-bearing and sham-injected limbs of WT and MMP-9$^{-/-}$ animals. μCT was also used to calculate the ratio of trabecular BV to TV (BV/TV) for tumor-injected and sham-injected WT and MMP-9$^{-/-}$ mice. *Points,* mean or individual sample quantitation; *bars,* SD. *, $P < 0.05$; *n.s.,* nonsignificant.

BV/TV ratio or with TRAcP to assess osteoclast number per millimeter of bone at the tumor-bone interface using Metamorph.

Immunoprecipitation, immunoblotting, and ELISA. Tumor and sham-injected tibias from WT or MMP null animals were harvested 9 d postinjection and flash frozen in liquid nitrogen. Tissue homogenates were generated by mortar and pestle, and total protein was subsequently extracted using a standard protein lysis buffer containing a complete protease inhibitor cocktail (Roche). Protein concentration in isolated samples was quantitated using a bicinchoninic acid assay as per manufacturer's instructions (Pierce). For immunoprecipitation and quantitation of soluble RANKL in the tumor-bone microenvironments, equal concentrations of total protein (1 mg) in 1 mL of PBS were precleared with 10 μL of protein G–sepharose beads (Amersham Biosciences) for 1 h at 4°C. Precleared lysates were then incubated with 2 μg of antibody directed to the NH_2 terminus of RANKL (Santa Cruz Biotechnology) for 1 h at 4°C. Subsequently, 10 μL of protein G–sepharose beads were added to the samples, and the bead-antibody-protein complexes were allowed to form overnight at 4°C. A nutator was used during all steps for agitation. The complexes were washed extensively [100 mmol/L NaCl, 50 mmol/L Tris-HCl (pH 7.5), 0.5% NP40] and then boiled in sample buffer [10% SDS, 0.5 mol/L Tris-HCl (pH 6.8), 30% glycerol, 1% β-mercaptoethanol, and 0.02% bromophenol blue] for 10 min before loading on to a 15% SDS-PAGE gel. Recombinant RANKL (462-TR-010/CF, R&D Systems) or MMP-7 solubilized RANKL [10 μg recombinant RANKL incubated with 100 ng active MMP-7 (Calbiochem) for 1 h at 37°C as previously described; ref. 14] were added as positive controls for the molecular weight of full-length and MMP-solubilized RANKL. Proteins were transferred to nitrocellulose membranes and blocked for 1 h at room temperature (5% milk powder in 1×TBS). The blots were then panned with an antibody directed to the NH_2 terminus of RANKL (1:1,000 dilution; Axxora LLC in 5% milk in 1 × TBST) overnight with rocking at 4°C. The following day, blots were washed extensively with 1 × TBST before the addition of a secondary IR-labeled anti-mouse antibody (1:5,000 dilution in 1×TBST, Rockland, Inc.) for 1 h at room temperature. After washing in 1×TBST, blots were developed and bands of interest were quantitated using the Odyssey system (LI-COR Biosciences). ELISA was also used for the quantitation of soluble RANKL in samples according to the manufacturer's instructions (Quantikine, R&D Systems).

Statistical analyses. For *in vivo* data, statistical analysis was performed using ANOVA and Bonferroni multiple comparison tests. *In vitro*, statistical

DOI:10.1158/0008-5472.CAN-08-3949

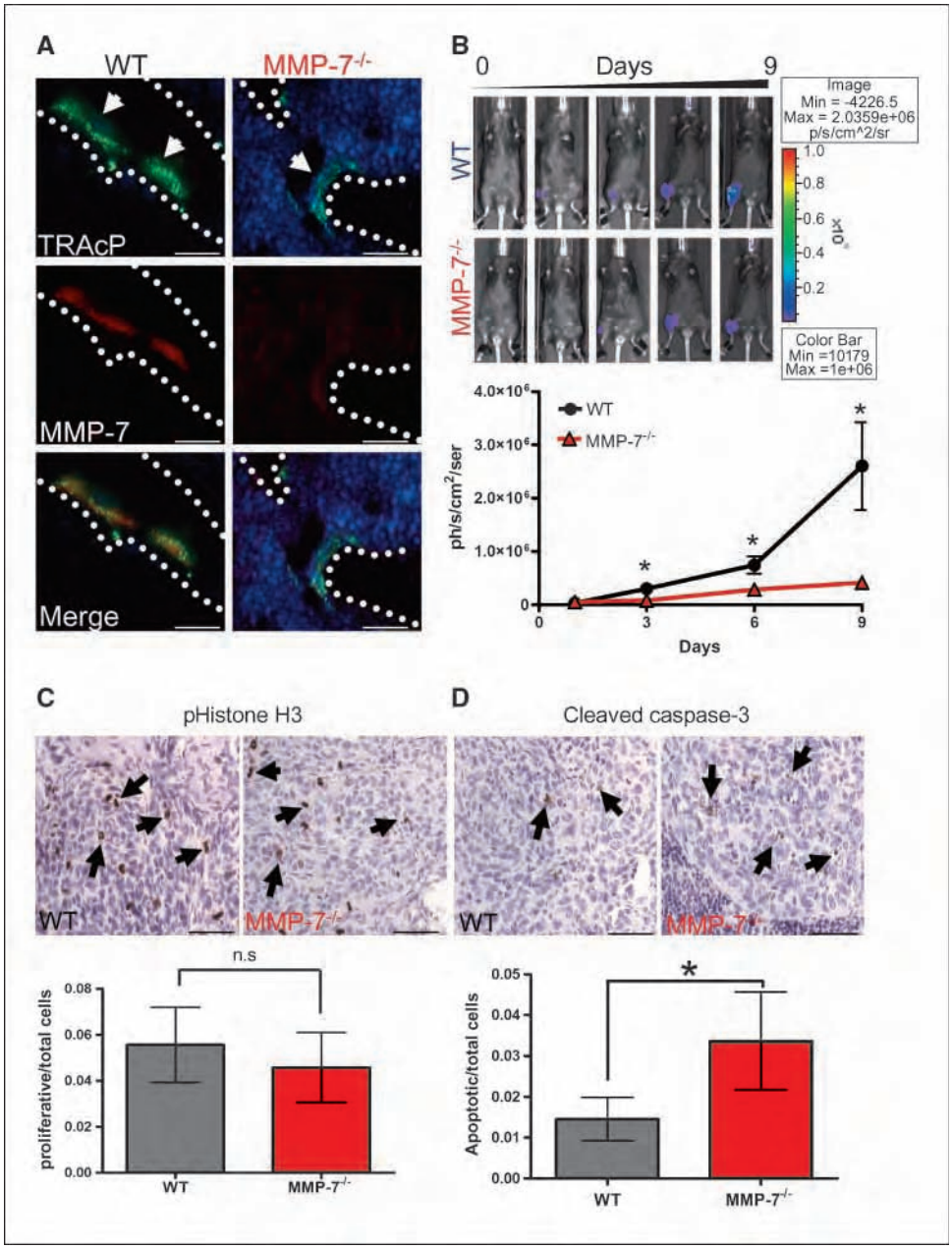

Figure 3. Host MMP-7 contributes to mammary tumor growth in the bone microenvironment. *A,* representative photomicrographs of MMP-7 (*red*) immunofluorescent localization merged with TRAcP (*green*) localization in WT and MMP-7$^{-/-}$ animals. DAPI (*blue*) was used as nuclear stain. *Arrows,* osteoclasts; *dashed line,* tumor-bone interface. *B,* PyMT-Luc cells were injected intratibially into RAG-2 null (WT; $n = 5$) or MMP-7 null (MMP-7$^{-/-}$; $n = 10$). The contralateral limb received a sham injection of saline. Luciferase activity was determined over a 9-d period and used as a measure of tumor growth. *C* and *D,* proliferative or apoptotic cells (*arrows*) in representative sections of WT- and MMP-7$^{-/-}$–injected tibias were identified by immunostaining of phosphorylated histone H3 (*pHistone H3*) or cleaved caspase-3, respectively. The number of positively stained cells per total number of cells was calculated. *Scale bars,* 50 μm. *Columns,* mean; *bars,* SD. *, $P < 0.05$; *n.s.,* nonsignificant.

significance was analyzed using a Student's t test. A value of $P < 0.05$ was considered significant. Data are presented as mean ± SD.

Results

MMP-7 and MMP-9 are expressed by osteoclasts in human breast-to-bone metastases. Previous observations using an animal model of tumor-bone interaction identified several MMPs as being highly expressed at the tumor-bone interface compared with the tumor area alone, namely MMP-2, MMP-3, MMP-7, MMP-9, and MMP-13 (14).[4] The expression of these MMPs was examined in human cases of frank breast-to-bone metastasis ($n = 11$). Interestingly, MMP-7 and MMP-9 were largely localized to the majority of mature TRAcP-positive multinucleated osteoclasts at the tumor-bone interface in human samples containing areas of osteolysis (10 of 11 samples; Fig. 1*A-C* and Supplementary Figs. S1 and S2). Other cells in the stromal compartment stained positively for MMP-7 and MMP-9, but remarkably, the tumor cells were negative for these metalloproteinases. MMP-2, MMP-3, and MMP-13 were also detected, but their expression was diffuse throughout the tumor/stroma compartment (data not shown). Because osteoclasts are the principal cells involved in bone resorption, we examined whether the ablation of host-derived MMP-7 or MMP-9 would affect the vicious cycle in terms of mammary tumor growth and/or mammary tumor–induced osteolysis.

Host-derived MMP-9 does not contribute to tumor growth or tumor-induced osteolysis. MMP-9 has previously been reported to be localized to osteoclasts, and MMP-9 null animals have been identified as having a delay in osteoclast recruitment

[4] S. Thiolloy and C.C. Lynch, unpublished observation.

DOI:10.1158/0008-5472.CAN-08-3949

during the development of long bones (19). Therefore, we initially tested the role of host-derived MMP-9 in tumor growth or tumor-induced osteolysis. Consistent with our observations in human samples, bone-resorbing osteoclasts in WT mice were positive for MMP-9 expression by immunofluorescent staining whereas, as expected, MMP-9 was not detected in MMP-9 null osteoclasts (Fig. 2*A*). Because MMP-9 null animals have a transient developmental bone phenotype, we determined the baseline trabecular BV as a function of TV (BV/TV) in WT and MMP-9 null animals at 6 weeks of age, which was the proposed time point for introduction of the PyMT-Luc tumor cells. No difference in the BV/TV between the WT and MMP-9 null animals was observed (Supplementary Fig. S3*A*).

To assess the contribution of host MMP-9 in mammary tumor growth in the bone microenvironment, the PyMT-Luc tumor cells, in which MMP-9 expression is undetectable *in vivo* (20), were injected into the tibia of syngeneic FVB WT or MMP-9 null mice. Surprisingly, quantitation of the bioluminescent signal from the tumor cells showed no difference in the tumor growth rate between the MMP-9 null and WT control mice (Fig. 2*B*). With respect to tumor-induced osteolysis, analysis of the BV/TV ratio by high-resolution micro–computed tomography (μCT) showed that the tumor-injected tibias of WT and MMP-9 null were significantly lower ($P < 0.05$) than their respective sham-injected control counterparts (Fig. 2*C*). However, a direct comparison of the BV/TV ratios between the WT and MMP-9 null tumor-injected limbs revealed no difference in BV/TV ratios (Fig. 2*C*). Furthermore, no differences in tumor growth as assessed by phosphorylated histone H3 for proliferation and cleaved caspase-3 immunohistochemistry for apoptosis, trabecular BV, and osteoclasts/millimeter bone by histomorphometry were observed between the WT and MMP-9 null groups (data not shown). These experiments with similar-sized groups were repeated on several occasions with similar results. These results using the intratibial model suggest that host MMP-9 does not contribute to mammary tumor growth in the bone or tumor-induced osteolysis and are consistent with studies examining the role of host MMP-9 in the prostate cancer-bone microenvironment (21).

Host MMP-7 contributes to mammary tumor growth in the bone microenvironment. This is the first report to document the expression of MMP-7 in human breast-to-bone metastases and in human osteoclasts (Fig. 1), although MMP-7 has previously been identified in rodent osteoclasts by our group (14). Recapitulating observations in human clinical samples, MMP-7 expression was identified in WT murine osteoclasts and not in MMP-7 null

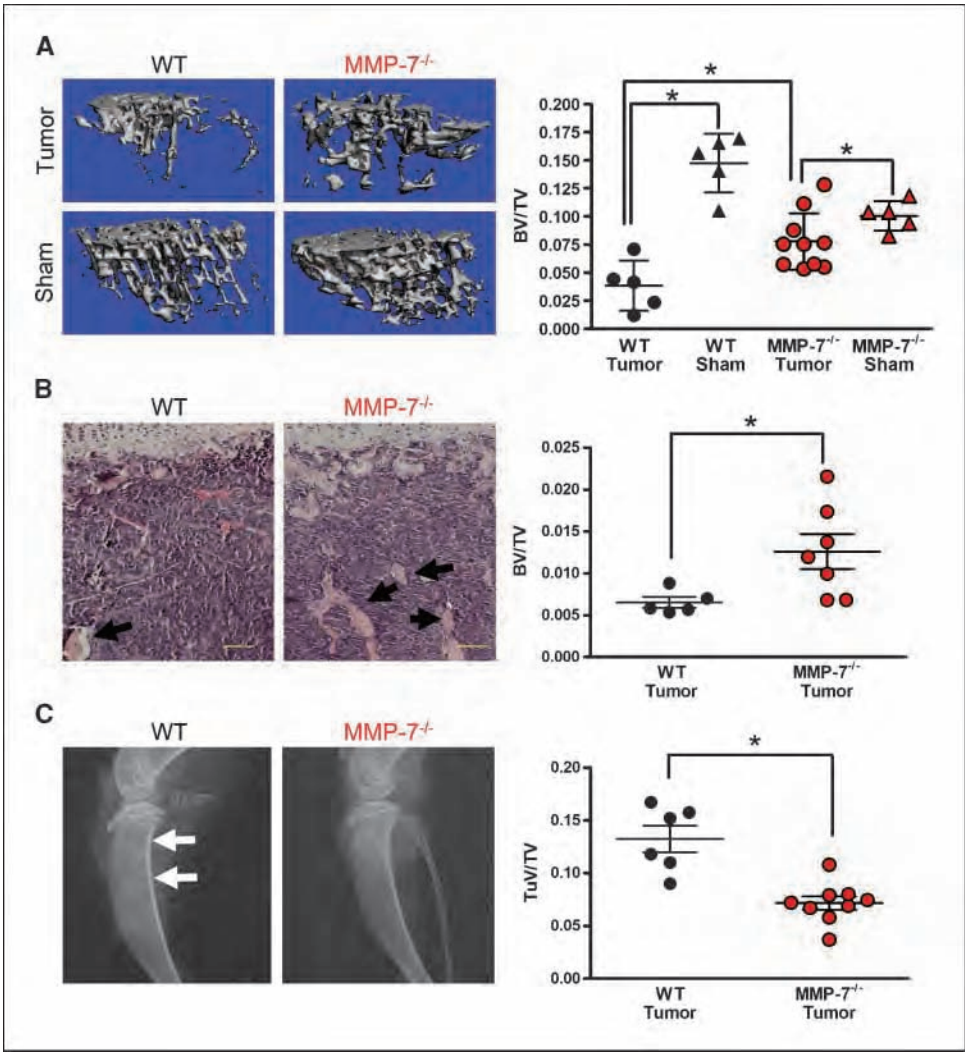

Figure 4. Tumor-mediated osteolysis is attenuated in the absence of host-derived MMP-7. *A,* μCT scans of trabecular bone from tumor-bearing and sham-injected limbs of WT and MMP-7$^{-/-}$ animals allowed for the calculation of the BV/TV ratio. *B,* representative H&E-stained photomicrographs of tumor-bearing tibias from WT and MMP-7$^{-/-}$ animals. *Arrows,* trabecular bone. *Scale bars,* 100 μm. The BV/TV ratio was determined in several nonserial sections of tumor-injected tibias obtained from WT ($n = 5$) and MMP-7 null animals ($n = 7$). *C,* representative radiographic images from tumor-injected WT and MMP-7$^{-/-}$ animals at day 9. *Arrows,* lytic tumor lesions in the WT animals. The TuV over TV for tumor-injected limbs of WT and MMP-7$^{-/-}$ animals was assessed. *Points,* individual sample quantitation mean; *bars,* SD. *, $P < 0.05$; *n.s.,* nonsignificant.

DOI:10.1158/0008-5472.CAN-08-3949

osteoclasts (Fig. 3*A*). Given that MMP-7 expression by osteoclasts is a relatively recent observation, studies into defining roles for MMP-7 in skeletal development have not been explored thus far. Therefore, before testing the effect of host-derived MMP-7 on the vicious cycle, the trabecular BV in noninjected, 6-week-old immunocompromised WT and MMP-7 null animals was examined using high-resolution μCT. Our results revealed no significant difference in the BV/TV ratio between WT and MMP-7 null animals, suggesting that, at this time point, MMP-7 null animals do not display an obvious bone phenotype compared with the WT controls (Supplementary Fig. S3*B*).

To determine the contribution of host MMP-7 to mammary tumor growth in the bone microenvironment, PyMT-Luc cells were injected into 6-week-old WT or MMP-7 null mice. Quantitation of the bioluminescent signal from the PyMT-Luc cells showed a significant decrease in the tumor growth rate in MMP-7 null mice compared with the WT controls (Fig. 3*B*). These experiments with similar-sized groups in terms of animal numbers were independently repeated on four occasions, and similar observations were noted. To further investigate the potential role of MMP-7 in tumor growth, tumor proliferation and apoptosis were assessed by immunohistochemistry for phosphorylated histone H3 and cleaved caspase-3, respectively, in multiple sections from at least five animals per group (Fig. 3*C* and *D*). Surprisingly, no difference in tumor proliferation was observed between the WT and MMP-7 null groups; however, tumor apoptosis was significantly higher in MMP-7 null mice compared with the WT controls ($P < 0.05$). Similar findings with respect to the effect of host MMP-7 on tumor growth using the 4T1-Luc cell line were also observed (Supplementary Fig. S4*A*–*C*). These results suggest that host-derived MMP-7 significantly contributes to mammary tumor growth in the bone by enhancing tumor cell survival.

Host-derived MMP-7 contributes to mammary tumor–induced osteolysis. The vicious cycle of tumor-bone interaction suggests that tumor growth/survival is dependent on osteoclast-mediated bone resorption. Because MMP-7 is primarily localized to bone-resorbing osteoclasts in the tumor-bone microenvironment, we assessed whether a lack of MMP-7 in osteoclasts affected tumor-induced osteolysis. Analysis of the BV/TV ratios from WT and MMP-7 null tumor-injected tibias using μCT (Fig. 4*A*) and histomorphometry (Fig. 4*B*) revealed that the MMP-7 null group had a significantly higher amount of trabecular bone, which is in keeping with our tumor growth data, i.e., less tumor growth in the MMP-7 null animal would lead to less osteolysis. X-ray analysis also revealed a significantly lower TuV in the MMP-7 null animals compared with WT controls (Fig. 4*C*). Studies using the 4T1-Luc cell line also showed that host-derived MMP-7 significantly affected tumor-induced osteolysis (Supplementary Fig. S5*A* and *B*). These results show that host-derived MMP-7 significantly affects mammary tumor–induced osteolysis.

MMP-7 mediates RANKL solubilization in the tumor-bone microenvironment. Next, we explored the potential molecular mechanism through which osteoclast-derived MMP-7 was affecting tumor-induced osteolysis. Given the acidity of the resorption lacunae (pH < 4) and the neutral activity profile of MMP-7, we suggest that MMP-7 does not function in direct bone matrix degradation but in the processing of factors that affect cell-cell communication within the tumor-bone microenvironment. MMP-7 has previously been shown to process a number of growth factors and cytokines to soluble active forms, including members of the tumor necrosis factor family TNF-α, Fas ligand (FasL), and RANKL

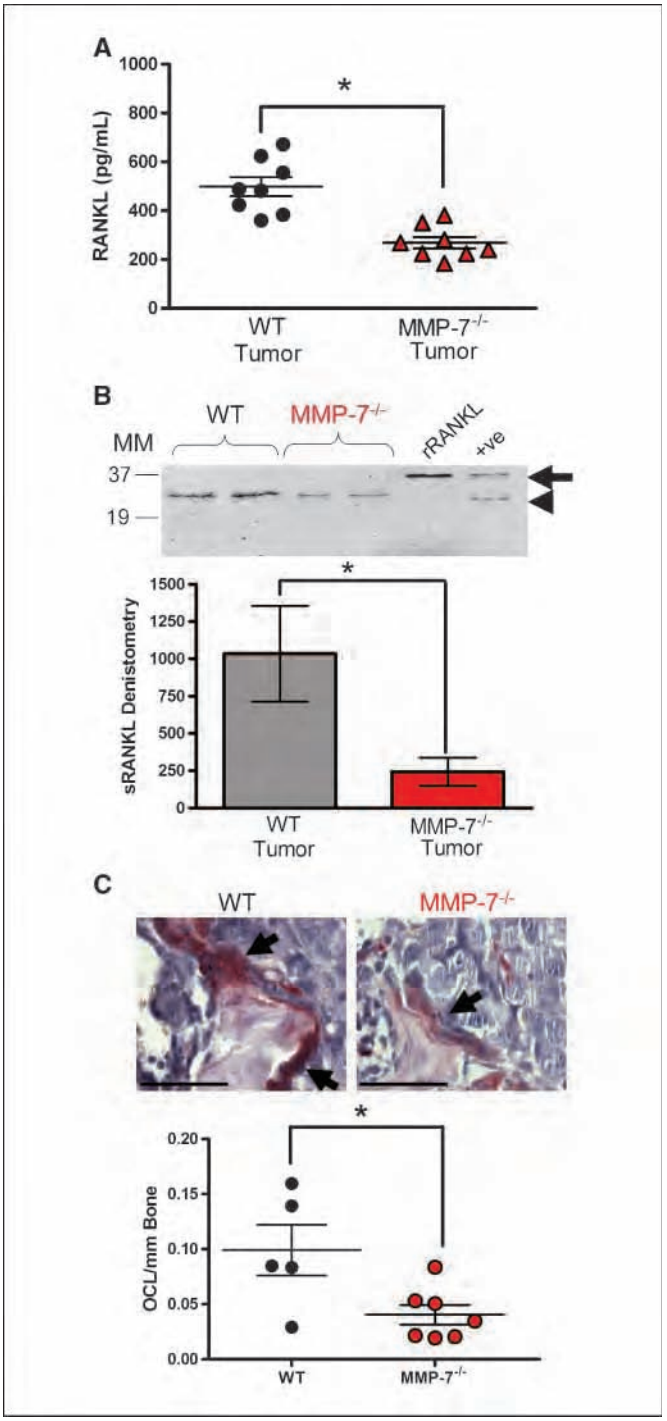

Figure 5. MMP-7 solubilization of RANKL in the tumor-bone microenvironment. *A,* ELISA analysis of soluble RANKL levels in lysates from tumor-injected tibias obtained from WT ($n = 8$) or MMP-7$^{-/-}$ ($n = 8$) animals. *B,* representative immunoprecipitation blot using antibodies directed toward the NH_2 terminus of RANKL for the detection of soluble RANKL in tumor-bearing tibias of WT and MMP-7$^{-/-}$ animals. *MM,* molecular weight marker in kDa. Unglycosylated full-length recombinant RANKL (*arrow*) was used as a positive control. In addition, MMP-7–solubilized RANKL (*arrowhead*) served as a further positive control (*+ve*). Densitometry was performed on the level of soluble RANKL in PyMT-Luc–bearing limbs derived from WT ($n = 11$) and MMP-7$^{-/-}$ null ($n = 12$) mice. *C,* TRAcP (*red*)-positive, multinucleated (*blue*) osteoclasts (*arrows*) at the tumor-bone interface in WT and MMP-7$^{-/-}$ animals. The number of osteoclasts at the tumor-bone interface was determined in multiple nonserial sections of tumor-injected tibias obtained from WT ($n = 5$) and MMP-7$^{-/-}$ ($n = 7$) animals. *Scale bars,* represent 100 μm. *Points,* individual sample quantitation mean; *bars,* SD. *, $P < 0.05$; *n.s.,* nonsignificant.

DOI:10.1158/0008-5472.CAN-08-3949

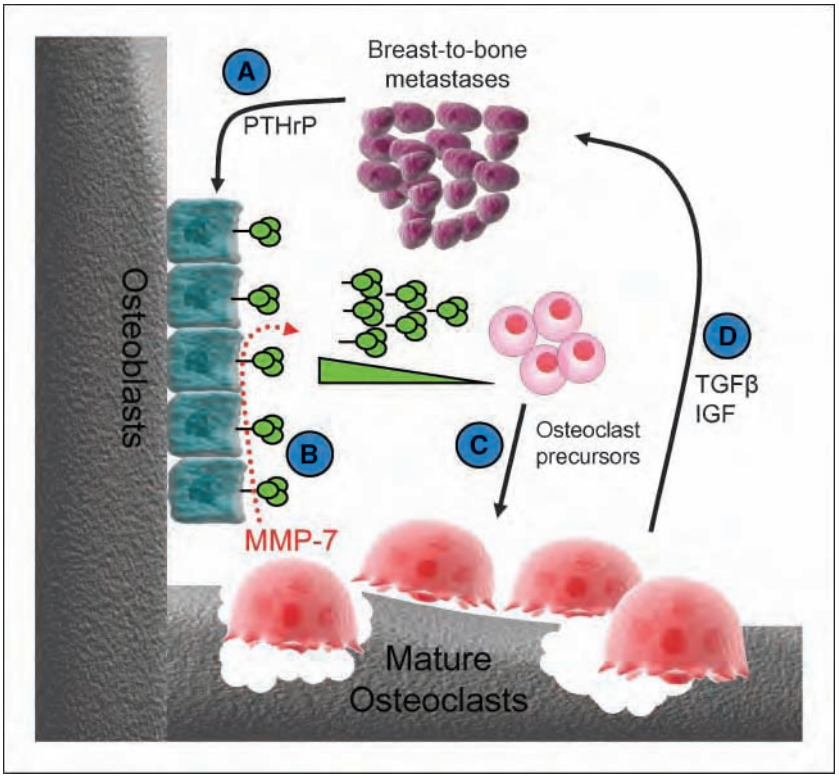

Figure 6. Hypothetical mechanism of osteoclast-derived MMP-7 action in the mammary tumor-bone microenvironment. *A,* metastatic tumor cells, through the secretion of factors such as parathyroid hormone related peptide (*PTHrP*), stimulate osteoblasts to express full-length membrane bound RANKL. *B,* osteoclasts express MMP-7, which can process membrane-bound RANKL to a soluble active form. *C,* soluble RANKL has been shown to be chemotactic for osteoclast precursors (25). In addition to acting as a potential chemotactic molecule, soluble RANKL can stimulate the maturation and activation of osteoclast precursors. *D,* activated osteoclasts, in turn, execute bone resorption leading to the release of growth factors such as TGF-β and IGFs that promote tumor survival and growth in the bone microenvironment.

(14, 22, 23). RANKL is essential for osteoclastogenesis and is a potent chemotactic molecule for monocytes and osteoclast precursor cells (24, 25). Therefore, we investigated if MMP-7 solubilization of RANKL was relevant in our model.

ELISA analysis revealed lower levels of total RANKL (membrane bound and soluble) in the tumor-injected tibias of MMP-7 null mice compared with WT control mice (Fig. 5*A*), whereas no difference was observed in the sham-injected control counterparts of each group (data not shown). Similar levels of osteoprotegerin, a soluble decoy receptor of RANKL, were found in the WT and MMP-7 null animals and were not present at a high enough concentration to interfere with the detection of RANKL by ELISA (data not shown). Immunoprecipitation and immunoblotting for soluble RANKL revealed significantly lower levels of soluble RANKL in PyMT-Luc or 4T1-Luc tumor-injected MMP-7 null animals compared with WT controls as assessed by densitometry (Fig. 5*B*, $P < 0.05$ and Supplementary Fig. S5*C*, $P < 0.05$).

Interestingly, soluble RANKL could still be detected in the tumor-bearing limbs of MMP-7 null animals. This suggests that RANKL solubilization is still occurring in the absence of MMP-7. We and others have previously identified that other metalloproteinases, such as MMP-1, MMP-3, MMP-14, a disintegrin and metalloproteinase-17 (ADAM-17), and the serine protease cathepsin G are capable of processing RANKL to a soluble active form, and therefore, these proteases may also be playing a role in the solubilization of RANKL in our model (14, 26–28). However, because the levels of RANKL are significantly lower in the MMP-7 null mice, we suggest that MMP-7 is the dominant protease involved in RANKL solubilization.

Next, because a decrease in the amount of soluble RANKL was detected in the tumor-bearing limbs of the MMP-7 null animals, we asked if there was concomitant decrease in the number of osteoclasts in the MMP-7 null tumor-bone microenvironment. We observed significantly lower numbers of TRAcP-positive multinucleated osteoclasts per unit length of tumor-bone interface in the MMP-7 null animals compared with the WT controls (Fig. 5*C*). Significantly lower numbers of osteoclasts were also recorded in MMP-7–deficient animals injected with 4T1-Luc cells compared with WT controls (Supplementary Fig. S5*D*). Given the importance of RANKL in mediating osteoclastogenesis, these data suggest that MMP-7 mediates mammary tumor–induced osteolysis by affecting the availability of a key factor for osteoclastogenesis, RANKL.

Discussion

Understanding the molecular mechanisms that control the vicious cycle is the key for the development of new therapeutics that will be effective not only in treating bone metastases but also in curing them. In the current study, we found that, in human cases of breast-to-bone metastasis, osteoclasts were a rich source of MMP-7 and MMP-9. Interestingly, our studies using two unrelated osteolytic-inducing tumor cell lines (PyMT-Luc and 4T1-Luc) revealed that only MMP-7 seemed to contribute to mammary tumor growth and tumor-induced osteolysis in the bone microenvironment. Furthermore, our data suggest that MMP-7 solubilization of the osteoclastogenic factor RANKL is the principal molecular mechanism underlying these observations. Previously, we have identified that MMP-7 processing of RANKL results in the generation of an active soluble form that can promote osteoclast maturation and activation (14). Therefore, in the context of breast-to-bone metastasis, we hypothesize that, in the absence of MMP-7–solubilized RANKL, there is a resultant decrease in osteoclast maturation and bone resorption at the tumor-bone interface, which in turn results in a decrease in bone-derived growth factors, such as TGF-β and IGF, which affect tumor survival and growth (Fig. 6).

DOI:10.1158/0008-5472.CAN-08-3949

Our results show that an osteoclast-derived protease, MMP-7, can promote osteoclast activation in the tumor-bone microenvironment by generating an active soluble form of the osteoclastogenic factor RANKL and suggest that selective inhibition of MMP-7 may be of benefit for the treatment of lytic metastases. Several studies support the rationale for the development of selective MMPIs for the treatment of bone metastases. Broad spectrum MMPIs, such as batimastat, have been identified as being effective in preventing tumor growth and tumor-induced osteolysis in the bone environment using animal models (10–12). However, conclusions from human clinical trials with the same inhibitors identified the necessity for highly selective MMPIs, which lack the deleterious side effects of broad spectrum inhibitors before their application in clinical settings (13). This requires an understanding of the precise roles of MMPs in the context of particular diseases, and in this regard, our studies suggest MMP-7 as an attractive target for the treatment of lytic metastases.

Whereas MMP-7 solubilization of RANKL is predicted here to be a mechanism underlying our observations, MMP-7 may contribute via other mechanisms. For example, MMP-7 processing of apoptotic factors, such as Fas ligand in the tumor-bone microenvironment, may directly affect tumor survival (22). In addition, the direct processing of the bone matrix by MMP-7 may also be a possibility. Acidification and cathepsin-K secretion into osteoclast resorption lacunae allows for the demineralization and collagenolysis of the bone matrix, respectively (6). By a process known as transcytosis, the osteoclast mediates the removal of bone products from the area of the bone undergoing resorption (29). Given the punctate localization of MMP-7 by immunofluorescent staining (Figs. 1*A* and 3*A*) it is tempting to speculate that MMP-7 contributes to the further processing of bone matrix components, such as osteopontin (30), or the release of growth factors from bone matrix components, such as TGF-β (31) and IGFs (32), within these transcytotic vesicles. The expression of MMP-7 from other cellular sources may also be a possibility. In the tumor-bone microenvironment, we observed that MMP-7 expression was largely confined to osteoclasts. However, MMP-7 has also been shown to be expressed by macrophages, and given the role of macrophages in tumor-induced osteolysis, the contribution of macrophage-derived MMP-7 in our model or in humans cannot be discounted (33, 34).

Given the apparent role of MMP-7 in osteoclast function in the pathologic setting of tumor-induced osteolysis, it is surprising that MMP-7 null animals seem to have a normal skeletal phenotype. Data presented here using μCT scan analysis show a similar BV/TV ratio between MMP-7 null and WT control mice at 6 weeks of age. Whereas a role for MMP-7 in bone development has not been explored, a number of reports have revealed that the phenotype of the MMP-7 null animals often becomes apparent in response to injury/challenges or disease. For example, in nonpathologic conditions such as herniated disc resorption, macrophage-derived MMP-7 is critical for the resorption of the herniated disc and in mammary and prostate involution; MMP-7 processing of FasL is important for initiating apoptosis (22, 23, 35). More often, phenotypes in the MMP-7 null animals have been observed in pathologic conditions such as pancreatitis, colon tumorigenesis, mammary gland tumorigenesis, and in innate defense wherein MMP-7 null animals show significant delays in disease progression or in response to infection (36–39). Therefore, although MMP-7 null mice lack an apparent skeletal phenotype, in the context of tumor-bone microenvironment, it is clear based on the results in the current study that host MMP-7 plays an important role in osteoclast biology. In addition, our observations defining a role for MMP-7 in bone diseases are consistent with previous reports that implicate roles for host MMP-7 in prostate cancer–induced osteolysis, osteoarthritis, and cartilage/periarticular bone destruction (14, 40, 41).

Although MMP-9 was localized to human and murine osteoclasts, the ablation of host MMP-9 did not seem to affect PyMT-Luc tumor growth and bone resorption compared with the WT controls. Analogous results were obtained by Nabha and colleagues, using the same intratibial model but in the context of prostate cancer progression in the bone (21). Given the importance of MMP-9 in osteoclast migration and recruitment in developing long bones (19), these results were surprising. It seems that, in the tumor-bone microenvironment, MMP-9 is not critical for osteoclast function. The possibility that tumor-derived MMP-9 could overcome the absence of host MMP-9 exists in our model; however, *in vivo* studies by our group have shown that MMP-9 expression by the PyMT-Luc tumor cells is not detectable (20). Therefore, the ability of tumor-derived MMP-9 to circumvent the loss of host-derived MMP-9 and affect tumor progression in the bone is unlikely. However, due to functional overlap among members of the MMP family, other MMPs produced by osteoclasts and other stromal cells in the tumor microenvironment may compensate for the absence of host MMP-9.

Whereas our data point toward MMP-9 as not being critical for mammary tumor growth or induced osteolysis, it is important to note that MMP-9 could contribute to other steps of metastasis that are not taken into account with the intratibial model. These include extravasation from the sinusoidal vasculature in the bone and initial survival, the latter of which has been shown to be an important role for host-derived MMP-9 in early lung metastasis (42). Furthermore, MMP-9 has been implicated in tumor angiogenesis by mediating the release of matrix-sequestered vascular endothelial growth factor (43). In the context of the prostate tumor-bone microenvironment, Nabha and colleagues showed a decrease in angiogenesis in MMP-9 null animals compared with WT controls (21). Therefore, the selective inhibition of MMP-9 may still prove useful in preventing the establishment and angiogenesis of bone metastases.

In conclusion, this study shows that osteoclast-derived MMP-7, but not MMP-9, significantly contributes to tumor-induced osteolysis by affecting osteoclast activation. We suggest that MMP-7–mediated solubilization of RANKL is a potential mechanism underlying this observation. Our data support the rationale for the generation of selective MMPIs for the treatment of osteolytic bone metastases and implies that the development of such reagents would expand the therapeutic options available to patients suffering with this incurable disease.

Disclosure of Potential Conflicts of Interest

No potential conflicts of interest were disclosed.

Acknowledgments

Received 10/14/08; revised 4/21/09; accepted 6/9/09.

Grant support: NIH grant 1 R01 CA84360 (L.M. Matrisian) and Susan G. Komen Foundation grant PDF 02 1394 (C.C. Lynch). C.C. Lynch and S. Thiolloy are supported by the Department of Defense awards W81XWH-07-1-0208 and BC051038, respectively.

Views and opinions of, and endorsements by, the authors (S. Thiolloy and C.C. Lynch) do not reflect those of the U.S. Army or Department of Defense.

The costs of publication of this article were defrayed in part by the payment of page charges. This article must therefore be hereby marked *advertisement* in accordance with 18 U.S.C. Section 1734 solely to indicate this fact.

We thank James Edwards and Steve Munoz of Vanderbilt Bone Center for their expertise.

DOI:10.1158/0008-5472.CAN-08-3949

References

1. Coleman RE, Rubens RD. The clinical course of bone metastases from breast cancer. Br J Cancer 1987;55:61–6.
2. Mundy GR. Metastasis to bone: causes, consequences and therapeutic opportunities. Nat Rev Cancer 2002;2:584–93.
3. Chirgwin JM, Guise TA. Molecular mechanisms of tumor-bone interactions in osteolytic metastases. Crit Rev Eukaryot Gene Expr 2000;10:159–78.
4. Compston JE. Bone marrow and bone: a functional unit. J Endocrinol 2002;173:387–94.
5. Delaisse JM, Engsig MT, Everts V, et al. Proteinases in bone resorption: obvious and less obvious roles. Clin Chim Acta 2000;291:223–34.
6. Delaisse JM, Andersen TL, Engsig MT, Henriksen K, Troen T, Blavier L. Matrix metalloproteinases (MMP) and cathepsin K contribute differently to osteoclastic activities. Microsc Res Tech 2003;61:504–13.
7. Saftig P, Hunziker E, Wehmeyer O, et al. Impaired osteoclastic bone resorption leads to osteopetrosis in cathepsin-K-deficient mice. Proc Natl Acad Sci U S A 1998;95:13453–8.
8. Chambers AF, Matrisian LM. Changing views of the role of matrix metalloproteinases in metastasis. J Natl Cancer Inst 1997;89:1260–70.
9. Lynch CC, Matrisian LM. Matrix metalloproteinases in tumor-host cell communication. Differentiation 2002;70:561–73.
10. Lee J, Weber M, Mejia S, Bone E, Watson P, Orr W. A matrix metalloproteinase inhibitor, batimastat, retards the development of osteolytic bone metastases by MDA-MB-231 human breast cancer cells in Balb C nu/nu mice. Eur J Cancer 2001;37:106–13.
11. Winding B, NicAmhlaoibh R, Misander H, et al. Synthetic matrix metalloproteinase inhibitors inhibit growth of established breast cancer osteolytic lesions and prolong survival in mice. Clin Cancer Res 2002;8:1932–9.
12. Nemeth JA, Yousif R, Herzog M, et al. Matrix metalloproteinase activity, bone matrix turnover, and tumor cell proliferation in prostate cancer bone metastasis. J Natl Cancer Inst 2002;94:17–25.
13. Coussens LM, Fingleton B, Matrisian LM. Matrix metalloproteinase inhibitors and cancer: trials and tribulations. Science 2002;295:2387–92.
14. Lynch CC, Hikosaka A, Acuff HB, et al. MMP-7 promotes prostate cancer-induced osteolysis via the solubilization of RANKL. Cancer Cell 2005;7:485–96.
15. Halpern J, Lynch CC, Fleming J, et al. The application of a murine bone bioreactor as a model of tumor: bone interaction. Clin Exp Metastasis 2006;23:345–56.
16. Aslakson CJ, Miller FR. Selective events in the metastatic process defined by analysis of the sequential dissemination of subpopulations of a mouse mammary tumor. Cancer Res 1992;52:1399–405.
17. Fingleton B, Powell WC, Crawford HC, Couchman JR, Matrisian LM. A rat monoclonal antibody that recognizes pro- and active MMP-7 indicates polarized expression *in vivo*. Hybridoma (Larchmt) 2007;26:22–7.
18. Filgueira L. Fluorescence-based staining for tartrate-resistant acidic phosphatase (TRAP) in osteoclasts combined with other fluorescent dyes and protocols. J Histochem Cytochem 2004;52:411–4.
19. Engsig MT, Chen QJ, Vu TH, et al. Matrix metalloproteinase 9 and vascular endothelial growth factor are essential for osteoclast recruitment into developing long bones. J Cell Biol 2000;151:879–90.
20. Martin M, Carter K, Thiolloy S, Lynch CC, Matrisian L, Fingleton B. Effect of ablation or inhibition of stromal matrix metalloproteinase-9 on lung metastasis in a breast cancer model is dependent on genetic background. Cancer Res 2008;68:6251–9.
21. Nabha SM, Bonfil RD, Yamamoto HA, et al. Host matrix metalloproteinase-9 contributes to tumor vascularization without affecting tumor growth in a model of prostate cancer bone metastasis. Clin Exp Metastasis 2006;23:335–44.
22. Powell WC, Fingleton B, Wilson CL, Boothby M, Matrisian LM. The metalloproteinase matrilysin (MMP-7) proteolytically generates active soluble Fas ligand and potentiates epithelial cell apoptosis. Curr Bio 1999;9:1441–7.
23. Haro H, Crawford HC, Fingleton B, Shinomiya K, Spengler DM, Matrisian LM. Matrix metalloproteinase-7-dependent release of tumor necrosis factor-α in a model of herniated disc resorption. J Clin Invest 2000;105:143–50.
24. Kong YY, Yoshida H, Sarosi I, et al. OPGL is a key regulator of osteoclastogenesis, lymphocyte development and lymph-node organogenesis. Nature 1999;397:315–23.
25. Breuil V, Schmid-Antomarchi H, Schmid-Alliana A, Rezzonico R, Euller-Ziegler L, Rossi B. The receptor activator of nuclear factor (NF)-κB ligand (RANKL) is a new chemotactic factor for human monocytes. FASEB J 2003;17:1751–3.
26. Lum L, Wong BR, Josien R, et al. Evidence for a role of a tumor necrosis factor-α (TNF-α)-converting enzyme-like protease in shedding of TRANCE, a TNF family member involved in osteoclastogenesis and dendritic cell survival. J Biol Chem 1999;274:13613–8.
27. Schlondorff J, Lum L, Blobel CP. Biochemical and pharmacological criteria define two shedding activities for TRANCE/OPGL that are distinct from the tumor necrosis factor α convertase. J Biol Chem 2001;276:14665–74.
28. Wilson TJ, Nannuru KC, Futakuchi M, Sadanandam A, Singh RK. Cathepsin G enhances mammary tumor-induced osteolysis by generating soluble receptor activator of nuclear factor-κB ligand. Cancer Res 2008;68:5803–11.
29. Blair HC. How the osteoclast degrades bone. Bioessays 1998;20:837–46.
30. Agnihotri R, Crawford HC, Haro H, Matrisian LM, Havrda MC, Liaw L. Osteopontin, a novel substrate for matrix metalloproteinase-3 (stromelysin-1) and matrix metalloproteinase-7 (matrilysin). J Biol Chem 2001;276:28261–7.
31. Imai K, Hiramatsu A, Fukushima D, Pierschbacher MD, Okada Y. Degradation of decorin by matrix metalloproteinases: identification of the cleavage sites, kinetic analyses and transforming growth factor-β 1 release. Biochem J 1997;322:809–14.
32. Miyamoto S, Yano K, Sugimoto S, et al. Matrix metalloproteinase-7 facilitates insulin-like growth factor bioavailability through its proteinase activity on insulin-like growth factor binding protein 3. Cancer Res 2004;64:665–71.
33. Burke B, Giannoudis A, Corke KP, et al. Hypoxia-induced gene expression in human macrophages: implications for ischemic tissues and hypoxia-regulated gene therapy. Am J Pathol 2003;163:1233–43.
34. Athanasou NA, Sabokbar A. Human osteoclast ontogeny and pathological bone resorption. Histol Histopathol 1999;14:635–47.
35. Fingleton B, Vargo-Gogola T, Crawford HC, Matrisian LM. Matrilysin [MMP-7] expression selects for cells with reduced sensitivity to apoptosis. Neoplasia 2001;3:459–68.
36. Sawey ET, Johnson JA, Crawford HC. Matrix metalloproteinase 7 controls pancreatic acinar cell transdifferentiation by activating the Notch signaling pathway. Proc Natl Acad Sci U S A 2007;104:19327–32.
37. Wilson CL, Heppner KJ, Labosky PA, Hogan BL, Matrisian LM. Intestinal tumorigenesis is suppressed in mice lacking the metalloproteinase matrilysin. Proc Natl Acad Sci U S A 1997;94:1402–7.
38. Wilson CL, Ouellette AJ, Satchell DP, et al. Regulation of intestinal α-defensin activation by the metalloproteinase matrilysin in innate host defense. Science 1999;286:113–7.
39. Rudolph-Owen LA, Matrisian LM. Matrix metalloproteinases in remodeling of the normal and neoplastic mammary gland. J Mammary Gland Biol Neoplasia 1998;3:177–89.
40. Gjertsson I, Innocenti M, Matrisian LM, Tarkowski A. Metalloproteinase-7 contributes to joint destruction in Staphylococcus aureus induced arthritis. Microb Pathog 2005;38:97–105.
41. Ohta S, Imai K, Yamashita K, Matsumoto T, Azumano I, Okada Y. Expression of matrix metalloproteinase 7 (matrilysin) in human osteoarthritic cartilage. Lab Invest 1998;78:79–87.
42. Acuff HB, Carter KJ, Fingleton B, Gorden DL, Matrisian LM. Matrix metalloproteinase-9 from bone marrow-derived cells contributes to survival but not growth of tumor cells in the lung microenvironment 1. Cancer Res 2006;66:259–66.
43. Bergers G, Brekken R, McMahon G, et al. Matrix metalloproteinase-9 triggers the angiogenic switch during carcinogenesis. Nat Cell Biol 2000;2:737–44.